UNIVERSIDAD NACIONAL AUTÓNOMA DE MÉXICO
POSGRADO EN CIENCIAS DEL MAR Y LIMNOLOGÍA

VARIABILIDAD DE LA ZONA DE OXÍGENO MÍNIMO Y SU RELACIÓN CON LA PRODUCTIVIDAD EN EL GOLFO DE TEHUANTEPEC DURANTE EL ÚLTIMO MILENIO

TESIS
QUE PARA OPTAR POR EL GRADO ACADÉMICO DE:
DOCTORA EN CIENCIAS
(GEOLOGÍA MARINA)

PRESENTA:
M. EN C. LAURA ALMARAZ RUIZ

TUTORA PRINCIPAL:
DRA. MA. LUISA MACHAIN CASTILLO
INSTITUTO DE CIENCIAS DEL MAR Y LIMNOLOGÍA, UNAM, CIUDAD DE MÉXICO
COMITÉ TUTOR:
DR. DAVID. A. SALAS DE LEÓN
INSTITUTO DE CIENCIAS DEL MAR Y LIMNOLOGÍA, UNAM, CIUDAD DE MÉXICO
DRA. MARGARITA E. CABALLERO MIRANDA
INSTITUTO DE GEOFÍSICA, UNAM
DR. JOAN ALBERT SÁNCHEZ CABEZA
INSTITUTO DE CIENCIAS DEL MAR Y LIMNOLOGÍA, UNAM, MAZATLÁN, SINALOA
DR. ABDELFFETTAH SIFEDDINE
INSTITUT DE RECHERCHE POUR LE DÉVELOPPEMENT EN MÉXICO

MÉXICO, CD. MX., JUNIO, 2023

VARIABILIDAD DE LA ZONA DE OXÍGENO MÍNIMO Y SU RELACIÓN CON LA PRODUCTIVIDAD EN EL GOLFO DE TEHUANTEPEC DURANTE EL ÚLTIMO MILENIO

TESIS

QUE PARA OBTENER EL GRADO ACADÉMICO DE:
DOCTORA EN CIENCIAS
(GEOLOGÍA MARINA)

PRESENTA:
M. EN C. LAURA ALMARAZ RUIZ

TUTORA PRINCIPAL:
DRA. MA. LUISA MACHAIN CASTILLO
INSTITUTO DE CIENCIAS DEL MAR Y LIMNOLOGÍA, UNAM, CIUDAD DE MÉXICO
COMITÉ TUTOR:
DR. DAVID. A. SALAS DE LEÓN
INSTITUTO DE CIENCIAS DEL MAR Y LIMNOLOGÍA, UNAM, CIUDAD DE MÉXICO
DRA. MARGARITA E. CABALLERO MIRANDA
INSTITUTO DE GEOFÍSICA, UNAM
DR. JOAN ALBERT SÁNCHEZ CABEZA
INSTITUTO DE CIENCIAS DEL MAR Y LIMNOLOGÍA, UNAM, MAZATLÁN, SINALOA
DR. ABDELFFETTAH SIFEDDINE
INSTITUT DE RECHERCHE POUR LE DÉVELOPPEMENT EN MÉXICO

MÉXICO, CD. MX., JUNIO, 2023

AGRADECIMIENTOS

Con todo mi amor para mi familia, amigos y aquellas personas que de alguna manera han contribuido a mi crecimiento personal y académico.

A mis hermanas Monse y Jaqui y a mis sobrinos Angie e Ismael.

A mi compañero de vida y compañero durante el doctorado a Xinantecatl A. Nava Fernández y en especial a nuestra hija Morelia Y. Nava Almaraz.

Gracias por su apoyo y por su amor incondicional.

TABLA DE CONTENIDO

INDICE DE FIGURAS

INDICE DE TABLAS

Resumen

El presente estudio tiene como objetivo comprender los cambios en el agua de fondo y su relación con la productividad superficial en los sedimentos laminados del Golfo de Tehuantepec (GT) durante el último milenio. Se utilizaron dos secuencias sedimentarias para complementar los últimos ~1000 años: el núcleo MD02-2521, en el cual se analizaron los primeros ~100 cm correspondientes de ~618 a ~1610 EC, y en el que se analizaron las asociaciones de diatomeas; y el núcleo Tehua XII E03 que abarcó de ~1500 a ~2014 EC en el que se analizaron foraminíferos bentónicos (FB), diatomeas y proxies geoquímicos (Mo, V, Cd, U, Re, Ni/Al, Cu/Al, C_{org}, NT, y $\delta^{15}N_{sed}$). El GT se encuentra en el Pacífico Tropical Nororiental (PTNO) y forma parte de una de las Zonas de Oxígeno Mínimo (ZOM) más grandes e intensas del mundo. Estacionalmente, el GT está influenciado por fuertes vientos llamados localmente Tehuanos y por la migración de la Zona de Convergencia Intertropical (ZCIT). Los Tehuanos provocan una intensa surgencia y mezcla de aguas superficiales y subsuperficiales ricas en nutrientes, lo que promueve una alta productividad primaria en el GT. A su vez, la productividad influye en la cantidad de materia orgánica que llega al fondo oceánico, y consecuentemente la cantidad de oxígeno disuelto (OD) consumido debido a la remineralización de la materia orgánica. Las diatomeas en el núcleo MD02-2521 revelaron que el Periodo Cálido Medieval (PCM, ~765 a ~1414 EC) se caracterizó por una asociación de aguas cálidas y baja productividad (*Neodelphineis pelagica* y *Thalassionema nitzschioides*), mientras que el inicio de la Pequeña Edad de Hielo (PEH, ~1426 a ~1610 EC) por una asociación de diatomeas de condiciones frías y alta productividad (esporas de *Chaetoceros* spp., *T. nitzschioides* y *Lioloma pacificum*). En el núcleo Tehua XII E03, la PEH (~1500 a ~1860 EC) se caracterizó por la dominancia de la asociación de FB tolerantes a las más bajas concentraciones de OD (*Epistominella sandiegoensis*, *Takayanagia delicata* y *Buliminella tenuata*), lo que sugiriere una ZOM más intensificada, lo

cual fue consistente con el enriquecimiento de Mo, V, Cd, U y Re, y una mayor desnitrificación (δ^{15}N). Durante este período, la productividad fue alta como lo revelaron la predominancia de la asociación de diatomeas de aguas frías y alta productividad (*T. nitzschioides*, esporas de *Chaetoceros* spp., *L. pacificum*, *Thalassiosira nanolineata* y *Rhizossolenia setigera*) y los valores altos de C_{org}, NT, Ni/Al y Cu/Al. El Periodo Cálido Actual (PCA, ~1860 EC al presente) se caracterizó por una asociación de FB más diversa con la predominancia de la asociación menos tolerante a las bajas concentraciones de OD (*Bolivina seminuda Epistominella* sp.1, *Gyroidina nitidula* y *Suggrunda eckisi*), así como un menor enriquecimiento de Mo, V, Cd, U, y Re, y menor desnitrificación, que en conjunto sugirieron una ZOM menos intensificada en el GT. Esta desintensificación de la ZOM durante el PCA fue asociada a una menor productividad superficial como así lo revelaron la predominancia de la asociación de aguas cálidas y de baja productividad (*N. pelagica*, *Fragillariopsis doliolus*, *Cyclotella litoralis*, *Thalassiosira oestrupii*, *Cymatodiscus*, *planetophorus*, *Nitzschia interruptestriata* y *Rhizossolenia bergonii*), en acuerdo con valores bajos de C_{org}, NT, Ni/Al y Cu/Al. Los cambios de la ZOM en el período estudiado fueron asociados principalmente a la variabilidad de la productividad superficial, la cual respondió a las variaciones de la actividad solar que afectaron la dinámica atmosférica y la posición de la ZCIT y la intensidad de los vientos Tehuanos. Estos resultados destacan la extensión tropical del PCM, la PEH y el PCA en el PTNO y su efecto en la ZOM y en la productividad superficial del GT.

Abstract

The present study aims to understand the bottom-water changes and their relationship with superficial productivity in laminated sediments from the Gulf of Tehuantepec (GoT) during the last millennium. Two sedimentary sequences were used: core MD02-2521 (top 100 cm from ~618 to ~1610 CE) in which diatom assemblages were analyzed; and core Tehua XII E03 (from ~1500 to ~2014 CE) in which benthic foraminifera (BF), diatoms and geochemical proxies (Mo, V, Cd, U, Re, Ni/Al, Cu/Al, C_{org}, TN, and $\delta^{15}N_{sed}$) were analyzed. The GoT is located in the Eastern Tropical North Pacific (ETNP), within one of the world's largest and more intense Oxygen Minimum Zones (OMZ). Seasonally the GoT is influenced by the Intertropical Converge Zone (ITCZ) migration and by strong winds locally called Tehuanos. These winds cause intense upwelling and mixing of nutrient-rich subsurface water, promoting high primary productivity in the GoT. In turn, productivity influences organic matter flux to the seabed and dissolved oxygen (DO) consumption in the bottom water. The diatoms in core MD02-2521 during the Medieval Warm Period (MWP, ~765 to ~1414 CE) were characterized by the warm-water and low-productivity assemblage (*Neodelphineis pelagica* and *Thalassionema nitzschioides*), and the onset of the Little Ice Age (LIA, ~1426 a ~1610 CE) was characterized by the cold and high productivity diatom assemblage (*Chaetoceros* spores, *T. nitzschioides* y *Lioloma pacificum*). In the core Tehua XII E03 the LIA (~1500 to ~1860 CE) was characterized by the dominance of the BF assemblage that withstands the lowest DO concentration (*Epistominella sandiegoensis*, *Takayanagia delicata*, and *Buliminella tenuata*), which suggests a more intensified OMZ than present, consistent with the enrichment of redox-sensitive metals (Mo, V, Cd, U and Re), and enhanced denitrification ($\delta^{15}N$). During this period, the productivity was higher, as revealed by the predominance of the cold-water and high-productivity diatom assemblage (*T. nitzschioides, Chaetoceros* spores, *L. pacificum, Thalassiosira nanolineata*, and *Rhizossolenia setigera*), as

well as high values of C_{org}, TN, Ni/Al, and Cu/Al. The CWP (~1860 CE to present) was characterized by a more diverse and less tolerant to low DO concentration BF assemblage (*Bolivina seminuda Epistominella* sp.1, *Gyroidina nitidula*, and *Suggrunda eckisi*) that suggested a less enhanced OMZ, supported by the lower enrichment in redox-sensitive metals, and $\delta^{15}N_{sed}$. During the CWP, the diatoms were characterized by the predominance of the warm-water and low-productivity assemblage (*N. pelagica, Fragillariopsis doliolus*, *Cyclotella litoralis*, *Thalassiosira oestrupii*, *Cymatodiscus. planetophorus*, *Nitzschia interruptestriata*, and *Rhizossolenia bergonii*) in agreement with low values of C_{org}, TN, Ni/Al, and Cu/Al. The OMZ changes in the period studied were mainly explained by the surface productivity variability, which responded to the solar activity variations affecting the ITCZ position and the Tehuano-winds intensity. These results highlight the tropical extent of MWP, LIA, and CWP in the ETNP and their effects on the OMZ and surface productivity in the GoT.

CAPÍTULO 1:

1. Introducción general

El clima repercute en casi todas las actividades humanas, por lo que comprender las causas y consecuencias de los diversos fenómenos climático-oceanográficos es fundamental. A lo largo del tiempo, el clima varía naturalmente a diversas escalas. Durante los últimos dos milenios, también conocidos como la Era Común (EC), el clima ha mostrado variaciones en escalas estacionales, interanuales, decadales y seculares (Jones y Mann, 2004). Además, durante este periodo han ocurrido importantes cambios en la irradiancia solar, donde destacan ciclos solares importantes (ej. ~11, ~22, ~80 y ~180 a 206 años), así como el máximo solar medieval de ~1100 a ~1250 EC, y los mínimos solares entre ~1290 y ~1830 EC (Cronin, 1999; Bard et al., 2000). Resultado de la variación de la actividad solar durante el último milenio, la Zona de Convergencia Intertropical (ZCIT, la cual determina el patrón precipitación en los trópicos y cuya posición migra estacionalmente siguiendo el cenit del sol) y las celdas de alta presión (que son regiones donde domina el movimiento descendente del aire), que en conjunto determinan la intensidad del gradiente de presión y tienen influencia en la fortaleza de los vientos, también han experimentado variaciones (ej. Barron y Bukry, 2007; Griffiths et al., 2016).

En la EC se reconocen cuatro eventos climáticos alternados entre periodos fríos y cálidos que son: el Periodo Cálido Romano de ~1 a ~400 EC (Neukom et al., 2019)1), el periodo frío de la Edad Oscura de ~400 a ~800 EC (Neukom et al., 2019), el Periodo Cálido Medieval (PCM) de ~950 a ~1250 EC (Mann et al., 2009), y la Pequeña Edad de Hielo (PEH) de ~1350 a ~1850 EC (Crowley et al., 2008; Mann et al., 2009). Asimismo, en los últimos ~150 años (~1850 EC) se reconoce una tendencia de calentamiento a nivel global, que ha sido atribuida a las actividades antropogénicas (IPCC, 2014). A este periodo se le ha nombrado el Periodo Cálido Actual (PCA)

(ej. Salvatteci et al., 2014; Griffiths et al., 2016), pero existe debate sobre cuánto y desde cuando el ser humano ha tenido influencia sobre el clima.

Durante el último siglo, se cuenta con registros instrumentales de diversos parámetros climáticos (ej. temperatura, viento, precipitación) que permiten evaluar cómo ha variado el clima. Sin embargo, debido a la multiplicidad de ciclos que presenta, es necesario estudiar a escalas mayores de tiempo para tener un mejor entendimiento de su comportamiento global. En ese contexto cobran relevancia los estudios paleoclimáticos, que permiten extender el registro climático más allá del registro instrumental. Para ello, se requiere del uso de indicadores (también conocidos como proxies), que previamente hayan sido calibrados con registros instrumentales.

El presente proyecto se desarrolló en el Golfo de Tehuantepec (GT), el cual se encuentra dentro de la zona de oxígeno mínimo (ZOM) del Pacífico Tropical Nororiental (PTNO) (Helly y Levin, 2004). Las condiciones de bajo oxígeno favorecen la preservación de sedimentos laminados (Thunell y Kepple, 2004; Blanchet et al., 2012; García-Gallardo et al., 2021; 2022), con un gran potencial para estudios de reconstrucciones paleoclimáticas, debido a su baja o nula bioturbación. El GT es además una de las regiones de mayor productividad biológica en México debido a la presencia de afloramientos estacionales de agua subsuperficial (Trasviña y Barton, 1997). Asimismo, es una región de interés oceanográfico dado que convergen dos grandes giros subtropicales, los del Pacífico Norte y Sur (Fiedler y Talley, 2006) (Fig. 1), por lo que estudios paleoclimáticos pueden ayudarnos a comprender y conocer los cambios de la circulación oceánica y hacer inferencias sobre la ocurrencia de fenómenos climático-oceanográficos a través del tiempo.

En este estudio, se propone el análisis de la variabilidad de la ZOM del GT durante el último milenio. Los cambios en oxigenación dependen tanto de la ventilación de las masas de

agua como del consumo del oxígeno, que depende principalmente de los cambios en la productividad superficial. Por lo tanto, se plantea analizar la relación que existe entre la ZOM y la productividad superficial. La hipótesis general es que, al aumentar/disminuir la productividad superficial aumenta/disminuye el flujo de materia orgánica transportada al lecho marino, cuyo proceso de oxidación consume oxígeno, y por lo tanto disminuye/aumenta la concentración de oxígeno disuelto (OD) en el agua de fondo, que, a su vez, aumenta/disminuye la intensidad de la ZOM. Para ello, se utilizarán a los FB, así como elementos redox-sensitivos (Mo, V, Cd, U, y Re) y el $\delta^{15}N$ como proxies de oxigenación, y como proxies de productividad se utilizarán a las diatomeas, el Carbono orgánico total (C_{org}), Nitrógeno total (NT), Ni/Al, Cu/Al, y $\delta^{13}C$. Para alcanzar un registro de ~1000 años, en este estudio, se utilizaron dos núcleos de sedimentos laminados: el núcleo MD02-2521 en el cual se analizaron diatomeas en los primeros ~100 cm de sedimento abarcando de ~618 a ~1610 EC; y el núcleo Tehua XII E03 con una longitud de 32.5 cm que abarcó de ~1500 a ~2014 EC en el que se analizaron foraminíferos bentónicos (FB), diatomeas y proxies geoquímicos (Mo, V, Cd, U, Re, Ni/Al, Cu/Al, C_{org}, NT, y $\delta^{15}N_{sed}$).

Los FB son protistas marinos ampliamente distribuidos en el fondo oceánico y sus poblaciones son afectadas principalmente por las concentraciones de oxígeno y flujos de materia orgánica (Bernhard y Sen Gupta, 1999). Por ello, algunas asociaciones de FB son usados como indicadores de la oxigenación del agua de fondo y cambios en la productividad en los registros sedimentarios de ambientes pobres en oxígeno (ej. Sen Gupta y Machain-Castillo, 1993; Bernhard y Sen Gupta, 1999; Murray et al; 2006; Moffitt et al., 2015).

Los elementos redox-sensitivos como el Mo, V, Cd, U y Re, también son utilizados como proxies de oxigenación. Estos metales se enriquecen bajo condiciones reductoras, y aunque presentan umbrales de oxigenación característicos y distintas vías de precipitación y acumulación, tienen en común que se acumulan bajo condiciones de bajo oxígeno. Por lo

anterior, son usados para inferir cambios en la oxigenación de las masas de agua de fondo de los ambientes en donde se depositaron (Tribovillard et al., 2006; Calvert y Pedersen, 2007).

El $\delta^{15}N$ es otro indicador habitual de paleoxigenación de la materia orgánica sedimentaria ya que, en ambientes pobres en oxígeno, la desnitrificación es un proceso dominante en la columna de agua. En estos ambientes de bajo oxígeno, donde además hay un alto flujo de materia orgánica al lecho marino, la desnitrificación es mediada por bacterias que llevan a cabo un fraccionamiento del nitrato consumiendo preferentemente el isotopo ligero ^{14}N lo cual resulta en un depósito residual de nitrato enriquecido en ^{15}N. En ambientes de surgencia donde estas aguas son llevadas a la superficie, y en el cual el nitrato es completamente consumido por el fitoplancton, esta señal isotópica del ^{15}N es transferida a la materia orgánica y es eventualmente depositada en los sedimentos (Robinson et al., 2012). Por lo tanto, el $\delta^{15}N$ es un proxy de desnitrificación ligado a los cambios de oxigenación de la columna de agua (Robinson et al., 2012; Deutsch et al., 2014; Tems et al., 2016).

Las diatomeas son uno de los principales componentes del fitoplancton marino. Su distribución está relacionada a las variaciones de los parámetros fisicoquímicos de las masas de agua, siendo la temperatura y la disponibilidad de nutrientes los más importantes (Crosta-Koc, 2007). En regiones de surgencia, el grupo de las diatomeas es predominante en la columna de agua superficial, y una parte de la producción que escapa de la zona fótica es enterrada y preservada en el fondo oceánico (Treguer et al., 1995). Las diatomeas preservadas en los sedimentos llevan la señal promedio de la productividad en la columna de agua superficial, así como de las condiciones paleoambientales predominantes (Treppke, 1996; Crosta y Koc, 2007). Este grupo han sido exitosamente usado para reconstruir las condiciones ambientales relacionadas a la productividad en diversas regiones, incluyendo el PTNO (ej. Barron et al., 2003; Barron y Bukry, 2007; Barron et al., 2013).

El contenido de C_{org} y NT también han sido usados como indicadores de productividad ya que son los constituyentes principales de la biomasa de fitoplancton. Asimismo, la razón C:N y el isotopo estable de ^{13}C han sido ampliamente utilizados como trazadores del origen de la materia orgánica (Lamb et al., 2006). Se utiliza la relación C:N debido a que el fitoplancton marino presenta una razón C:N menor a 10; mientras que la vegetación terrestre tiene valores de C:N > 12 (Lamb et al., 2006). De igual forma, el fitoplancton marino tiene una señal característica del $\delta^{13}C$ entre ~-22 y ~-18 ‰. Ambas señales son transferidas a los sedimentos marinos a través de la materia orgánica particulada (Lamb et al., 2006).

Otros indicadores de productividad son el Ni y el Cu, micronutrientes esenciales para el fitoplancton (Calver y Pedersen, 2007). No obstante, estos elementos pueden ser afectados por la entrada de terrígenos continentales (Tribovillard et al., 2006; Calver y Pedersen, 2007), por lo que su normalización con algún elemento terrígeno (como el Al o Ti) remueven la señal terrestre. La contaminación por impacto humano (ej. Ruiz-Fernández et al., 2004) y los procesos redox también pueden afectar la señal del Ni y Cu (Tribovillard et al., 2006; Calver y Pedersen, 2007). Sin embargo, cuando estos elementos exhiben una tendencia similar a otros proxies de productividad (ej. diatomeas, C_{org}, sílice biogénico), se considera que están reflejando esta variable.

Se ha sugerido que la variabilidad de la ZOM y la productividad superficial en el Pacífico Nororiental durante el último milenio está influenciada por los eventos climáticos del PCM, la PEH y el PCA (ej. Goni et al., 2006; Barron y Bukry, 2007; Juárez et al., 2014; Deutsch et al., 2014; Tems et al., 2016; Choumiline et al., 2019). Sin embargo, hace falta información sobre la extensión e intensidad de estos eventos climáticos en latitudes más tropicales, lo cual será abordado en el presente estudio. Este trabajo contribuye con la generación de información del

último milenio para la reconstrucción de los cambios en la oxigenación del agua de fondo y la productividad en el GT a través de un enfoque multiproxie.

2. Antecedentes

2.2. Antecedentes en el Pacífico Oriental

Las series y mediciones instrumentales de la concentración de OD en el medio marino reportadas a la fecha sugieren una disminución de la concentración de oxígeno en el océano global (Keeling et al., 2010 y citas allí referenciadas) y la expansión e intensificación de las ZOMs (Stramma et al., 2008; 2010; Helm et al., 2011) en casi todos los océanos (Stramma et al. 2010). Además, esta tendencia se ha agudizado en las regiones tropicales (Stramma et al., 2008), principalmente en la capa de agua intermedia (~200 y 700 m) (Stramma et al., 2010). Esta tendencia puede deberse a que la Circulación Meridional de Retorno en la cuenca del Pacífico se ha ralentizado desde 1970s por el decremento de los vientos Alisios ecuatoriales del Este (McPhaden y Zhang, 2002). Dado que no existen series de tiempo instrumentales largas que permitan evidenciar los cambios de la ZOM, es necesario analizar periodos de tiempo más largos, especialmente antes del siglo XX. En ese sentido los estudios paleoceanográficos pueden ayudar a entender y comprender la variabilidad de la ZOM en el Pacífico Tropical Oriental.

En el Golfo de California, las fluctuaciones de la ZOM de los últimos ~1200 años, analizados a través del $\delta^{15}N_{sed}$, han sido asociados con la Oscilación Decadal del Pacífico, los ciclos solares de ~80 (Gleissberg) y ~206 año (Suess), así como a los cambios latitudinales de la ZCIT (Tems et al., 2016). Mientras que en los último ~150 años, la ZOM ha mostrado una tendencia general de desintensificación, como lo sugiere la disminución del $\delta^{15}N_{sed}$ durante la mayor parte del siglo XX, asociada a la variación de los vientos Alisios (Deutsch et al., 2014).

En el Pacífico Suroriental, la ZOM de Perú ha mostrado cambios importantes en los últimos 2000 años (Sifeddine et al., 2008; Agnihotri et al., 2008; Gutiérrez et al., 2009; Salvatteci et al., 2014; Briceno-Zuluaga et al., 2016). Durante la PEH, en la que predominaron condiciones de mayor humedad (posición de la ZCIT más al sur cercana al Ecuador) y baja productividad, se encontró una ZOM más débil (Sifeddine et al., 2008; Gutiérrez et al., 2009, Salvatteci et al., 2014; Briceno-Zuluaga et al., 2016). Sin embargo, en la mayor parte del PCM y el PCA, donde predominaron condiciones secas y de mayor productividad, se vio una ZOM intensificada (Salvatteci et al., 2014; Briceno-Zuluaga et al., 2016).

Estas observaciones de la ZOM durante la PEH son opuestas a las encontradas en el hemisferio norte (ej. Ricaurte-Villota et al., 2013; Deutsch et al. 2014; Tems et al., 2016; Choumiline 2019; Ontiveros-Cuadras et al., 2019), pero pueden ser explicadas por las migraciones latitudinales de la ZCIT. Cuando en el hemisferio norte la ZCIT está más al sur, se registran condiciones secas en el centro de México (Cuna et al., 2014; Rodríguez-Ramírez et al., 2015) y en la cuenca de Cariaco (Haug et al., 2001; 2003). Pero, en la región de Perú, dado que la ZCIT se encuentra más cercana al Ecuador, transporta mayor humedad a esta región, debilitando los patrones de viento, lo que a su vez ocasiona una disminución en las surgencias y la productividad y, consecuentemente, un menor consumo de oxígeno dentro de la ZOM, lo que se refleja como un debilitamiento de la misma.

Las variaciones de la ZOM durante el PCM en el PTNO han sido menos estudiadas (ej. Ricaurte-Villota et al., 2013), y se ha observado que las condiciones atmosféricas durante este periodo también son opuestas entre el hemisferio norte y sur. Durante el PCM se infieren condiciones más húmedas en el centro de México debido a una migración más al norte de la ZCIT (Barron y Bukry, 2007; Rodríguez-Ramírez et al., 2015); mientras que en la región de Perú se infiere que predominaron condiciones más secas, patrones de vientos más intensos, que

conllevaron a surgencias más intensas, una mayor productividad y consecuentemente una ZOM más intensificada (Salvatteci et al., 2014; Briceno-Zuluaga et al., 2016).

En estudios sobre productividad, en el Golfo de California se ha encontrado la influencia de los ciclos solares de ~11, ~22 y ~50 años en la frecuencia del número anual de conglomerados de *Thalassiothrix longissima*, una diatomea indicadora de alta productividad (Pike and Kemp, 1997). Variaciones de mayor escala ~100 y ~200 años han sido encontrados en las asociaciones de diatomeas y silicoflagelados del Golfo de California vinculados con el forzamiento solar (Barron et al., 2003; Barron y Bukry, 2007). No existen estudios de esta resolución temporal en el GT, por lo que se desconoce si las señales de los ciclos solares y los eventos de la PEH y el PCM quedaron registrados a estas latitudes. Sin embargo, existen varios trabajos realizados en el continente (en el centro y sur del país) donde se han documento la influencia de la PEH y el PCM (ej. Lozano-García et al., 2007; Cuna et al., 2014; Rodríguez-Ramírez et al., 2015), por lo que se espera que en el registro sedimentario del GT se encuentren evidencias de estos eventos.

2.2. Antecedentes en el Golfo de Tehuantepec

Las asociaciones de FB en el GT también han sido relacionadas con la variación de la concentración de OD en el agua de fondo y la profundidad. Se reconoce una asociación de plataforma media (100-150 m) formada por *Hanzawaia nitidula* y *Cassidulina* sp *A* en concentraciones de OD entre 0.5 y 0.3 mL/L y una asociación de plataforma externa (150-200 m) caracterizada por *Epistominella bradyana*, *Bolivina seminuda*, y *Bolivina plicata* en concentraciones < 0.3 mL/L de OD (Pérez-Cruz y Machain-Castillo, 1990). En fauna viva, se han identificado tres asociaciones: la asociación caracterizada por *B. seminuda* distribuida a 70-750 m de profundidad y OD < 1.0 mL/L; la asociación dominada por *Hanzawaia concentrica* localizada en la plataforma interna con valores de OD > 1.0 mL/L; y la asociación dominada por

E. bradyana distribuida de 860 a 1200 m en concentraciones de 0.1 a 0.08 mL/L de OD (Machain-Castillo et al., 2006).

Las asociaciones de FB también han revelado que la concentración de OD entre ~1925 y ~1942 EC fue < 0.5 mL/L, mientras que de ~1943 a ~1981 EC el OD fue relativamente > 0.5 mL/L, pero menor a 0.3 mL/L (Almaraz-Ruiz, 2017). En estudio más largos, las asociaciones de FB sugieren que el OD del agua de fondo del GT ha permanecido en concentraciones < 1.0 mL/L en los últimos ~4791 (Medina-Sánchez, 2010) y ≤ 0.3 mL/L pero mayores a 0.1mL/L en los últimos 55 ka (Cuesta-Castillo, 2011). Además, en un registro de los últimos ~6 mil años, los FB revelan una disminución en el OD en los últimos ~2500 años en respuesta a la transición de condiciones frías a cálidas relacionadas con la migración al sur de la ZCIT, asimismo, se observaron ciclicidades de ~1470 años, probablemente relacionadas con ciclos Bond sugiriendo una conexión climática entre los océanos Atlántico y Pacífico (García-Gallardo et al. 2021).

Con respecto a la productividad, los estudios en el GT han sido enfocados principalmente a identificar la variación de la productividad estacional. Se ha encontrado que en la época de surgencias (noviembre) las diatomeas suelen predominar en la región occidental del golfo, mientras que en el resto del GT se presenta una mezcla de varios grupos, a diferencia de cuando el periodo de surgencias se establece y las diatomeas dominan la región (Meave del Castillo y Hernández-Becerril, 1998). En un estudio con trampas de sedimento (febrero-julio 2006), a resolución semanal, ha permitido identificar las asociaciones de diatomeas de la época de surgencias y no surgencias en el GT (Almaraz-Ruiz, 2013).

En los últimos ~100 años, las asociaciones de diatomeas reflejaron una disminución de la productividad en el GT que comienza ~1940 EC, así como una tendencia de calentamiento que se evidencia posterior a ~1980 EC (Almaraz-Ruiz, 2017). En un estudio de mayor alcance temporal que se extiende hasta 23,400 cal AP (años calendario antes del presente), las

asociaciones de diatomeas indicaron cambios en la productividad asociados a el Último Máximo Glacial, la deglaciación y el Holoceno (Tobón-Velásquez, 2015).

3. Justificación e importancia

El presente estudio contribuye con la generación de nuevo conocimiento para una mejor comprensión de la variación de la ZOM en el GT, y a su vez comprender la de otras zonas. La variación de las ZOMs tiene implicaciones en la distribución y adaptación de los organismos marinos, gestión de recursos marinos, así como influencia en la biogeoquímica marina y el secuestro/liberación de gases invernadero como el CO_2 y CH_4.

Este estudio de alta resolución ha permitido reconocer variaciones en la concentración del OD del agua de fondo y de la productividad que en estudios de menor resolución han sido imperceptibles, pero no por ello menos importantes, ya que entre más ciclos identifiquemos, ampliaremos más nuestro conocimiento acerca de cuáles son los procesos que intervienen en su variación.

Además, en este estudio se relaciona las variaciones de la ZOM con la productividad superficial (a través de las poblaciones de diatomeas), con el fin de identificar su influencia sobre la variación del OD del agua de fondo del GT y, por lo tanto, inferir la relación entre las señales climático-oceánicas de la superficie del océano con las variaciones del agua de fondo.

Puesto que los trabajos previos de la ZOM se han realizada en el Pacífico Nororiental y Suroriental, un estudio de esta naturaleza en la región del GT revela si las variaciones encontradas en la región norte y sur se extienden a latitudes tropicales. Por otra parte, el estudio de los últimos 1000 años permite evidenciar como era la variación de la ZOM y la productividad antes de la tendencia de calentamiento del siglo XX.

4. Preguntas de investigación e hipótesis

En el presente trabajo se plantean cuatro preguntas principales que son:

1) ¿Cómo ha variado la productividad en los últimos 1000 años en el GT?

2) ¿Cómo ha variado la ZOM en el mismo lapso?

3) ¿Cómo se relaciona la variación de la ZOM con la productividad en esta región?

4) ¿Qué influencia tiene las señales climáticas de escala decadal a secular, los ciclos solares, los eventos climáticos del PCM, PEH y la reciente tendencia de calentamiento del PCA sobre la variación de la ZOM y la productividad en el GT?

Las hipótesis planteadas fueron:

Se infiere que los cambios en la productividad serán reflejados en el contenido de OD de la ZOM, debido a que, la cantidad de materia orgánica transportada es el principal factor que consume el OD del agua de fondo. Dichas variaciones de oxígeno se evidenciarán con los cambios en las asociaciones de FB, así como en los elementos redox-sensitivos (Mo, V, Cd, Ni, U y Re) y el $\delta^{15}N_{sed}$. Por lo tanto, se espera que las variaciones de la ZOM estén influenciadas por las señales climáticas como ciclos solares, los eventos climáticos del PCM, la PEH y la reciente tendencia de calentamiento del PCA.

Se espera que la ZOM durante los periodos cálidos (PCM y PCA) será menos intensa debido a una menor productividad superficial, ya que en un escenario de condiciones cálidas se intensifica la estratificación de la columna de agua, la termoclina es más profunda y la disponibilidad de nutrientes está más restringida, lo que conlleva a una menor productividad,

menor transporte de materia orgánica al fondo oceánico y disminuye el consumo de OD. Por el contrario, se espera que condiciones opuestas ocurran durante el periodo frío de la PEH.

5. Objetivos

Objetivo general:

Establecer la variabilidad de la ZOM y la productividad a través de indicadores biológicos (diatomeas y FB) y geoquímicos (C_{org}, NT, Mo, V, Cd, U, Re, Ni/Al, Cu/Al, $\delta^{13}C$, y $\delta^{15}N_{sed}$) en los sedimentos laminados del GT durante el último milenio.

Objetivos específicos:

- Determinar los cambios en la productividad a partir de las asociaciones de diatomeas y del contenido de C_{org}, NT, Ni/Al, y Cu/Al en el núcleo Tehua XII E03 que abarca del periodo ~1500 al ~2014 EC (Capítulo 2).

- Identificar los cambios en la ZOM a través de las asociaciones de FB, elementos redox-sensitivos (Mo, V, Cd, U y Re) y $\delta^{15}N_{sed}$ en el núcleo Tehua XII E03 que abarca del periodo ~1500 al 2014 EC (Capítulo 3).

- Determinar los cambios en la productividad a partir de las asociaciones de diatomeas en el núcleo MD02-2521 que abarca del periodo ~618 a ~1610 EC (Capítulo 4).

6. Área de estudio

El GT se ubica al sur del Pacífico Mexicano, localizado al sur de los estado de Oaxaca y Chiapas (14.30° a 16.12° N; 92.17° y 96.00° O; Fig. 1) (Lara-Lara et al, 2008). Presenta una plataforma continental asimétrica que se extiende hasta los 250 m de profundidad (Lugo, 1986). La plataforma presenta una amplitud de 4 a 6 km en su lado occidental y se ensancha hacia el lado oriental alcanzando más de 100 km (Carranza-Edwards et al., 1998). El talud superior se encuentra a profundidades de ~250 a ~400 m, formando una planicie considerable en la region

mas interna del golfo. Posteriomente se encuentra el talud continental a profundidades de 2500 a 3000 m y se mantiene constante en una amplitud de 25 a 50 km (Lugo, 1986).

Anualmente se reconocen dos escenarios climáticos bien definidos en el GT. Durante el invierno y la primavera, la ZCIT y los sistemas de alta presión en el PTNO están en su posición más sureña (Lavín et al., 1992; Amador et al., 2006). Estas condiciones causan que flujos de aire provenientes del Golfo de México sean canalizados a través del paso de montaña del Istmo de Tehuantepec, que en el GT son conocidos localmente como vientos Tehuanos (Trasviña y Barton, 1997). Los eventos de vientos Tehuanos suelen tener una duración de 3-5 días en intervalos de 10 -15 días, ráfagas de vientos intensos > 20 m/s (Romero-Centeno et al., 2007), y llegan perpendiculares a la costa del GT. Estos eventos causan procesos de mezcla y surgencias sobre el eje del viento que rompen la estratificación y promueven el ascenso de aguas frías y ricas en nutrientes desde la subsuperficie a la superficie del océano (Lavín et al., 1992), fertilizando la zona fótica y promoviendo una alta productividad biológica (Meave del Castillo y Hernández-Becerril, 1998). Durante el verano y otoño, los sistemas de alta presión se debilitan y los vientos Tehuanos son relativamente esporádicos y débiles (Romero-Centeno et al., 2007). Además, durante esta época del año la ZCIT migra a su posición más norteña llevando más humedad a esta región, lo que ocasiona lluvias intensas en el sur de México (Amador et al., 2006).

La circulación oceánica superficial también exhibe una variación de acuerdo con el posicionamiento de la ZCIT (Fiedler y Talley, 2006). Durante el invierno y principios de la primavera, remanentes de aguas frías subsuperficiales de la Corriente de California pueden llegar a extenderse hacia los trópicos (hasta los 13°N), lo cual restringe la influencia de las aguas cálidas de la Corriente Costera de Costa Rica (CCCR) sobre el GT (Kessler, 2006) (Fig. 1). Durante el verano y otoño, la CCCR es más intensa, logra atravesar el GT alcanzando más allá de los 15°N

y posteriormente la CCCR se desvía al oeste para unirse a la Corriente Norecuatorial (Kessler, 2006) (Fig. 1).

En el sitio de estudio se identifican cuatro masas de agua: Agua Ecuatorial Superficial, Agua Subtropical Subsuperficial, Agua Intermedia del Pacífico Norte, y Agua Profunda del Pacífico (Fiedler y Talley, 2006; Machain-Castillo et al., 2008). Durante las dos condiciones climatico-oceanográficas descritas, las masas de agua exhiben diferente extensión vertical. En la época de Tehuanos, las masas de agua muestran una inclinación de oeste a este, con mayor profundidad del lado occidental del golfo (Machain-Castillo et al., 2008).

La ZOM en el GT se extiende de los ~100 a ~800 m de profundidad (Cline y Richards, 1972). El límite superior de la ZOM en el GT exhibe una variación estacional: durante el invierno y la primavera se encuentra más cercana a la superficie a ~25 m de profundidad; en contraste, en la época de verano esta se hunde hasta ~80 m (García-Gallardo et al., 2021).

La concentración de nutrientes en el GT también exhibe una variación estacional, según Machain-Castillo et al., (2008) en la época de Tehuanos, en el eje del la concentración de nitratos es > 5 µM, y en gran parte del golfo los nitratos son ligeramente superiores a 1 µM, mientras que en la época de verano, la concentración de nitratos en casi todo el golfo son menores a 1 µM.
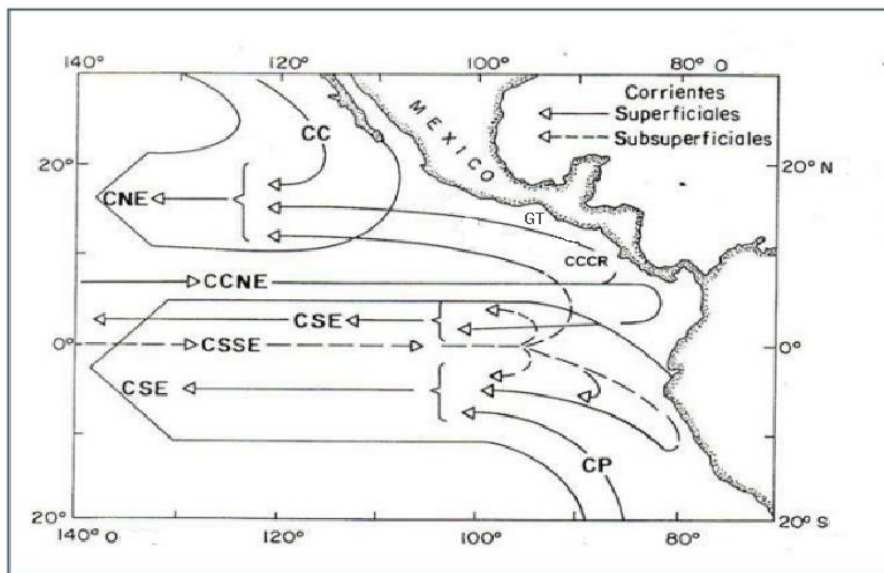
Figura 1. Patrón de circulación de las corrientes oceánicas en el PTNO. Tomada de Molina-Cruz y Martínez-López (1994).

7. Referencias

Agnihotri, R., M. A. Altabet, T. D. Herbert, and J. E. Tierney. 2008, Subdecadally resolved paleoceanography of the Peru margin during the last two millennia, Geochem. Geophys. Geosyst., 9, Q05013, doi:10.1029/2007GC001744.

Almaraz-Ruiz, L., 2017. Variabilidad de las surgencias en el golfo de Tehuantepec durante el último siglo a través del registro sedimentario de diatomeas y foraminíferos bentónicos. Tesis Maest. Universidad Nacional Autónoma de México.

Amador, J.A., Alfaro, E.J., Lizano, O.G., Magaña, V.O., 2006. Atmospheric forcing of the eastern tropical Pacific: A review. Prog. Oceanogr. 69, 101–142. https://doi.org/https://doi.org/10.1016/j.pocean.2006.03.007

Bard, E., Raisbeck, G., Yiou, F., Jouzel, J., 2000. Solar irradiance during the last 1200 years based on cosmogenic nuclides. Tellus, Ser. B Chem. Phys. Meteorol. 52, 985–992. https://doi.org/10.1034/j.1600-0889.2000.d01-7.x

Barron, J.A., Bukry, D., Bischoff, J.L., 2003. A 2000-yr-long record of climate from the Gulf of California, in: West, G.J. and Blomquist, N.L. (Ed.), Proceedings of t h e Nineteenth Pacific Climate Workshop. Asilomar, Pacific Grove, CA, pp. 1–15.

Barron, J.A., Bukry, D., 2007. Solar forcing of Gulf of California climate during the past 2000 yr suggested by diatoms and silicoflagellates. Mar. Micropaleontol. 62, 115–139. https://doi.org/10.1016/j.marmicro.2006.08.003

Barron, J.A., Bukry, D., Bischoff, J.L., 2003. A 2000-yr-long record of climate from the Gulf of California, in: West, G.J. and Blomquist, N.L. (Ed.), Proceedings of t h e Nineteenth Pacific Climate Workshop. Asilomar, Pacific Grove, CA, pp. 1–15.

Bernhard, M. J. y B. K. Sen Gupta. 1999. Foraminifera: Foraminífera of oxygen-depleted enviroments. In: Sen Gupta, B. K. (Ed.), Modern Foraminifera. Kluver Academic Publisher. Dordrecht. 37-55 p.

Briceño Zuluaga, F., Sifeddine, A., Caquineau, S., Cardich, J., Salvatteci, R., Gutierrez, D., et al. (2016). Terrigenous material supply to the Peruvian central continental shelf (Pisco 14_ S) during the last 1000 yr: paleoclimatic implications. Clim. Past 12, 787–798. doi: 10.5194/cpd-12-787-2016

Calvert, S.E., Pedersen, T.F., 2007. Elemental proxies for palaeoclimatic and palaeoceanographic variability in marine sediments: interpretation and application. In: Hillaire-Marcel, C., De Vernal, A. (Eds.), Developments in Marine Geology 1. Elsevier B.V, Amsterdam, pp. 576–644.

Carranza-Edwards. A., Morales de la Garza y L. Rosales. 1998. Tectónica, sedimentología y geoquímica. En Tapia, G. M. (ed). *El Golfo de Tehuantepec: el ecosistema y sus recursos.* Universidad Autónoma Metropolitana-Iztapalapa, México. Cap.1: 1-12.

Cronin, T. M. 1999. Paleoclimates: understanding Climate Change Past and Present. New York Columbia University Press. 448 p.

Choumiline, K., Pérez-Cruz, L., Gray, A.B., Bates, S.M., Lyons, T.W., 2019. Scenarios of Deoxygenation of the Eastern Tropical North Pacific During the Past Millennium as a

Window Into the Future of Oxygen Minimum Zones. Front. Earth Sci. 7. https://doi.org/10.3389/feart.2019.00237

Cline, J. D. y F. A. Richards. 1972. Oxygen deficit conditions and nitrate redactor in the Eastern Tropical North Pacific. *Ocean. Limnol. Oceanogr.* 17 (6): 885-900.

Crosta, X., Koc, N., 2007. Diatoms: From Micropaleontology to Isotope Geochemistry. Dev. Mar. Geol. 1, 327–369. https://doi.org/10.1016/S1572-5480(07)01013-5

Crowley, T.J., Zielinski, G., Vinther, B., et al. 2008. Volcanism and the little ice age. *PAGES News* 16(2): 22–23

Cuesta-Castillo, L. B. 2011. Reconstrucción Paleoceanográfica del Golfo de Tehuantepec durante los últimos 55 ka A. P., a través de los Foraminíferos bentónicos, Carbono orgánico y Carbonato de calcio. Tesis de Maestría, UNAM, México. 65 p.

Cuna, E., Zawisza, E., Caballero, M., Ruiz-Fernández, A.C., Lozano-García, S., Alcocer, J., 2014. Environmental impacts of Little Ice Age cooling in central Mexico recorded in the sediments of a tropical alpine lake. J. Paleolimnol.51,1–14. https://doi.org/10.1007/s10933-013-9748-0

Deutsch, C., Berelson, W., Thunell, R., Weber, T., Tems, C., McManus, J., Crusius, J., Ito, T., Baumgartner, T., Ferreira, V., Mey, J., van Geen, A., 2014. Centennial changes in North Pacific anoxia linked to tropical trade winds. Science 345, 665–668.

Fiedler, P.C., Talley, L.D., 2006. Hydrography of the eastern tropical Pacific: A review. Prog. Oceanogr. 69, 143–180. https://doi.org/10.1016/j.pocean.2006.03.008

García-Gallardo, Á., Almaraz-Ruiz, L., & Machain-Castillo, M. L. (2022). Paleoceanography of the Gulf of Tehuantepec during the Medieval Warm Period. *Marine Micropaleontology*, *170*(August 2021). https://doi.org/10.1016/j.marmicro.2021.102081

García-Gallardo, Á., Machain-Castillo, M.L., Almaraz-Ruiz, L., 2021. Paleoceanographic evolution of the Gulf of Tehuantepec (Mexican Pacific) during the last ~6 millennia. Holocene 31, 529–544. https://doi.org/10.1177/0959683620981724

Griffiths, M.L., Kimbrough, A.K., Gagan, M.K., Drysdale, R.N., Cole, J.E., Johnson, K.R., Zhao, J.X., Cook, B.I., Hellstrom, J.C., Hantoro, W.S., 2016. Western Pacific hydroclimate linked to global climate variability over the past two millennia. Nat. Commun. 7, 1–9. https://doi.org/10.1038/ncomms11719

Gutiérrez, D., Sifeddine, A., Field, D.B., Ortlieb, L., Vargas, G., Chávez, F.P., Velazco, F., Ferreira, V., Tapia, P., Salvatteci, R., Boucher, H., Morales, M.C., Valdés, J., Reyss, J.L., Campusano, A., Boussafir, M., Mandeng-Yogo, M., García, M., Baumgartner, T., 2009. Rapid reorganization in ocean biogeochemistry off Peru towards the end of the Little Ice Age. Biogeosciences 6, 835–848. https://doi.org/10.5194/bg-6-835-2009

Haug GH, Hughen KA, Sigman DM et al. 2001. Southward migration of the Intertropical Convergence Zone through the Holocene. *Science* 293(5533): 1304–1308.

Haug, Gerald & Günther, Detlef & Peterson, Larry & Sigman, Daniel & Hughen, Konrad & Aeschlimann, Beat. 2003. Climate and the Collapse of Maya Civilization. Science (New York, N.Y.). 299. 1731-5. 10.1126/science.1080444.

Helly, John & Levin, Lisa. (2004). Global distribution of naturally occurring marine hypoxia on continental margins. Deep Sea Research Part I: Oceanographic Research Papers. 51. 1159-1168. 10.1016/j.dsr.2004.03.009.

Helm, K. P., Bindoff, N. L., and Church, J. A. 2011, Observed decreases in oxygen content of the global ocean, *Geophys. Res. Lett.*, 38, L23602, doi:10.1029/2011GL049513.

IPCC, 2014. Climate Change 2014: Synthesis Report. Contribution of Working groups I, II and III to the Fifth Assessment Report of the Intergovernmental Panel on Climate Change. Geneva, Switzerland.

Jones, P. & Mann, Michael. (2004). Climate over Past Millennia. Reviews of Geophysics. 42. RG2002. 10.1029/2003RG000143.

Keeling, R. E., Körtzinger, A. y N. Gruber. 2010. Ocean Deoxygenation in Warming World. Annual Review Marine Science. 2:199-229.

Kessler, W. S. 2006. The circulation of the eastern tropical Pacific: A review. *Progr. Oceanogr.* 69: 181-217. doi:10.1016/j.pocean.2006.03.009.

Lamb, A.L., Wilson, G.P., y M, J. Leng. 2006. A review of coastal palaeoclimate and relative sea-level reconstructions using δ13C and C/N ratios in organic material. *Earth-Science Reviews* 75(1–4): 29–57.

Lara-Lara, J. R., Arenas, F. V., Bazán, G. C., Díaz, C. V., Escobar, B. E., García, A. M., Gaxiola, C., L. A. Tapia, G. M. y J. E. Valdez-Holguín. 2008. Los ecosistemas marinos. En: Capital natural de México, vol. I: Conocimiento actual de la biodiversidad. CONABIO, México. 135-159 p.

Lavín, M.F., Fiedler, P.C., Amador, J.A., Ballance, L.T., Färber-Lorda, J., Mestas-Nuñez, A.M., 2006. A review of eastern tropical Pacific oceanography: Summary. Prog. Oceanogr. 69, 391–398. https://doi.org/10.1016/j.pocean.2006.03.005

Lozano-García, M.D.S., Caballero, M., Ortega, B., Rodríguez, A., Sosa, S., 2007. Tracing the effects of the Little Ice Age in the tropical lowlands of eastern Mesoamerica. Proc. Natl. Acad. Sci. U. S. A. 104, 16200–16203. https://doi.org/10.1073/pnas.0707896104

Lugo, H. J. 1986. Morfoestructuras del fondo oceánico mexicano. *Boletín del Instituto de Geografía*, 5, UNAM, México. 9-39

Machain-Castillo, M. L., Monreal-Gómez, M. A., Arellano-Torres, E., Merino-Ibarra, M. and González-Chávez, G. 2008. Recent planktonic foraminiferal distribution patterns and their relation to hydrographic conditions of the Gulf of Tehuantepec, Mexican Pacific. *Marine Micropaleontology*. 66: 103-119.

Machain-Castillo, M. L., Diego-Casimira, G., Ruiz-Fernández, A. C. y Cuesta-Castillo, L. B. 2006. Living (rose bengal stained) benthic foraminifera from the oxygen minimum zone in the Gulf of Tehuantepec, Mexican Pacific. European Geosciences Union General Assembly. Viena, Austria, 2-7 abril.

Mann, M.E., Zhang, Z., Rutherford, S., Bradley, R.S., Hughes, M.K., Shindell, D., Ammann, C., Faluvegi, G., Ni, F., 2009. Global Signatures and Dynamical Origins of the Little Ice Age and Medieval Climate Anomaly. Science 326, 1256–1260.

McPhaden, M. J. y D. Zhang. 2002. Slowdown of the meridional overturning circulation in the upper Pacific Ocean. 415: 603-607.

Meave del Castillo, M.A., Hernández-Becerril, D.U., 1998. "Fitoplancton," in: M. Tapia–García. (Ed.), El Golfo de Tehuantepec: El Ecosistema y Sus Recursos. Universidad Autónoma Metropolitana (Unidad Iztapalapa), México, D. F., pp. 59–74.

Medina-Sánchez, A. N. 2010. Diferencias entre faunas glaciares y recientes de foraminíferos bentónicos y su relación con Zonas de Oxígeno Mínimo en el Golfo de Tehuantepec, México. Tesis de Licenciatura, Universidad Nacional Autónoma de México. D. F. México.

Moffitt SE, Hill TM, Roopnarine PD et al. 2015. Response of seafloor ecosystems to abrupt global climate change. *Proceedings of the National Academy of Sciences* 112: 4684–4689.

Molina-Cruz, A. y M. Martínez-López. 1994. Oceanography of the Gulf of Tehuantepec, Mexico, indicated by Radiolarian remains. Palaeogeography, Palaeoclimatology, Palaeecology. 110 (3-4), 179-195.

Murray JW (2006) *Ecology and applications of Benthic Foraminifera*. Cambridge: Cambridge University Press.

Neukom, R., Steiger, N., Gómez-Navarro, J.J. *et al.* No evidence for globally coherent warm and cold periods over the preindustrial Common Era. *Nature* **571**, 550–554 (2019). https://doi.org/10.1038/s41586-019-1401-2

Perez-Cruz, L L. y M. L. Machain-Castillo. 1990. Benthic foraminifera of the oxygen minimum zone, continental shelf on the gulf of Tehuantepec, Mexico. Journal of Foraminiferal Research. 20(4): 312-325.

Pike, J., Kemp, A.E.S., 1997. Early Holocene decadal-scale ocean variability recorded in Gulf of California laminated sediments. Paleoceanography 12 (2), 227–238.

Robinson, R., Kienast, M., Alburquerque, A. L. Altabet, M., Contreras, S., de Pol Holz, R., Dubois, N. Francois, R. 2012. A review of nitrogen isotopic alteration in marine sediments. *Paleoceanography.*27: PA4203.

Rodríguez-Ramírez A, Caballero M, Roy P et al. (2015) Climatic variability and human impact during the last 2000 years in western Mesoamerica: Evidence of late Classic (AD 600-900) and Little Ice Age drought events. *Climate of the Past* 11(9): 1239–1248.

Romero-Centeno, R., Zavala-Hidalgo, J., Raga, G.B., 2007. Midsummer gap winds and low-level circulation over the eastern tropical Pacific. J. Clim. 20, 3768–3784. https://doi.org/10.1175/JCLI4220.1

Ruiz-Fernández, A.C., Páez-Osuna, F., Machain-Castillo, M.L. et al. 2004. 210Pb geochronology and trace metal fluxes (Cd, Cu and Pb) in the Gulf of Tehuantepec, South Pacific of Mexico. *Journal of Environmental Radioactivity*, *76*(1–2): 161–175.

Salvatteci, R., Gutiérrez, D., Field, D., Sifeddine, A., Ortlieb, L., Bouloubassi, I., Boussafir, M., Boucher, H., Cetin, F., 2014. The response of the Peruvian Upwelling Ecosystem to centennial-scale global change during the last two millennia. Clim. Past 10, 715–731. https://doi.org/10.5194/cp-10-715-2014

Sen Gupta, B. K. y M. L. Machain-Castillo. 1993. Benthic foraminifera in oxygen poor habitats. Marine Micropaleontology. 20:183-201.

Sifeddine, A., Gutiérrez, D., Ortlieb, L., Boucher, H., Velazco, F., Field, D., Vargas, G., Boussafir, M., Salvatteci, R., Ferreira, V., García, M., Valdés, J., Caquineau, S., Mandeng Yogo, M., Cetin, F., Solis, J., Soler, P., Baumgartner, T., 2008. Laminated sediments from the central Peruvian continental slope: A 500 year record of upwelling system productivity, terrestrial runoff and redox conditions. Prog. Oceanogr. 79, 190–197. https://doi.org/10.1016/j.pocean.2008.10.024

Stramma, L., Johnson, G. C., Sprintall, J. y V. Mohrholz. 2008. Expanding oxygen-minimum zones in the tropical oceans. Science. 320: 655-658.

Stramma, L., Schmidtko, S., Levin, L. A. y G. C. Johnson. 2010. Ocean oxygen minima expansions and their biological impacts. Deep-Sea Research Part-I Oceanographic Research Papers, 57: 587-595.

Tems, C.E., Berelson, W.M., Thunell, R., Tappa, E., Xu, X., Khider, D., Lund, S., Gonzalez-Yajimovich, O., Hamann, Y., 2016. Decadal to centennial fluctuations in the intensity of the eastern tropical North Pacific oxygen minimum zone during the last 1200years. Paleoceanography 31 (8), 1138–1151. https://doi.org/10.1002/ 2015PA002904.

Tobón-Velázquez, N. I. 2015. Reconstrucción paleoclimática del golfo de Tehuantepec determinado por el registro sedimentario de diatomeas durante el Pleistoceno tardío-Holoceno. Tesis de Licenciatura. Facultad de ciencias, UNAM. 71 p.

Trasviña, A. y E. D. Barton. 1997. Los "Nortes" del Golfo de Tehuantepec: La circulación costera inducida por el viento. M. F. Lavín. Contribuciones a la Oceanografía Física en México. Monografía No. 3. Unión Geofísica Mexicana. 25-46 p.

Treguer, P., Nelson, D. M., Van Bennekom, A. J., DeMaster, D. J., Leynaert, A. y B. Queguiner. 1995. The balance of silica in the world ocean: a reestimate. Science. 268: 375-379.

Treppke, F.U., Lange, C. and Wefer, G., 1996. Vertical fluxes of diatoms and silicoflagellates in the eastern equatorial Atlantic, and their contribution to the sedimentary record. Mar. Micropaleontol. 28, 73–96.

Tribovillard N, Algeo TJ, Lyons T et al. (2006) Trace metals as paleoredox and paleoproductivity proxies: An update. Chemical Geology 232: 12–32.

CAPÍTULO 2: Diatom-based paleoproductivity and climate change record of the Gulf of Tehuantepec (Eastern Tropical Pacific) during the last ~500 years.

Laura Almaraz-Ruiz[1], laura.almaraz.ruiz@gmail.com

María Luisa Machain-Castillo[2], machain@cmarl.unam.mx

Abdelfettah Sifeddine[3-4], abdel.sifeddine@ird.fr

Ana Carolina Ruiz-Fernández[5], caro@ola.icmyl.unam.mx

Joan-Albert Sanchez-Cabeza[5], jasanchez@cmarl.unam.mx

Alejandro Rodríguez-Ramírez[2], alerdz@unam.mx

Perla Guadalupe López-Mendoza[1], pergualome@gmail.com

Mercedes Mendez-Millan[3], mercedes.mendez@ird.fr

Sandrine Caquineau[3], sandrine.caquineau@ird.fr

[1]Posgrado en Ciencias del Mar y Limnología, Universidad Nacional Autónoma de México; Av. Universidad 3000, Ciudad Universitaria Coyoacán, C.P. 04510, Ciudad de México, México.

[2]Unidad Académica de Procesos Oceánicos y Costeros, Instituto de Ciencias del Mar y Limnología, Universidad Nacional Autónoma de México, Circuito Exterior s/n, Ciudad Universitaria, 04510, México.

[3]IRD, CNRS, SU, MNHN, IPSL, LOCEAN: Laboratoire d'Océanographie et du Climat: Expérimentations et Approches Numériques, 93143 Bondy, France.

[4]ERC2- Université Quisqueya. Port au Prince-Haïti.

[5]Unidad Académica Mazatlán, Instituto de Ciencias del Mar y Limnología, Universidad Nacional Autónoma de México, Calz. Montes Camarena s/n, Col. Playa Sur, 82040 Mazatlán, Sinaloa, México.

Corresponding author. E-mail address: machain@cmarl.unam.mx (M.L. Machain-Castillo), +5215556225691

ABSTRACT

Changes in marine productivity of the last five centuries in the Gulf of Tehuantepec were investigated using a high-resolution record of diatoms, organic carbon (C_{org}), total nitrogen (TN), Ni/Al, and Cu/Al. The laminated sediments were dated by using ^{210}Pb and ^{14}C, with a bayesian age model providing a new $\Delta R = 247 \pm 30$ yr for the bulk sediment. The Little Ice Age (LIA) (~1500 to ~1858 CE) was characterized by the predominance of cold-water and high productivityhigh-productivity diatoms (*Chaetoceros* spores*, Thalassionema nitzschioides*, *Lioloma pacificum, Thalassiosira nanolineata*, and *Rhizossolenia setigera*) and high values of geochemical productivity proxies. A transition period (~1860 to ~1919 CE) towards warmer conditions related to the end of the LIA and the beginning of the Current Warm Period (CWP), was indicated by the appearance of warm-water diatoms (*Neodelphineis pelagica*, *Thalassiosira tenera*, and *Rhizossolenia bergonii*), as well as lower values of C_{org}, TN, Ni/Al, and Cu/Al. The most recent period of the CWP (~1920 CE to today) was characterized by the increased abundance warm-water taxa (*N. pelagica*, *Cymatodiscus planetophorus*, *T. tenera*,

Plagiogramma minus, *Nitzschia interruptestriata*, and *R. bergonii*), and by the prevalence of low values of C_{org}, TN, Ni/Al, and Cu/Al. These changes in productivity during the LIA and CWP were likely driven by changes in solar irradiance and the migration of the Intertropical Convergence Zone. This study highlights the spatial extent of the LIA in the Eastern Tropical North Pacific and contributes to the knowledge of the productivity response to climate in tropical regions.

Keywords: Little Ice Age, Current Warm Period, Gulf of Tehuantepec, paleoproductivity, diatoms, upwelling.

1. Introduction

The climate of the Eastern Tropical North Pacific (ETNP) is primarily modulated by changes in the strength of the trade winds and the latitudinal shifts of the Intertropical Convergence Zone (ITCZ) (Lavín et al., 2006). Also, variations at diverse scales (centennial, decadal and interannual) have impacted the ETNP climate in the last half millennium. A prolonged cold period called the Little Ice Age (LIA ~1250 to ~1850 CE, e.g., Crowley et al., 2008; Miller et al., 2012; ~1400 to ~1700 CE, e.g., Mann et al., 2009) has been related to the lowest solar irradiance in the past millennium (Spörer, Maunder and Dalton solar minima, Bard et al., 2000; Lean, 2018), and increased volcanic activity (Crowley et al., 2008). Although the LIA has been widely studied, its timing and impact on a global scale are still being discussed, mainly in tropical regions (Juárez et al., 2014) and in the ETNP (Goni et al., 2006; Barron and Bukry, 2007; Staines-Urías et al., 2009; Juárez et al., 2014; Choumiline et al., 2019). In paleolimnological studies in central and southern Mexico, the LIA has been associated with temperature decrease of ~2.0°C and mountain glacier advance (Lozano-García et al., 2007; Vázquez-Selem, 2011). A change to warmer condition is documented worldwide since ~1850

(IPCC, 2014) identified as the Current Warm Period (CWP) (e.g., Salvatteci et al., 2014; Griffiths et al., 2016).

The Gulf of Tehuantepec (GoT) is in the ETNP (Fig. 1). Water masses in the GoT are: Equatorial Surface Water (ESW, up to 29°C and salinity > 34), Subtropical Subsurface Water (SSW, < 25°C and salinity > 35), North Pacific Intermediate Water (NPIW, 4 to 9°C and salinity < 34.5), and North Deep Pacific Water (NDPW, 1.2 to 2°C, < 34.5) (Fiedler and Talley, 2006; Machain-Castillo et al., 2008); and their vertical distribution is influenced by the atmospheric circulation regime.

During winter and early spring seasons, the ITCZ is located at its southernmost position, and easterly trade winds across southern Mexico and Central America are stronger than the rest of the year (Amador et al., 2006). These conditions allow the high-pressure systems south-eastward migration associated with cold-air outbreaks coming from the northwestern United States. The outbreaks generate airflows channelled through the low elevation gap of the Sierra Madre del Sur and reach the GoT as intense northerly winds (Amador et al., 2006), locally named Tehuanos (Trasviña et al., 1995). Tehuanos are perpendicular to the coast and cause mixing and stress curling of the surface water column on the wind axis (Trasviña et al., 1995). These winds can break up the stratification or raise the thermocline near the surface (Kessler, 2006) to even less than ~30 m depth (Lluch-Cota et al., 1997), and cold (~20 °C), nutrient-rich subsurface waters fertilize the euphotic zone resulting in high primary productivity, including diatom blooms, as revealed by high chlorophyll-*a* concentrations (Fig. 1). At this time, the ESW occupied the upper 35-40 to 70 m, the SSW is found until 430-470 m, the NPIW to 900-1200 m, and the NDPW below this depth (Machain-Castillo et al., 2008).

In contrast, during the summer and autumn seasons, the ITCZ is at its northernmost position, rainfall dominates in the ETNP due to the associated convective belt of the ITCZ, and trade winds are weaker than during the winter-spring period (Amador et al., 2006). Surface water circulation is dominated by tropical waters from the equatorial region flowing north through the Costa Rica Coastal Current (Kessler, 2006). The ESW is found between 55-70 m, SSW until 450 m, and the NPIW and NDPW depth limits are similar to winter (Fiedler and Talley, 2006; Machain-Castillo et al., 2008). Tehuanos are relatively sporadic and weak (Romero-Centeno et al., 2007), and the thermocline is deeper at ~70 m (Lluch-Cota et al., 1997). Hence upwelling and productivity decrease (Meave del Castillo and Hernández-Becerril, 1998), and the highest sea surface temperatures (SST) ~30.0 °C are found (Fig. 1).
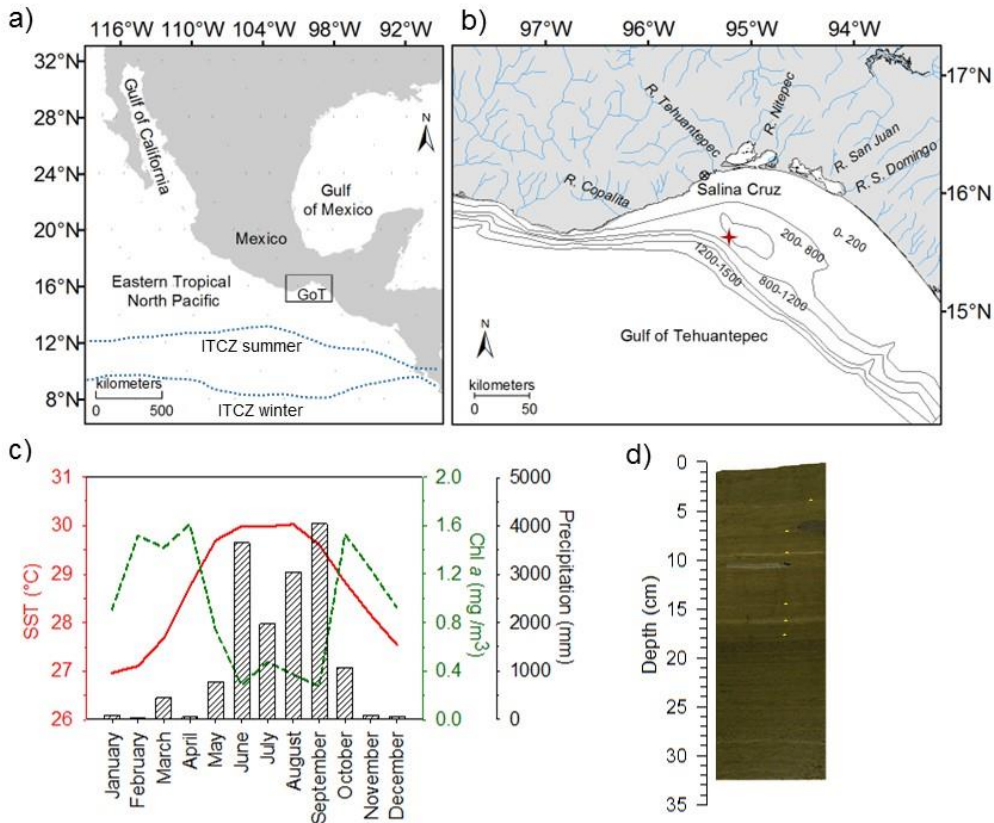
Figure 1. a) Gulf of Tehuantepec (GoT) location in the Eastern Tropical North Pacific and mean position of the ITCZ in summer and winter (Amador et al., 2016). b) sampling site of core Tehua XII E03 (red star) and main rivers in the Tehuantepec coast. c) Monthly average of Sea Surface Temperature (SST), Chlorophyll *a* (Chl *a*), and Precipitation in the study area (data taken from IRI, 2015). D) Photography of core Tehua XII E03*b*, the yellow asterisks indicate the key laminae used to correlate subcores.

Diatoms are unicellular algae and one of the main components of phytoplankton in the GoT, together with cyanophytes, dinoflagellates, and coccolithophorids (Meave del Castillo and Hernández-Becerril, 1998). One must consider that preserved diatoms silicate frustules on the seafloor may be a mixed assemblage (freshwater, marine, benthic, and planktonic). Furthermore, most of the information is lost during settling to the seafloor by dissolution, grazing, transport, reworking, and bioturbation (Crosta and Koc, 2007). However, upwelling regions with high productivity usually reflect the overlaying hydrographic conditions of the surface waters (Treppke et al., 1996), and have been used to reconstruct ocean environmental conditions during climate episodes such as the LIA and the Medieval Warm Period (MWP ~900 to ~1200 CE, e.g., Barron et al., 2003; Barron and Bukry, 2007). In addition, geochemical proxies such as organic carbon (C_{org}) and total nitrogen (TN) in sediments have been widely used to infer exported production to the seabed (Sifeddine et al., 2008; Salvatteci et al., 2014; Choumiline et al., 2019). The C:N ratio and $\delta^{13}C$ have been used to track the origin of sedimentary C_{org}, since marine phytoplankton and land vegetation carry a distinct C:N and $\delta^{13}C$ signal (Lamb et al., 2006). Ni and Cu concentrations are also used as productivity tracers since they are used as a micronutrient for the phytoplankton (Tribovillard et al., 2006; Smrzka et al., 2019). Although, these elements can be affected by terrestrial input (Calver and Pedersen, 2007; Smrzka et al., 2019), the normalization with a terrigenous element (such as Al or Ti) removes the terrestrial signal.

Contamination by human impact is another factor that can alter trace element concentrations in sedimentary records (e.g., Ruiz-Fernández et al., 2004). In the GoT coastal zone, previous studies have reported increments in trace metal associated with the development of anthropogenic land-based activities, mainly oil production, urban wastes, and agricultural residues (Pica-Granados et al., 1994; Ruiz-Fernández et al., 2004). Ruiz-Fernandez et al. (2004) reported that Cu background level in sediments (before 1860) was 138.9 mg/kg, and a moderate anthropic influence on Cu (from 150 to 480 mg/kg) since the 1980s off Salina Cruz at ~240 m water depth. Concerning Ni, Pica-Granados et al. (1994) reported current high Ni concentrations in water (from 49.8 to 81.7 mg/l) collected near the "Antonio Dovalí Jaime" oil refinery (~5 km from Salina Cruz Port, Fig. 1) at < 5 m water depth.

Redox processes can also affect the Ni and Cu signals deposited in hypoxic environments (Calver and Pedersen, 2007; Smrzka et al., 2019). However, when Ni and Cu profiles have similar trends to other productivity proxies, such as C_{org} and biogenic silica, they can be considered as reliable productivity tracers.

In the GoT, most of the studies on phytoplankton have been focused on taxa distribution, species richness (Torres-Ariño et al., 2019 and references therein), and seasonal variability (e.g., Meave del Castillo and Hernández-Becerril, 1998; Moreno-Ruiz et al., 2011). This study provides the first high-resolution reconstruction of paleoproductivity based on diatoms, C_{org}, TN, Ni/Al, and Cu/Al of the last five centuries in a sequence of laminated sediments from the GoT and its relationship to ocean-climate variability. The study site is in a more tropical latitude. Nevertheless, we expect that the climate variability of the last centuries seen in more northern regions (e.g., Goni et al., 2006; Barron and Bukry, 2007; Staines-Urías et al., 2009; Juárez et al., 2014; Choumiline et al., 2019) can also be registered in the GoT sediments. . Tropical climates

are naturally sensitive to climate variations (e.g., Yamaguchi and Suga, 2019; Li et al., 2020), as small SST increases further strengthen upper water column stratification (Fiedler and Talley, 2006; Amador et al., 2006), affecting productivity due to lower nutrient availability (Yamaguchi and Suga, 2019; Li et al., 2020). Therefore, this study helps to understand the effects of warming on tropical regions and their implications for future climate and ocean dynamics.

2. Material and Methods

2.1. Sediment core

The present study is based on a Reineck box core, retrieved in March 2014 from the GoT (Tehua XII E03, 15.6442° N and 95.3071° W) at 743 m water depth, aboard the R/V "El Puma" from the National Autonomous University of Mexico (UNAM) (Fig. 1). Two subcores were obtained; subcore Tehua XII E03a (34.5 cm long, 6.5 cm diameter) was used for ^{210}Pb dating, Ni, and Cu analysis, and subcore Tehua XII E03b (32.5 cm long and 14 x 14 cm wide and high; Fig. 1) was used for diatom, and the rest of geochemical analyses (C_{org}, TN, and δ^{13}C), and radiocarbon (^{14}C) dating.

2.2. Age dating

The radiochronology of the upper core segment (0 − 20 cm) of the subcore Tehua XII E03a was estimated through the ^{210}Pb age dating method at 1 cm resolution (Table S1). ^{210}Pb activities were determined at the laboratory of Isotopic Geochemistry and Geochronology at UNAM (Mexico) through high-resolution gamma ray spectrometry (HPGe well detector, Ortec-Ametek) as described by Díaz-Asencio et al. (2020). For validation, ^{239,240}Pu was determined in selected sediment samples by alpha spectrometry (Ortec-Ametek Alpha Spectrometry system) (Ruiz-Fernández et al., 2014). Data quality was assessed through the analysis of the reference

material IAEA-300 (Radionuclides in Baltic Sea sediment) and the results were within the reported range of recommended values.

Radiocarbon ages were determined by accelerator mass spectrometry (AMS), at the National Platform LMC14, France, on five bulk sediment samples (4.0-4.5, 8.0-8.5, 20.0-20.5, 25.0-25.5, and 29.0-29.5 cm depth) of the subcore Tehua XII E03*b* (Table S2). We used the bulk sediment because of the poor preservation (Arellano-Torres et al., 2013) and recalcification of planktonic foraminiferal shells (Gibson et al., 2016). Previous studies in the GoT using AMS[14]C age dating on bulk sediment (Table 1) have shown that this method is reliable in the area (e.g., Pichevin et al., 2010; Blanchet et al., 2012; Arellano-Torres et al., 2013; García-Gallardo et al., 2021). To produce an integrated ^{210}Pb-^{14}C age model, both subcores were stratigraphically correlated by identifying common key laminae (light laminae visually identified in both subcores; Fig. 1, Table S1) and ^{210}Pb-derived dates for subcore Tehua XII E03a were transferred to subcore Tehua XII E03*b* (Table S1).

2.3. Geochemical procedures

Twenty-four dry sediment samples (~0.5 cm each) ground in a porcelain mortar, were used for geochemical analyses at the ALYSES platform (IRD/SU, Bondy France). The content of C_{org} and TN and the stable carbon isotopic ratio ^{13}C/^{12}C of the organic matter were determined on a Flash HT 2000 elemental analyzer, coupled to an isotopic ratio mass spectrometer Delta Vplus via a combustion-ConFlow IV interface from Thermo Fischer Scientific. The samples for C_{org} and δ^{13}C analysis were treated with HCl 10% for removal of the carbonate fraction. Bulk sediment was used for TN analysis. The stable carbon isotopic ratio ^{13}C/^{12}C of OM is reported in the conventional δ-notation with respect to the PDB (Pee Dee Belemnite) carbonate standard

defined with the equation $\delta^{13}C = \frac{^{13}C/^{12}C_{sample} - ^{13}C/^{12}C_{standard}}{^{13}C/^{12}C_{standard}} * 1000$. The analytical precision was determined by replicates of the certified reference materials and was always below 0.12% for C_{org} and TN, and lower than ± 0.2‰ for $\delta^{13}C$. The $\delta^{13}C$ values are expressed in ‰ against the international standard PDB.

To evaluate the productivity changes along the core, Ni and Cu concentrations were used as productivity proxies (Tribovillard et al., 2006; Smrzka et al., 2019). As the Ni and Cu concentration in the sediments can be affected by terrestrial input, we normalized them with Al concentrations (Calver and Pedersen, 2007). Ni, Cu, and Al concentrations were determined on thirty-five samples (~1 cm each) by X-ray fluorescence spectrometry (XRF, Spectrolab Xepos-3). Analytical precision was assessed through the replicate analysis (n=3) of a single sediment sample, and the coefficients of variation were < 0.6% for Ni and Cu, and < 0.01% for Al). The accuracy of the measurements was evaluated through the analysis of the reference material IAEA-158 with results obtained within the reported certified values.

2.4. Diatom processing

Ninety-two sediment samples (~0.4 cm average thickness and ~6 years temporal resolution average; Table S3) were obtained for diatom analysis. Samples were processed at the Micropaleontology Laboratory of the Marine Sciences and Limnology Institute, UNAM. Laminae were visually recognized and separated using an x-ray digitalized acetate template. The dry weight of each sediment lamina was registered for abundance calculations. Sediment samples (~0.2 to ~0.5 g dry weight) were added with HCl 10% to eliminate carbonates and digested at ~80°C with H_2O_2 30% and HNO_3 70% to remove organic matter. Acids and salts were removed

through several washes with distilled water, settled for at least 24 h, and the liquid was discarded. The samples were diluted to a standard volume (30 mL).

For diatom slides, samples were homogenized and 200 µL aliquots were taken. In most samples, dilution was needed owing to the large number of particles, these volumes were considered for the calculation of total abundance. Aliquots were placed on coverslips (18 mm diameter) and dried at room temperature. Slides were mounted in Naphrax resin (refraction index = 1.74). All diatoms were identified at the genera or species taxonomic level using Cupp (1943), Round et al. (1990), Moreno et al. (1996), Hasle and Syvertsen (1997), Hernández-Becerril et al. (2021), and specialized literatures. The samples were counted by transects (Schrader and Gersonde, 1978), at least 500 valves per sample were identified under a light microscope (Nikon eclipse Ni) at 1000x magnification with Nomarski interference contrast. The precision of the diatom analysis was evaluated through the replicate analysis (n=8) of diatom slides; the relative standard deviation was < 8%. The species composition is reported as relative abundance (%).

2.5. Data analysis

In order to quantitatively define assemblages' zone (periods) in the studied core, a CONISS (CONstrained Incremental Sums of Squares; Grimm, 1987) analysis was applied to a simplified diatom species matrix (taxa with total abundances > 0.8%; Table S3) together with geochemical data (C_{org}, TN, $\delta^{13}C$, C:N, Ni/Al, and Cu/Al). A squared Euclidian matrix approach was used to quantify the dissimilarity between samples, and the number of statistically significant zones was established with a broken stick model (Benett, 1996). These procedures were performed with the R packages "rioja" (Juggins, 2020) and "vegan" (Oksanen et al., 2020).

3. Results

3.1. Age-depth model

The ^{210}Pb chronology was established a) with the Constant Flux model (Sanchez-Cabeza and Ruiz-Fernández, 2012), with uncertainties estimated through a Monte Carlo method with 10^6 simulations (Sanchez-Cabeza et al., 2014), and b) with a bayesian method (Aquino-López et al., 2018) by using the R package rplum (Blaauw et al., 2021), which has been successfully used in contrasting aquatic environments, including marine sediment cores (Aquino-López et al., 2020). Both chronologies were almost identical and were successfully validated with the ^{239,240}Pu onset, which is a robust age-dating marker in regions far from nuclear testing grounds (Sanchez Cabeza et al., 2021) (Figure 2).
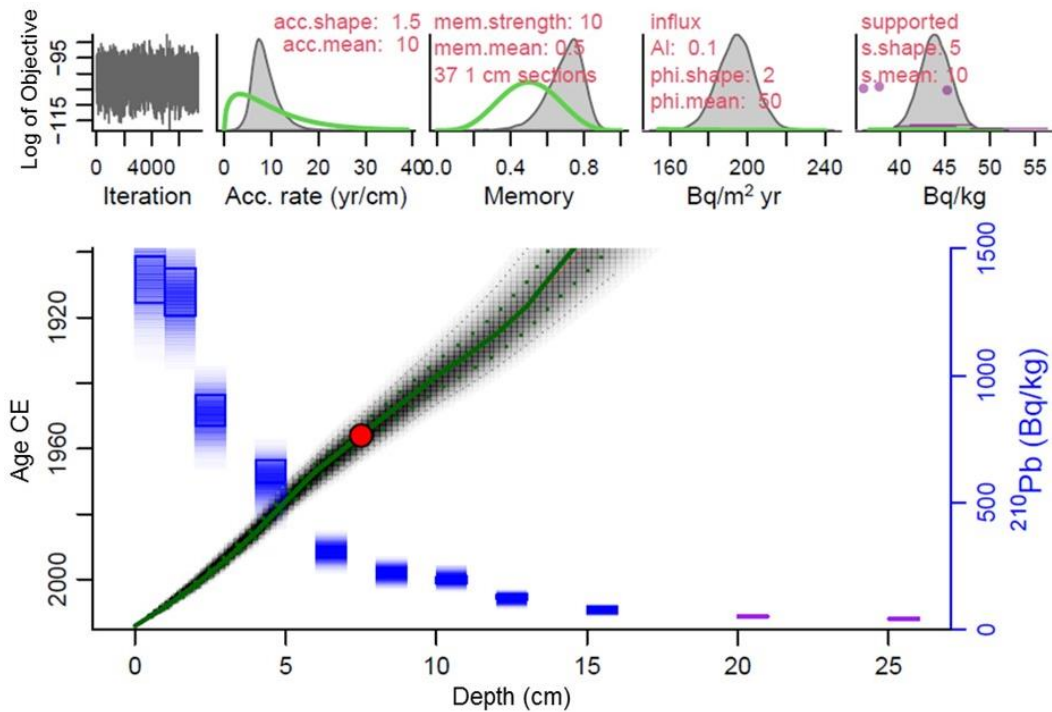

Figure 2. ^{210}Pb-derived age model for the core Tehua XII E03 using the Constant flux (green line) and Plum models (red line). The blue squares represent the ^{210}Pb activities ($\pm 2\sigma$; right axis). The red point represents the ^{239,240}Pu onset (red point) in 1954 CE (Common Era), used to validate the age model.

Following common practice, the radiocarbon ages were calibrated with the Marine20 curve (Heaton et al., 2020) and corrected for a regional marine reservoir age (ΔR) of 456 ± 51 yr (Berger et al., 1966), but ages of sections 4.0-4.5 and 8.0-8.5 were significantly older than the ^{210}Pb-derived ones (Table S1-S2). These discrepancies have been attributed to regional differences in the marine reservoir age (e.g., Thunell and Kepple, 2004; Hendy and Pedersen, 2006), which can be large in upwelling areas (Goodfriend and Flessa, 1997; Gutiérrez et al., 2009).

To estimate the local ΔR, we followed the method described by Reimer and Reimer (2016), which has been successfully used with ^{210}Pb in the Baja California continental margin, also affected by upwelling (Treinen-Crespo et al., 2021). To calculate uncertainties, we used a Monte Carlo approach with the R language (R core team, 2021). The ^{210}Pb-derived ages were expressed as BP (before present; age BP $= 1950 -$ calendar age) and produced 10^6 simulations of the ^{210}Pb age BP (*pb210.bp*) and the sample radiocarbon age (*c14*) following normal distributions. Simulated ^{210}Pb BP ages younger than 1950 were discarded as they could not be calibrated with the MARINE20 curve. Each *pb210.bp* simulation was reverse-calibrated with the MARINE20 curve (*pb210.c14*) by using the *calBP.14C* function of the IntCal package (Blaauw, 2022). Then, the ΔR simulations were determined as the difference between the sample radiocarbon age simulations (*c14*) and the ^{210}Pb reverse-calibrated age simulations (*pb210.c14*) as $\Delta R = c14 - pb210.c14$. Finally, ΔR and its uncertainty were determined as the mean and standard deviation of all simulations, respectively ($\Delta R = 247 \pm 30$ yr, 1 sigma).

The integrated ^{210}Pb-^{14}C age-model was produced by a bayesian approach (Blaauw and Christen, 2011) with the rbacon R package (Blaauw et al., 2022). We used all ^{210}Pb-derived ages and the three radiocarbon ^{14}C ages beyond the validated ^{210}Pb chronology (sections below 20.0

cm), with the MARINE20 curve and the calculated ΔR. The integrated age-model showed a satisfactory agreement between ^{210}Pb and ^{14}C ages, and a common and smooth trend (Figure 3).
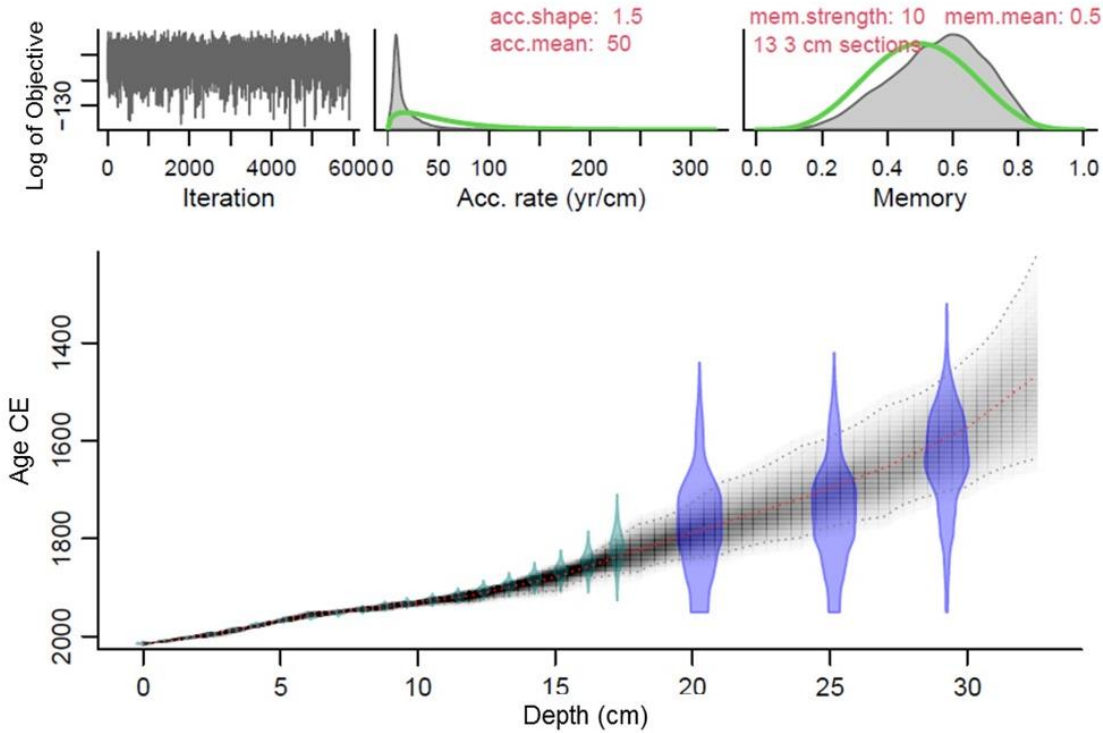
Figure 3. Integrated bayesian age model of the core Tehua XII E03 using MARINE20 curve and the calculated ΔR = 247 ± 30 yr. ^{210}Pb dates in cyan color and ^{14}C dates in blue. CE = Common Era.

The integrated ^{210}Pb and ^{14}C age model indicated that the base of the core reached ~1500 CE (Table S4; Fig. 3). The average sediment accumulation rate from ~1907 to ~2014 CE was 0.14 ± 0.07 cm/yr; whereas for the older sediment, the sedimentation rate was of 0.08 ± 0.06 cm/yr (Table S1-2).

3.2. Geochemistry

The C_{org} (%) and TN (%) trends were similar along the core, with values ranging from 4.94 to 7.33 % (average C_{org} = 6.35%) and 0.52 to 0.87 % (average TN = 0.68%), respectively.

Both elements displayed the highest values between ~1717 and ~1820 CE. The $\delta^{13}C$ varied from -21.24 to -18.22‰ (average $\delta^{13}C$ = -19.40‰) (Fig. 4; Table S3). The Ni/Al ranged from 0.01 to 0.11 (average = 0.50), Cu/Al from 3.55 to 8.25 (average = 5.58) (Table S3). From ~1500 to ~1847 CE, Ni/Al and Cu/Al showed the highest concentrations (Fig. 4).

3.3. Diatoms

A total of 103 taxa belonging to 54 genera were determined; marine taxa were predominant and benthic and freshwater taxa represented only < ~9% of all studied sample. Specimens in the sediment core Tehua XII E03 were common to adjacent tropical Pacific regions and other upwelling areas. Seventeen taxa with a total relative abundance > 0.8% made up 85.8% (Fig. 4; Plate 1; Table S3). *Thalassionema nitzschioides* (20.9%) and *Chaetoceros* spores (mainly *C. affinis*, *C. costatus*, *C. curvisetus*, and *C. radicans*) (18.5%) were the dominant taxa, reaching up to 57% of total assemblages in the samples; followed by *Neodelphineis pelagica* (8.5%), *Thalassionema bacillare* (6.6%), *Lioloma* pacificum (5.8%), *Thalassionema nitzschioides* var. *parvum* (5.0%), *Fragillariopsis doliolus* (4.4%), *Cyclotella litoralis* (3.1%), *Thalassiosira oestrupii* (3.0%), *Thalassiosira nanolineata* (2.4%), *Rhizosolenia setigera* (1.5%), *Thalassiosira lineata* (1.4%), *Thalassiosira tenera* (1.4%), *Nitzschia interruptestriata* (1.1%), *Rhizosolenia bergonii* (0.9%), *Plagiogramma minus* (0.8%), and *Cymatodiscus planetophorus* (0.8%).

3.4. Ecological affinity of the main diatom taxa in the Gulf of Tehuantepec

Thalassionema nitzschioides is widely distributed from tropical to temperate waters (Hasle and Syvertsen, 1997) and usually appears throughout the year (Sancetta, 1995; Meave del Castillo and Hernández-Becerril, 1998; Meave del Castillo, 2002; Romero et al., 2009a); however, its largest abundance in subtropical to tropical regions occurs during the most productive season (e.g., Schrader et al., 1993; Sancetta, 1995; Treppke et al., 1996; Barron et al.,

2010; Romero et al., 2011; Almaraz-Ruiz, 2017). Similarly, the *Chaetoceros* genus is usually predominant in regions with high nutrient availability (Rines and Hargraves, 1988; Treppke et al., 1996; Hasle and Syvertsen, 1997; Lange et al., 1997; Meave del Castillo and Hernández-Becerril, 1998; Romero et al., 2001; Meave del Castillo, 2002; Romero et al., 2009a), where it is commonly represented by resting spores in the sediment (e.g., Sancetta, 1995; Romero et al., 2009a; Ren et al., 2014). Unpublished data from sediment traps (~500 m depth) in the sediment core location during an ENSO-neutral year (February to July 2006) indicate that *T. nitzschioides* was more abundant during the most productive season, together with the *Chaetoceros* genus and *L. pacificum*, where *Chaetoceros* was represented mainly by coastal species in their vegetative forms (*C. affinis, C. compressus, C. costatus*, *C. curvisetus, C. decipiens, C. diversus, C. laciniosus, C. lorenzianus,* and *C. radicans*). Resting spores were only found for *C. affinis, C. compressus*, *C. costatus*, *C. curvisetus*, and *C. radicans* (Plate 1). In the sediments of core Tehua XII E03, no vegetative forms were found, only resting spores. We identified mainly four resting spore forms (*C. affinis*, *C. costatus*, *C. curvisetus*, and *C. radicans*; Plate 2, 7-10) that correspond to the most abundant *Chaetoceros* taxa found in the sediment traps during the upwelling season. Also, in the core sediments, the highest abundances of *Chaetoceros* spores occurred with *T. nitzschioides* and *L. pacificum*, as in the sediment traps during upwelling events. Therefore, we considered that the association of *Chaetoceros* spores, *T. nitzschioides* and *L. pacificum* recovered from the GoT sediments reflects the upwelling season conditions.

Rhizossolenia setigera is sometimes found together with *Chaetoceros* in the California Current System, reflecting high productivity (Sautter and Sancetta, 1992; Sancetta, 1995; Lange et al., 1997). *Thalassiosira nanolineata* is recorded in Panama Basin as a coastal taxon; however, the species also showed a high factor score in the high productivity group (Romero et al., 2011, Table 1). Since in this study *T. nanolineata* exhibited its highest abundance together with *T.*

nitzschioides, *Chaetoceros* spores, *L. pacificum*, and *R. setigera*, it was considered part of the assemblage of cold-waters and high-productivity taxa.
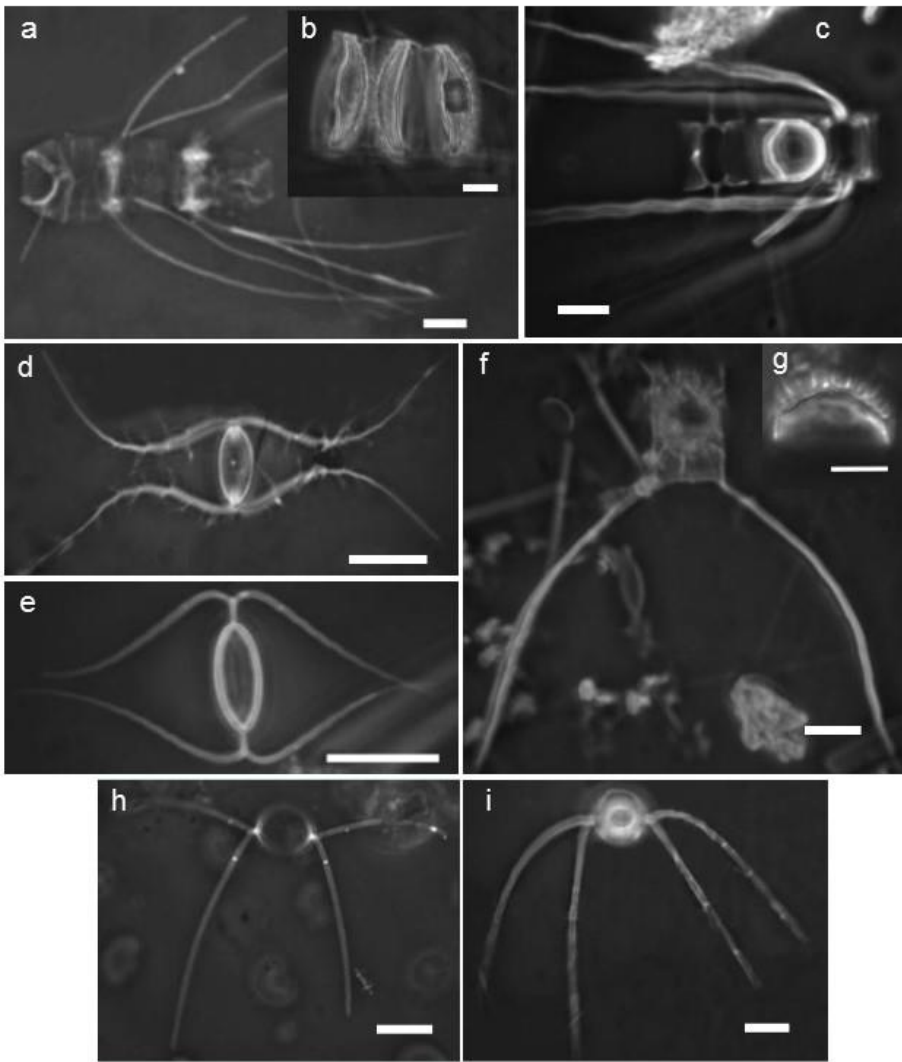
Plate 1. Light microscope photographs of vegetative cells with their resting spores of some of the predominant *Chaetoceros* species in the sediment traps from the GoT. a) chain valves and b) chain resting spores of *Chaetoceros costatus*. c) chain valves and resting spore of *Chaetoceros compressus*. d) valve of *Chaetoceros radicans* and e) its resting spore. f-g) terminal valve and resting spore of *Chaetoceros affinis*. h) valve of *Chaetoceros curvisetus* and i) its resting spore. The scale bar is 10 μm in all images.

In the California Current System and the Eastern Equatorial Pacific, during warm and low productivity conditions, diatom assemblages are composed of one or more of the following species: *F. doliolus*, *T. oestrupii*, *N. interruptestriata* (Lange et al., 1987; Lange et al., 1990; Sancetta, 1992; Sautter and Sancetta, 1992; Schrader et al., 1993; Sancetta, 1995; Barron et al., 2010; Romero et al., 2011; Barron et al., 2013), *T. bacillare* (Baumgartner et al., 1985), *T. nitzschioides* var. *parvum* (Romero et al., 2011), *T. lineata*, *R. bergonii* (Baumgartner et al., 1985; Lange et al., 1987; Kemp et al., 2000), *C. litoralis* (Sancetta, 1995; Barron et al., 2004; Barron et al., 2005; Barron and Bukry, 2007), *C. planetophorus* (Estrada et al., 2022), *N. pelagica* (Almaraz-Ruiz, 2017), and other taxa in minor amounts. In particular, *R. bergoni* is a deep-dwelling taxon (up to ~130 m, Kemp et al., 2000) that indicates strong stratification in the water column in tropical to subtropical regions (Baumgartner et al., 1985; Lange et al., 1987; Lange et al., 1994; Kemp et al., 2000; Romero et al., 2011). For example, in the Santa Barbara Basin, *R. bergonii* (and other warm-water diatoms) showed high abundances during the 1983 El Niño (Lange et al., 1987). This trend also was observed in the Guaymas Basin during the 1957-1959, 1965, 1968-1969, and 1972 El Niño events (Baumgartner et al., 1985). El Niño on the Eastern North Pacific coast are characterized by a strong upper water column stratification and a deeper thermocline, which limit nutrients availability, and consequently low productivity (Pennington et al., 2006), where *R. bergonii* is one of the common species. However, some of these species have also been observed in temperate water, such as *F. doliolus* (Lange et al., 1994; Sancetta, 1995; Treppke et al., 1996; Almaraz-Ruiz, 2017), *T. oestrupii* (Sautter and Sancetta, 1992; Hasle and Syvertsen, 1997; Romero et al., 2009b; Almaraz-Ruiz, 2017), *T. bacillare* (Sancetta, 1995), *T. nitzschioides* var. *parvum* (Schrader et al., 1993; Treppke et al., 1996; Almaraz-Ruiz, 2017), and *C. litoralis* (Lange and Syvertsen, 1989; Romero et al., 2009a; Romero et al., 2011). Therefore, in this study *T. bacillare*, *F. doliolus*, *T. nitzschioides* var. *parvum*, *C. litoralis*, and *T.*

oestrupii were considered temperate to warm-water taxa. *Thalassiosira tenera* is reported as cosmopolitan, except for polar regions (Hasle and Syvertsen, 1997; Naya, 2012; Li et al., 2013) and *P. minus*, as a widely distributed species (Guiry and Guiry, 2020); since these taxa exhibited in our record a similar distribution to warm-water *N. pelagica*, *C. planetophorus*, *N. interruptestriata*, *T. lineata*, and *R. bergonii*, they were interpreted as such (Fig. 4).
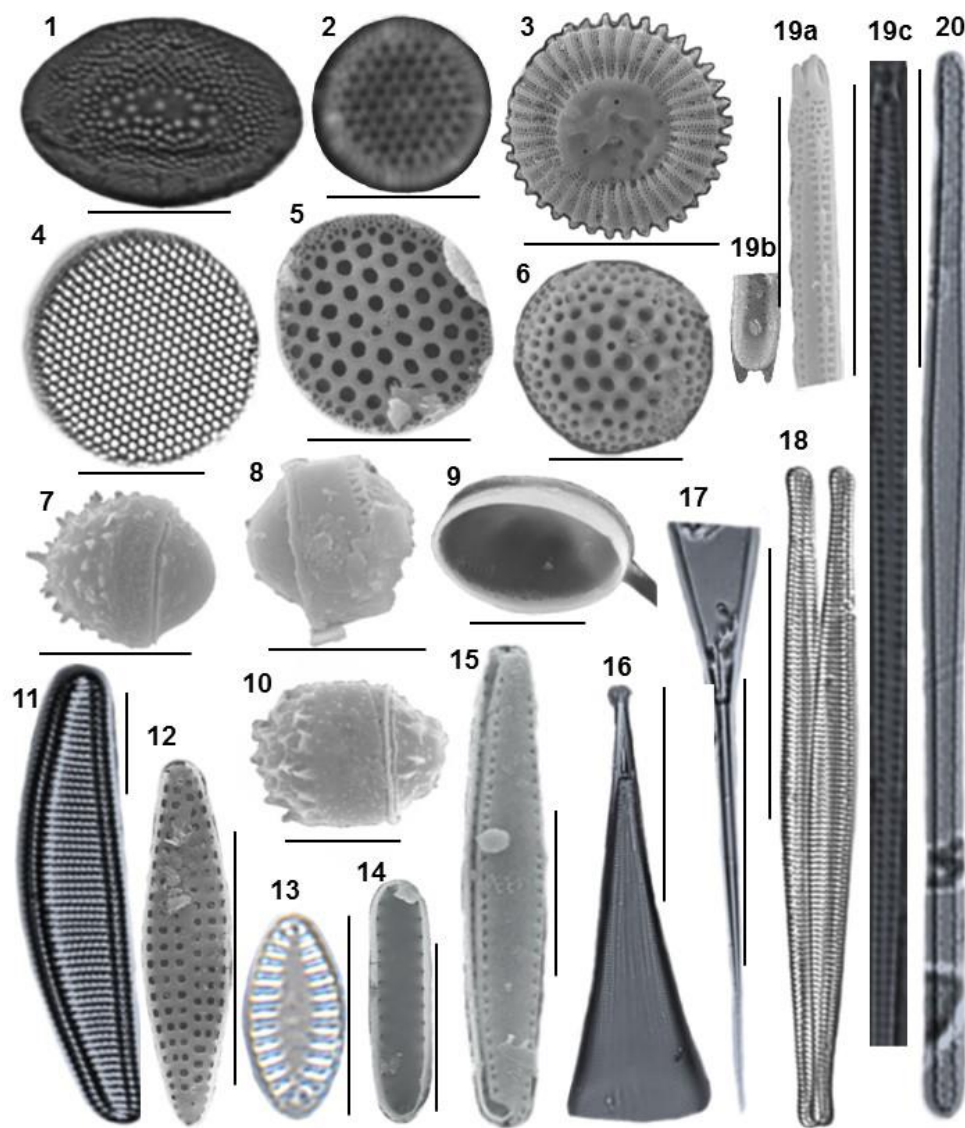

Plate 2. Scanning Electron Microscope (SEM) and Light Microscope (LM) images of the most abundant diatom taxa in the sediment core Tehua XII E03. 1) *Cymatodiscus planetophorus* (LM),

2) *Thalassiosira tenera* (LM), 3) *Cyclotella litoralis* (SEM), 4) *Thalassiosira lineata* (LM), 5) *Thalassiosira nanolineata* (SEM), 6) *Thalassiosira oestrupii* (SEM), 7) *Chaetoceros affinis* resting spore (SEM), 8) *Chaetoceros curvisetus* resting spore (SEM), 9) *Chaetoceros radicans* resting spore (internal view of the flat secondary valve, SEM), 10) *Chaetoceros costatus* resting spore (SEM), 11) *Fragillariopsis doliolus* (LM), 12) *Neodelphineis pelagica* (SEM), 13) *Plagiogramma minus* (LM), 14) *Thalassionema nitzschioides* var. *parvum* (SEM), 15) *Thalassionema nitzschioides* (SEM), 16) *Rhizosolenia bergonii* (LM), 17) *Rhizosolenia setigera* (LM), 18) *Nitzschia interruptestriata* (LM), 19) *Lioloma pacificum* (a-b SEM, c LM), and 20) *Thalassionema bacillare* (LM). Scale bar: 5 µm (7-10); 10 µm (1-6 and 11-15); 30 µm (16-18), and 20 µm (19a-c and 20).

3.5. CONISS analysis

According to the abundance of the main diatom species and their ecological affinities based on the literature, three broad ecological assemblages were adopted: cold-water and high productivity taxa, temperate to warm-water taxa, and warm-water and low productivity taxa (Figure 4). These assemblages and the CONISS zonation are described below.

Visual observation of the CONISS and the broken stick model (Fig. S1) suggest four significant zones (at the 12.1 of total sum of squares) in the studied core (Fig. 4). The classification on the first hierarchical level presents two significant diatom assemblage zones, the lower part of the core between ~1500 and ~1919 CE (32.5 to 11.5 cm), and the upper part between ~1920 and ~2014 CE (11.4 to 0 cm). The classification on the second level subdivides the lower part into two zones from ~1500 to ~1858 CE (32.5 cm to 16.6 cm) and ~1860 to ~1919 CE (16.5 to 11.5 cm). Finally, a third level separates another zone between ~1500 and ~1648 CE (32.5 to 28.0 cm).

The lowest zone (~1500 to ~1648 CE) was characterized by the predominance of cold-water and high productivity taxa (*T. nitzschioides*, *Chaetoceros* spores, *L. pacificum, T. nanolineata,* and *Rhizosolenia setigera*) and most temperate to warm-taxa (*T. nitzschioides* var. *parvum*, *C. litoralis*, and *T. oestrupii*). The zone from ~1650 to ~1858 CE showed a relative increase of the temperate to warm-taxa (*T. bacillare, F. doliolus*, *T. nitzschioides var. parvum*, and *C. litoralis*). From ~1860 to ~1919 CE some cold-water and high productivity taxa (*T. nitzschioides*, *Chaetoceros* spores, and *L. pacificum*) and most warm-water and low productivity diatoms (*N. pelagica*, *T. tenera*, and *R. bergonii*) increased. The upper part (~1920 to ~2014 CE) was characterized by high abundances of all warm-water and low productivity taxa and almost all temperate to warm-water taxa (except *T. nitzschioides* var. *parvum*) (Figs. 4-5).
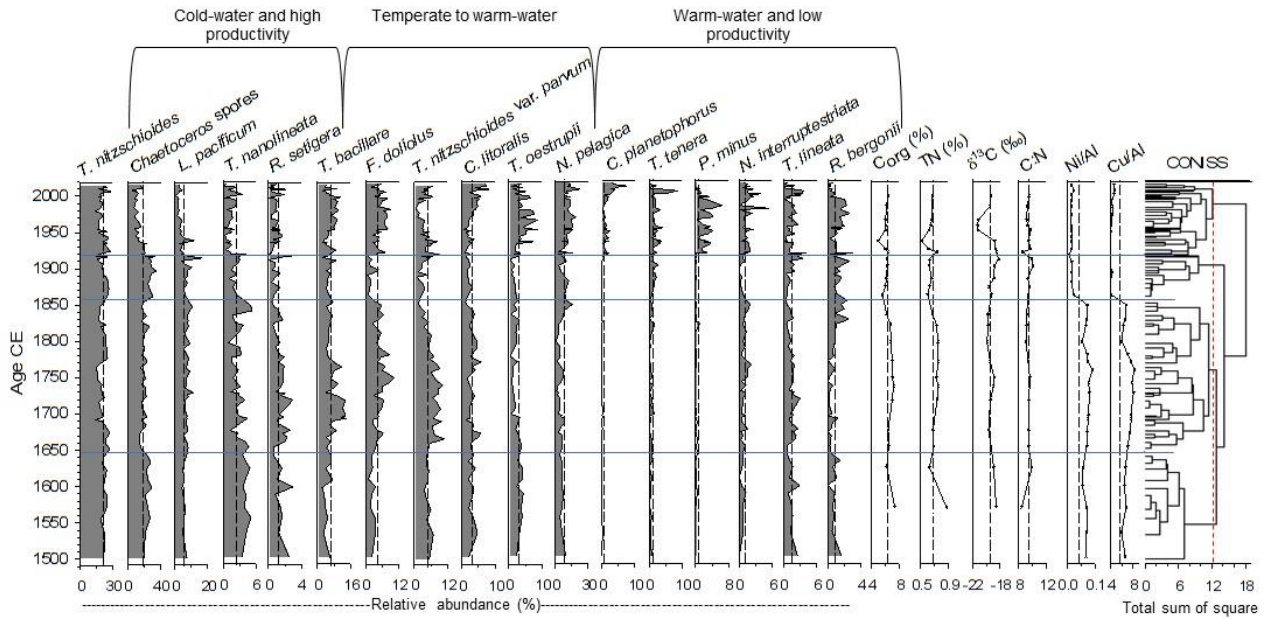

Figure 4. Relative abundance (%) and ecological group for the most common diatoms (> 0.8%), C_{org} (%), TN (%), $\delta^{13}C$ (‰), C:N, Ni/Al, Cu/Al, and CONISS dendrogram of the Tehua XII E03. Vertical dashed lines indicate the average values of each set. Horizontal (blue) lines indicate the

four zones defined by CONISS analysis (at the 12.1 of total sum of squares indicated in red dotted line).

4. Discussion

4.1. Chronology and sedimentation rate

The ^{210}Pb dating is the most suitable method to obtain the chronology of recent sediments (~100 years) (Sanchez-Cabeza and Ruiz-Fernández, 2012), whereas the ^{14}C method is widely used to date sediments beyond the 1700 - 1800s (e.g., Gutiérrez et al., 2009; Staines-Urías et al., 2009; Choumiline et al., 2019). Although there are several palaeoceanographic studies in the GoT, these studies were focused on climate changes at the millennial scale and according to their reported ages they do not cover the last hundred years (e.g., Thunell and Kepple, 2004; Hendy and Pedersen, 2006; Pichevin et al., 2010; Arellano-Torres et al., 2013; García-Gallardo et al., 2021) (Table 1). This is the first high-resolution study in the region of the last ~500 years, where the environmental changes, linked to climatic variability, are based on an integrated ^{210}Pb-^{14}C age model.

A new ^{14}C reservoir age ($\Delta R = 247 \pm 30$ years; Fig. 3) was calculated for bulk sediments of the core Tehua XII E03 (section 2.2). This ΔR value is higher than the reference reservoir age of the GoT proposed by Berger et al. (1966) (456 ± 51 years, $\Delta R = 18 + 50$ years), the marine reservoir effect applied by Thunell and Kepple (2004) (400 yr), and Hendy and Pedersen (2006) (Table 1). Our reservoir age is consistent with the independently obtained ^{210}Pb dates (Fig. 2; Tables S1-S2), which are reliably validated by the Pu onset (Fig. 2).

The method to estimate ΔR has been used in sediment cores at Soledad Basin, Baja California, Mexico (Treinen-Crespo et al., 2021), where different ΔRs are found for organic matter and planktonic foraminifera. This suggests that the reservoir age in *Turritella leverostoma*

shell (Berger et al., 1966) cannot be used for bulk sediment. In recent and high-resolution sedimentary records (such as Tehua XII E03), it is essential to obtain reliable local reservoir corrections, as ages can be shifted by decades, or even centuries (Treinen-Crespo et al., 2021), thus invalidating the paleoreconstructions.

The sedimentation rate for the last century was 0.14 ± 0.07 cm/yr, within the range reported by Ruiz-Fernández et al. (2009) of 0.03 to 0.21 cm/yr for the GoT. The sedimentation rate of 0.08 ± 0.04 cm/yr for the older sediments was similar to values obtained in previous studies in GoT for the late Holocene of ~0.1 cm/yr (Table 1) (Thunell and Kepple, 2004; Hendy and Pedersen, 2006; Blanchet et al., 2012; Arellano-Torres et al., 2013; García-Gallardo et al., 2021).

4.2. Origin of organic matter in the Tehua XII E03

The origin of sedimentary organic matter was inferred through the C:N ratio and $\delta^{13}C$ that indicate the relative contributions of organic matter from different sources (Lamb et al., 2006). Typically, C:N ratio values above 12 and $\delta^{13}C$ values that range from -33 to -25 ‰ suggest the predominance of terrestrial organic matter. C:N ratio values between 4 and 10, and $\delta^{13}C$ values ranging from -21 to -18 ‰ indicate a marine origin (Lamb et al., 2006). Thus, our values of C:N ratio (~9) and $\delta^{13}C$ (~-22 to ~-18 ‰) suggest that the organic matter preserved in the GoT sediments is predominantly of marine origin (Fig. 4; Table S3).

4.3. Productivity variation in the Gulf of Tehuantepec over the last five centuries

The diatom abundance and geochemical proxies used in this study (C_{org}, TN, $\delta^{13}C$, Ni/Al, and Cu/Al) suggest relative productivity changes related to LIA and CWP conditions during the last five centuries. According to CONISS analysis, four significant zones were recognized within these two conditions (Fig. 4). These periods are compared below (Fig. 5) with solar irradiance

(Lean, 2018), temperature records (Goni et al., 2006; Mann et al., 2009; Staines-Urías et al., 2009), and the Pacific Walker Circulation strength through the Southern Oscillation Index (SOI) (Griffiths et al., 2016). Also, we compared our record with other ETNP exported productivity records (Barron and Bukry, 2007; Barron et al., 2013; Juárez et al., 2014; Choumiline et al., 2019).
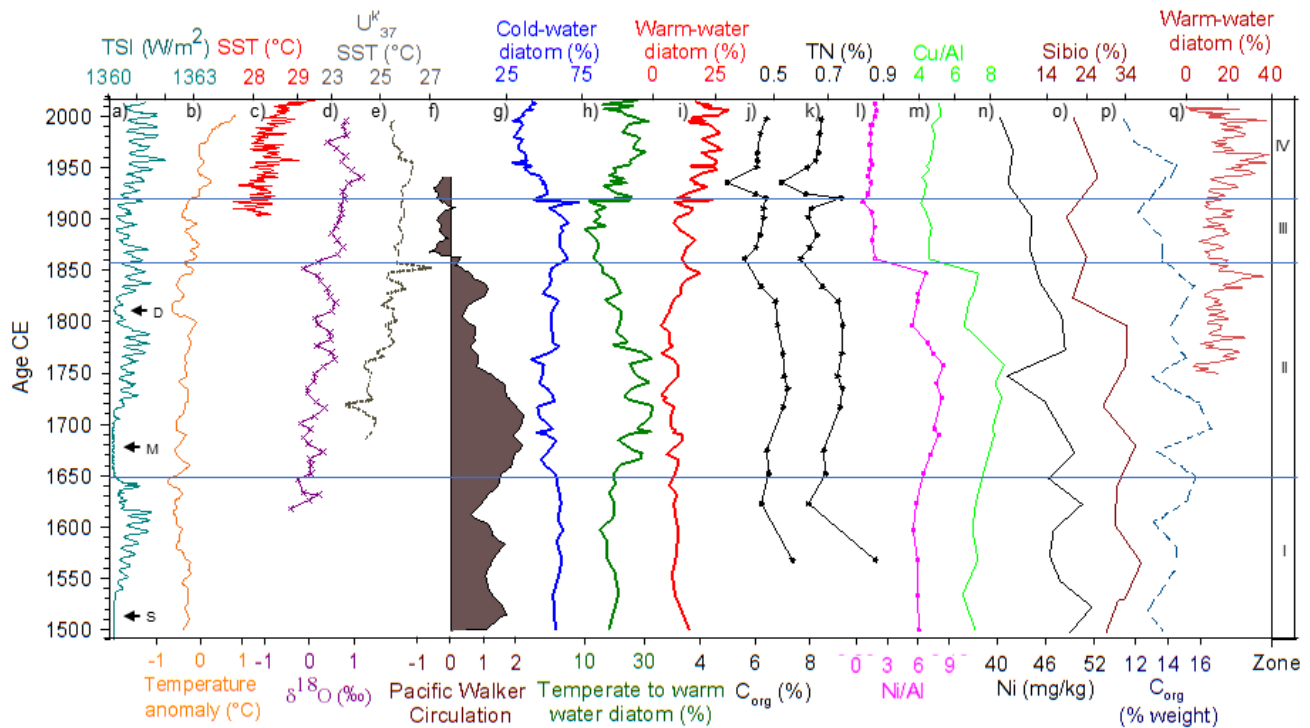
Figure 5. Paleoclimate records and the Tehua XII E03 record during the studied period. a) Total Solar Irradiance (TSI, W/m^2), Spörer (S), Maunder (M) and Dalton (D) minima (Lean, 2018). b) Surface temperature anomaly (°C) from the Northern Hemisphere (Mann et al., 2009). c) SST (°C) from GoT (IRI, 2015). d) stratification of the water column (Staines-Urías et al., 2009) from Gulf of California. e) Alkenone-derived SST (U$^{k'}_{37}$ °C) from Guaymas Basin (Goni et al., 2006). f) Pacific Walker Circulation strength (Griffiths et al., 2016). g) Cold-water diatom (%), h) temperate-water diatom (%), i) warm-water diatom (%), j) C$_{org}$ (%), K) TN (%), l) Ni/Al, and m) Cu/Al from GoT (this study). n) Ni concentration (mg/kg) (Choumiline et al., 2019) and o)

biogenic silica (Sibio %) (Barron and Bukry, 2007) from Gulf of California. p) C_{org} (weight %) from off the Baja California margin (Juárez et al., 2014). q) Warm-water diatom from Santa Barbara Basin (Barron et al., 2013). Horizontal lines indicate the periods (I to IV) identified with CONISS analysis.

4.3.1. Little Ice Age (zone I ~1500 to ~1648 CE and zone II ~1650 to ~1858 CE)

During the LIA period, the predominance of cold-water and high productivity assemblage and the low abundance of temperate to warm-water and warm-water taxa, as well as the highest values of C_{org}, TN, Ni/Al, and Cu/Al (Figs. 4-5), overall suggest the presence of upwelling and high productivity, presumably linked to LIA. Similar findings are observed in the Gulf of California and Baja California margin records during the LIA (Barron et al., 2003; Barron and Bukry, 2007; Juárez et al., 2014; Choumiline et al., 2019) (Fig. 5).

The LIA in the Northern Hemisphere has often been observed as negative surface temperature anomalies (~-0.7 to ~-0.3°C, Mann et al., 2009), associated with lower solar irradiance (Bard et al., 2000; Lean, 2018). Under these conditions, the mean position of the ITCZ is displaced southward (Haug et al., 2001; Sachs et al., 2009; Griffiths et al., 2016) related with a strengthened Pacific Walker Circulation (Griffiths et al., 2016). Although during the LIA, presumably, La Niña-like conditions were predominant (Yan et al., 2011; Griffiths et al., 2016; Beaufort and Grelaud. 2017), as it is suggested by the SOI (Fig. 5, Griffiths et al., 2016), the temporal resolution of our samples does not allow direct comparison with ENSO variability.

The southern position of the ITCZ reinforced northeasterly trade winds into the Gulf of Mexico and the Caribbean Sea (Black et al., 1999; Nyberg et al., 2002), which reached the Pacific coast of Central America (Glynn et al., 1983) and the GoT. Also, a southward migration of the high-pressure systems may have resulted in more frequent outbreaks, particularly during winters

(Lozano et al, 2007; Nyberg et al., 2002). As a result, strong Tehuanos winds blowing during the LIA, likely enhanced mixing and upwelling and therefore caused high productivity due to the nutrient input from subsurface waters into the photic zone (Lluch-Cota et al.,1997; Pennington et al., 2006). In the Gulf of Papagayo, close to the GoT, Glynn et al. (1983) reported the demise of coral reefs likely caused by low SST, triggered by an increase in duration or intensity of seasonal upwelling during the LIA (~1600 to ~1900 CE).

Our diatom record suggests that the LIA was not a homogeneous cold period. The increased abundance of the temperate to warm-water assemblage (Fig. 4) suggests less cold and less productive conditions from ~1650 to ~1858 CE (zone II), although our geochemical productivity proxies in this interval show a slight decrease after ~ 1850, similar to those found in the Gulf of California (biogenic silica %, Barron and Bukry, 2007) and the Baja California margin (C_{org}, Juarez et al., 2014) (Fig 5).

The relative decrease in productivity suggested by our diatom record between ~1650 and ~1858 CE is associated with the increase in solar irradiance after the Maunder minimum and the decrease in Pacific Walker Circulation (Fig.5). Other studies in the ETNP have also indicated the heterogeneity of the LIA, also attributed to solar activity variations (Barron et al., 2003; Barron and Bukry, 2007; Lozano-García et al., 2007; Staines-Urías et al., 2009; Cuna et al., 2014; Rodríguez-Ramírez et al., 2015; Choumiline et al., 2019).

4.3.2. Transition period (zone III ~1860 to ~1919 CE)

Although there is still no consensus in the ETNP records about the end of the LIA, we identified a transition period from ~1860 to ~1919 CE that could be interpreted as the end of LIA and the beginning of the CWP. The records closest to the GoT report the end of LIA at about ~1750 CE (Ricaurte-Villota et al., 2013), ~1820 CE (Juárez et al., 2014), ~1850 CE (Barron et

al., 2003; Barron and Bucky, 2007; Cuna et al., 2014; Del Castillo-Batista et al., 2018; Choumiline et al., 2019), and even ~1900 (Hodell et al., 2005).

In this interval, though some cold-water and high productivity taxa (*Chaetoceros* spores, *T. nitzschioides*, and *L. pacificum*) remained abundant, the increased abundance of warm-water and low productivity taxa (*N. pelagica*, *T. tenera*, and *R. bergonii*) characterized the period, indicating the transition toward warmer and less productive conditions (Fig. 4). Likewise, the sediments from this period were characterized by lower values of C_{org}, TN, Ni/Al, and Cu/Al ratio, suggesting a reduction in the productivity of the GoT, similarly to some productivity proxies from Gulf of California and off the Baja California margin (Barron et al., 2003; Barron and Bukry, 2007, Juárez et al., 2014; Choumiline et al., 2019) (Fig. 5).

As mentioned in section 3.4, *R. bergonii* is a deep-dwelling taxon that indicates strong stratification in the water column (Baumgartner et al., 1985; Lange et al., 1987; Lange et al., 1994; Kemp et al., 2000; Romero et al., 2011). In the GoT, greater stratification occurs during the summer and autumn when the thermocline and nutricline are found beyond ~50 m (~30 m during winter), and the upwelling and mixing events are restricted (Lluch-Cota et al., 1997). Also, this taxon is common during El Niño events on the Eastern North Pacific coast. Thus, the increased abundance of *R. bergonii* suggests that the GoT water column became more stratified around the mid-1800s, similar to the findings of Staines-Urías et al. (2009) (Fig. 4).

The general trend of this period shows a progressive warming since ~1850 CE (IPCC, 2014) largely associated with solar irradiance (Hoyt and Schatten, 1993; Lean et al., 1995; Bard et al., 2000) and global warming (IPCC, 2014). This warming trend is also observed in the Gulf of California by Staines-Urías et al. (2009), who pointed out rapid warming since the mid-1800s and enhanced water column stratification. Also, Goni et al. (2006) found a general trend of

increased SST of 1 to 2°C in Guaymas and Cariaco Basins since ~1800 CE (Fig. 5) and related them to the end of the LIA. Likewise, this period coincides with the weakening of the Pacific Walker Circulation since ~1860 CE (Yan et al., 2011; Griffiths et al., 2016) and the northward migration of the ITCZ (Sachs et al., 2009). Lacustrine sediments from central Mexico recorded wetter conditions after the LIA, coinciding with the ITCZ's northward displacement (Cuna et al., 2014). These conditions probably led to a weakening of the northeasterly trade winds over the Caribbean Sea (Nyberg et al., 2002), as well as to lesser frequent polar outbreaks over the Gulf of Mexico (Lozano-García et al., 2007), which would result in weaker Tehuanos winds in the GoT and consequently less upwelling and lower productivity. These findings together with those reported in the northwestern region of Mexico suggest warmer climate conditions and a likely decline in productivity during this transitional period in the ETNP.

4.3.3. Current Warm Period (zone IV ~1920 CE to ~today)

The most recent period is characterized by the highest abundance of the warm-water and oligotrophic assemblage together with a high abundance of moderate to warm conditions taxa (Fig. 4). High abundances of *N. interruptestriata*, *T. nitzschioides* var. *parvum*, and *F. doliolus* have been interpreted in La Paz , to reflect an incursion of tropical/subtropical water during anomalously warm periods (Acevedo-Acosta et al., 2021). Also, the rapid increase up to ~7.4% of the *C. planetophorus* (Fig. 4), a tropical taxon commonly found at temperatures above 23.3°C in the northwestern coasts of Mexico (Estrada-Gutiérrez et al., 2022), supports the idea that warmer conditions prevailed during this period. Diatom sedimentary records (Esparza-Alvarez et al., 2007; Martínez-López et al. 2007; Barron and Bukry, 2007; Barron et al., 2013) and planktonic foraminifera (Field et al., 2006) from the Eastern North Pacific also showed evidence of the global warming trend. For example, the percentage of warm-water diatoms (and

silicoflagellates, not graphed in Fig. 5) from Santa Barbara Basin exhibited a clear increase since ~1920 CE (Barron et al., 2013), in agreement with the peak of Alkenone-derived SST ($U^{k'}_{37}$) from the Guaymas Basin during the same time (Goni et al., 2006) (Fig. 5). Goni et al. (2006) attributed this increase in $U^{k'}_{37}$ SST to the northernmost Subtropical High and ITCZ migration in response to the Northern Hemisphere insolation. Under boreal summer conditions, the atmospheric regime results in weak winds over the central and southern regions of the Gulf of California; consequently, upwelling shuts down, leading to progressive warming and thermal stratification in the Guaymas Basin. In addition, the $U^{k'}_{37}$ SST peak after ~1920 CE could also reflect the northernmost incursion of warmer tropical water in the Eastern Tropical Pacific, similar to El Niño conditions in this region (e.g., Lavín et al., 1997).

On the other hand, our C_{org}, TN, Ni/Al, and Cu/Al records also remain with low values (Figs. 4-5; Table S6). Similarly, geochemical productivity proxies from the Gulf of California indicated reduced productivity in this period (Barron and Bukry, 2007; Juárez et al., 2014; Choumiline et al., 2019) (Fig. 5). In the GoT, human impact contamination has been identified by the increase in trace metals in the coastal and shelf zones (Pica-Granados et al., 1994; Ruiz-Fernández et al., 2004); however, since our sedimentary record is further seaward and deeper, our Ni and Cu concentrations were lower (16. 8 mg/kg for Ni and 47.0 mg/kg for Cu) than in the coastal and shelf zones. Therefore, we considered that our Ni and Cu records are not masked by human impact. Also, these elements' trend has been decreasing since ~1860 CE (together with those of the other productivity proxies) before the anthropic influence was evident (~1980) in the region (Ruiz-Fernández et al. 2004).

During this period, a generalized warming trend is observed in diverse records (Mann et al., 2009; IPCC, 2014), including the Eastern North Pacific (Goni et al., 2006; Staines-Urías et

al., 2009; Barron et al., 2013). In the SST record of the GoT, the evident warming trend of surface water in the 20th century (IRI, 2015) (Fig.5) leads us to infer that the reduced productivity during the CWP is associated with the warming trend, which caused a sharp upper ocean stratification, as is observed in the $\delta^{18}O$ of the planktonic foraminiferal record from the Gulf of California (Staines-Urías et al., 2009; Fig. 5).

Our observations document the dominance of warm conditions and low productivity since ~1920 CE in a more tropical area (~15°N latitude). These results agree with previous studies further north; therefore, this study documented the regional scale of the warming trend and its consequence on productivity in the tropical oceans.

5. Conclusions

This study provides a new $\Delta R = 247 \pm 30$ yr for the last five hundred years in the Gulf of Tehuantepec, estimated through the combinations of ^{210}Pb and ^{14}C methods in a bayesian model.

The diatom and geochemical proxies analyzed in the Gulf of Tehuantepec sediments reflected two predominant productivity conditions during the last five centuries, higher productivity conditions during the Little Ice Age and lesser productivity conditions during the Current Warm Period.

During the part of the LIA found in our record, low solar irradiance (Spörer, Maunder and Dalton minima) promoted the southward migration of the Intertropical Convergence Zone, which likely promoted more Tehuanos winds in the Gulf of Tehuantepec. This scenario resulted in enhanced upwelling and higher productivity as evidenced by the prevalence of cold and high productivity taxa (*Chaetoceros* spores*, T. nitzschioides, L. pacificum T. nanolineata*, and *R. setigera*) and high values of C_{org}, TN, Ni/Al, and Cu/Al. Temperate conditions and lesser

productivity from ~1650 to ~1858 CE, were suggested by the increase of some temperate to warm-water taxa (*T. bacillare*, *T. nitzschioides* var. *parvum*, *F. doliolus*, and *T. lineata*).

A transitional period (~1860 to ~1919 CE) towards the Current Warm Period was indicated by the appearance of most warm-water taxa (*N. pelagica*, *T. tenera*, and *R. bergonii*) as well as lower values of C_{org}, TN, Ni/Al, and Cu/Al. From ~1920 to ~2014 CE, the dominance of temperate to warm-water and mainly warm-water taxa (*T. bacillare*, *F. doliolus*, *C. litoralis*, *T. oestrupii*, *N. pelagica*, *C. planetophorus*, *T. tenera*, *P. minus*, *N. interruptestriata*, *T. lineata*, and *R. bergonii*) and low values of geochemical productivity proxies indicated even warmer conditions and lower productivity. These conditions were associated with diminished upwelling, and probably increased upper water column stratification and deeper thermocline derived from prevalence of warming trend, the northward migration of the ITCZ and weakening of the Pacific Walker Circulation.

Our findings highlight the importance of high-resolution productivity reconstructions and contribute to the knowledge of the response of the tropical regions to the Little Ice Age and Current Warm Period climates.

Acknowledgments

Declaration of Conflicting Interests: None.

References

Acevedo-Acosta JD, Martínez-López A, Morales-Acoltzi T et al. (2021) Self-organization maps (SOM) in the definition of a "transfer function" for a diatoms-based climate proxy. *Climate Dynamics* 56(1–2): 423–437.

Almaraz-Ruiz L (2017) *Variabilidad de las surgencias en el golfo de Tehuantepec durante el último siglo a través del registro sedimentario de diatomeas y foraminíferos bentónicos*. MSc thesis. Universidad Nacional Autónoma de México.

Amador JA, Alfaro EJ, Lizano OG et al. (2006) Atmospheric forcing of the eastern tropical Pacific: A review. *Progress in Oceanography* 69(2): 101–142.

Aquino-López MA, Blaauw M, Christen JA et al. (2018) Bayesian analysis of 210 Pb dating. *Journal of Agricultural, Biological, and Environmental Statistics* 23(3): 317–333.

Aquino-López MA, Ruiz-Fernández AC, Blaauw M et al. (2020) Comparing classical and Bayesian 210Pb dating models in human-impacted aquatic environments. *Quaternary Geochronology* 60.

Arellano-Torres E, Machain-Castillo ML, Contreras-Rosales LA et al. (2013) Foraminiferal faunal evidence for Glacial-Interglacial variations in the ocean circulation and the upwelling of the Gulf of Tehuantepec (Mexico). *Marine Micropaleontology* 100: 52–66.

Bard E, Raisbeck G, Yiou F et al. (2000) Solar irradiance during the last 1200 years based on cosmogenic nuclides. *Tellus, Series B: Chemical and Physical Meteorology* 52(3): 985–992.

Barron JA and Bukry D (2007) Solar forcing of Gulf of California climate during the past 2000 yr suggested by diatoms and silicoflagellates. *Marine Micropaleontology* 62(2): 115–139.

Barron JA, Bukry D and Bischoff JL (2003) A 2000-yr-long record of climate from the Gulf of California. In: N.L. West, G.J. and Blomquist (ed.) *Proceedings of the Nineteenth Pacific Climate Workshop*. Asilomar, Pacific Grove, CA 1–15.

Barron JA, Bukry D and Bischoff JL (2004) High resolution Paleoceanography of the Guaymas Basin, Gulf of California, During the Past 15 000 Years. *Marine Micropaleontology* 50(3): 185–207.

Barron JA, Bukry D and Dean WE (2005) Paleoceanographic history of the Guaymas Basin, Gulf of California, during the past 15,000 years based on diatoms, silicoflagellates, and biogenic sediments. *Marine Micropaleontology* 56(3–4): 81–102.

Barron JA, Bukry D and Field D (2010) Santa Barbara Basin diatom and silicoflagellate response to global climate anomalies during the past 2200 years. *Quaternary International* 215(1–2): 34–44.

Barron JA, Bukry D, Field DB et al. (2013) Response of diatoms and silicoflagellates to climate change and warming in the California Current during the past 250 years and the recent rise of the toxic diatom Pseudo-nitzschia australis. *Quaternary International* 310: 140–154.

Baumgartner T, Ferreira-Bartrina V, Schrader H et al. (1985) A 20-year varve record of siliceous phytoplankton variability in the central Gulf of California. *Marine Geology* 64(1–2): 113–129.

Beaufort L and Grelaud M (2017) A 2700-year record of ENSO and PDO variability from the californian margin based on coccolithophore assemblages and calcification. *Progress in Earth and Planetary Science* 4(1).

Bennett KD (1996) Determination of the number of zones in a biostratigraphical sequence. *New Phytologist* 132(1): 155–170.

Berger R, Taylor RE and Libby WF (1966) Radiocarbon content of marine shells from the California and Mexican West coast. *Science* 153(3738): 864–866.

Blaauw M (2022) Package "IntCal". Radiocarbon Calibration Curves. CRAN 28.

Blaauw M and Christen JA (2011) Flexible paleoclimate age-depth models using an autoregressive gamma process. *Bayesian Analysis* 6(3): 457–474.

Blaauw M, Christen JA, Aquino-Lopez MA et al. (2021) Package "rplum". Bayesian Age-Depth Modelling of Cores Dated by Pb-210. CRAN 12.

Blaauw M, Christen JA, Aquino-Lopez MA et al. (2022) Package " rbacon ". Age-Depth Modelling using Bayesian Statistics. CRAN 53.

Black DE, Peterson LC, Overpeck JT et al. (1999) Eight centuries of North Atlantic ocean atmosphere variabitity. *Science* 286(5445): 1709–1713.

Blanchet CL, Kasten S, Vidal L et al. (2012) Influence of diagenesis on the stable isotopic composition of biogenic carbonates from the Gulf of Tehuantepec oxygen minimum zone. *Geochemistry, Geophysics, Geosystems* 13(4): 1–20.

Calvert SE and Pedersen TF (2007) Chapter Fourteen Elemental Proxies for Palaeoclimatic and Palaeoceanographic Variability in Marine Sediments: Interpretation and Application. *Developments in Marine Geology* 1(07): 567–644.

Choumiline K, Pérez-Cruz L, Gray AB et al. (2019) Scenarios of deoxygenation of the eastern tropical North Pacific during the past millennium as a window Into the future of oxygen minimum zones. *Frontiers in Earth Science* 7(September): 1–23.

Crosta X and Koc N (2007) Diatoms: From Micropaleontology to Isotope Geochemistry. *Developments in Marine Geology* 1: 327–369.

Crowley TJ, Zielinski G, Vinther B et al. (2008) Volcanism and the little ice age. *PAGES News* 16(2): 22–23.

Cuna E, Zawisza E, Caballero M et al. (2014) Environmental impacts of Little Ice Age cooling in central Mexico recorded in the sediments of a tropical alpine lake. *Journal of Paleolimnology* 51(1): 1–14.

Cupp EE (1943) Marine Plankton Diatoms of the West Coast of North America. *Bulletin of The Scripps Institution of Oceanography* 5(1): 1–238.

Del Castillo-Batista AP, Figueroa-Rangel BL, Lozano-García S et al. (2018) 1580 years of human impact and climate change on the dynamics of a Pinus-Quercus-Abies forest in west-central Mexico. *Revista Mexicana de Biodiversidad* 89(1): 208–225.

Díaz-Asencio M, Sanchez-Cabeza JA, Ruiz-Fernández AC et al. (2020) Calibration and use of well-type germanium detectors for low-level gamma-ray spectrometry of sediments using a semi-empirical method. *Journal of Environmental Radioactivity* 225(September).

Esparza-Alvarez MA, Herguera JC and Lange C (2007) Last century patterns of sea surface temperatures and diatom (> 38 μm) variability in the Southern California Current. *Marine Micropaleontology* 64(1–2): 18–35.

Estrada Gutiérrez KM, Hernández Almeida OU, Siqueiros Beltrones DA et al. (2022) First record of *Cymatodiscus planetophorus* (Bacillariophyta) for littorals of NW Mexico; ecological remarks. *Revista Bio Ciencias* 9(322): 1–13.

Fiedler PC and Talley LD (2006) Hydrography of the eastern tropical Pacific: A review. *Progress in Oceanography* 69(2–4): 143–180.

Field DB, Baumgartner TR, Charles CD, Ferreira-Bartrina V, Ohman MD (2006) Planktonic Foraminifera of the California Current Reflect 20th-Century Warming. *Science Translational Medicine* 311(5757): 63–66.

García-Gallardo A, Machain-Castillo ML and Almaraz-Ruiz L (2021) Paleoceanographic evolution of the Gulf of Tehuantepec (Mexican Pacific) during the last ~6 millennia. *The Holocene* 31(4): 529–544.

Glynn PW, Druffel EM and Dunbar RB (1983) A dead Central American coral reef tract: possible link with the Little Ice Age (Costa Rica, Gulf of Papagayo, Gulf of Panama). *Journal of Marine Research* 41(3): 605-637.

Goni MA, Thunell RC, Woodwort MP et al. (2006) Changes in wind-driven upwelling during the last three centuries: Interocean teleconnections. *Geophysical Research Letters* 33(15): 3–6.

Goodfriend GA and Flessa KW (1997) Radiocarbon reservoir ages in the Gulf of California: roles of upwelling and flow from the Colorado river. *Radiocarbon* 39(2): 139–148.

Griffiths ML, Kimbrough AK, Gagan MK et al. (2016) Western Pacific hydroclimate linked to global climate variability over the past two millennia. *Nature Communications* 7: 1–9.

Grimm EC (1987) CONISS: A FORTRAN 77 program for stratigraphically constrained cluster analysis by the method of incremental sum of squares. *Computers & Geosciences* 13: 13–35.

Guiry MD, Guiry GM (2020) *AlgaeBase. World-wide electronic publication, National University of Ireland, Galway.* Available at: https://www.algaebase.org (accessed 9.1.22).

Gutiérrez D, Sifeddine A, Field DB et al. (2009) Rapid reorganization in ocean biogeochemistry off Peru towards the end of the Little Ice Age. *Biogeosciences* 6(5): 835–848.

Hasle GR and Syvertsen EE (1997) Marine Diatoms. In: CR Tomas (ed.) *Identifying Marine Diatoms*. San Diego, California: Academic Press 5–386.

Haug GH, Hughen KA, Sigman DM et al. (2001) Southward migration of the Intertropical Convergence Zone through the Holocene. *Science* 293(5533): 1304–1308.

Heaton TJ, Köhler P, Butzin M et al. (2020) Marine20 - The Marine Radiocarbon Age Calibration Curve (0-55,000 cal BP). *Radiocarbon* 62(4): 779–820.

Hendy IL and Pedersen TF (2006) Oxygen minimum zone expansion in the Eastern Tropical North Pacific during deglaciation. *Geophysical Research Letters* 33(20): 1–5.

Hernández-Becerril DU, Barón-Campis SA, Ceballos-Corona JGA et al. (2021) *Catálogo de fitoplancton del Pacífico central mexicano, Cruceros "MareaR" (2009-2019). B/O "El Puma." Universidad Nacional Autónoma de México*. México: Universidad Nacional Autónoma de México.

Hodell DA, Brenner M, Curtis JH et al. (2005) Climate change on the Yucatan Peninsula during the Little Ice Age. *Quaternary Research* 63(2): 109–121.

Hoyt DV and Schatten KH (1993) A discussion of plausible solar irradiance variations, 1700-1992. *Journal of Geophysical Research: Space Physics* 98(A11): 18895–18906.

IPCC (2014) *Climate Change 2014: Synthesis Report. Contribution of Working groups I, II and III to the Fifth Assessment Report of the Intergovernmental Panel on Climate Change*. Edited by LA Pachauri, RK Meyer. Geneve Switzerland.

IRI (2015) *Dataset GOSTA gisst22 sst*. Available at: http://iridl.ldeo.columbia.edu/SOURCES/.GOSTA/.gisst22/.sst/Y/%2815.66N%29%2815.66N%29RANGEEDGES/X/%2895.32W%29%2895.32W%29RANGEEDGES/ (accessed 8.17.21).

Juárez M, Sánchez A and González-Yajimovich O (2014) Variabilidad de la productividad biológica marina en el Pacífico nororiental durante el último milenio. *Ciencias marinas* 40(4): 211–220.

Juggins S (2020) The Rioja Package. Analysis of Quaternary Science Data 54.

Kemp AES, Pike J, Pearce RB et al. (2000) The "Fall dump" - A new perspective on the role of a "shade flora" in the annual cycle of diatom production and export flux. *Deep-Sea Research Part II: Topical Studies in Oceanography* 47(9–11): 2129–2154.

Kessler WS (2006) The circulation of the eastern tropical Pacific: A review. *Progress in Oceanography* 69(2–4): 181–217.

Lamb AL, Wilson GP and Leng MJ (2006) A review of coastal palaeoclimate and relative sea-level reconstructions using δ13C and C/N ratios in organic material. *Earth-Science Reviews* 75(1–4): 29–57.

Lange CB and Syvertsen EE (1989) *Cyclotella litoralis* sp. nov. (Bacillariophyceae), and its relationship to *C. striata* and *C. Stylorum*. *Nova Hedwigia* 48(3–4): 341–356.

Lange CB, Burke SK and Berger WH (1990) Biological production off Southern California is linked to climatic change. *Climate Change* 16: 319–329.

Lange CB, Treppke UF and Fischer G (1994) Seasonal diatom fluxes in the Guinea Basin and their relationships to trade winds, hydrography and upwelling events. *Deep-Sea Research Part I* 41(5–6).

Lange CB, Berger WH, Burke SK et al. (1987) El Niño in Santa Barbara Basin: Diatom, radiolarian and foraminiferan responses to the "1983 El Niño" event. *Marine Geology* 78(1–2): 153–160.

Lange CB, Weinheimer AL, Reid FMH et al. (1997) Sedimentation patterns of diatoms, radiolarians, and silicoflagellates in Santa Barbara Basin, California. *California Cooperative Oceanic Fisheries Investigations Reports* 38(August 1993): 161–170.

Lavín MF, Beier E, Badan A (1997) Estructuras hidrográficas y circulación del Golfo de California: Escalas estacional e interanual. Contribuciones a la Oceanografía Física en México. *Monografía* 3: 141-171.

Lavín MF, Fiedler PC, Amador JA et al. (2006) A review of eastern tropical Pacific oceanography: Summary. *Progress in Oceanography* 69(2–4): 391–398.

Lean JL (2018) Estimating Solar Irradiance Since 850 CE. *Earth and Space Science* 5(4): 133–149.

Lean J, Beer J and Bradley R (1995) Reconstruction of solar irradiance since 1610: Implications for climate change. *Geophysical Research Letters* 22(23): 3195–3198.

Li G, Cheng L, Zhu J et al. (2020) Increasing ocean stratification over the past half-century. *Nature Climate Change* 10(12): 1116–1123.

Li Y, Zhao Q and Lü S (2013) The genus *Thalassiosira* off the Guangdong coast, South China Sea. *Botanica Marina* 56(1): 83–110.

Lluch-Cota SE, Álvarez-Borrego SA, Santamaría del Angel EM et al. (1997) El Golfo de Tehuantepec y áreas adyacentes: variación espaciotemporal de pigmentos fotosintéticos derivados de satélite. *Ciencias Marinas* 23(3): 329–340.

Lozano-García MDS, Caballero M, Ortega B et al. (2007) Tracing the effects of the Little Ice Age in the tropical lowlands of eastern Mesoamerica. *Proceedings of the National Academy of Sciences of the United States of America* 104(41): 16200–16203.

Machain-Castillo ML, Monreal-Gómez MA, Arellano-Torres E, Merino-Ibarra M and González-Chávez G (2008) Recent planktonic foraminiferal distribution patterns and their relation to hydrographic conditions of the Gulf of Tehuantepec, Mexican Pacific. *Marine Micropaleontology* 66(2): 103–119.

Mann ME, Zhang Z, Rutherford S et al. (2009) Global Signatures and Dynamical Origins of the Little Ice Age and Medieval Climate Anomaly. *Science* 326(5957): 1256–1260.

Martinez -Lopez A, Baumgartner TR and Lange C (2007) Effects of Climate Change on Production of Siliceous Phytoplankton Over the Twentieth Century as Recorded in Sediments of the Santa Barbara Basin off Southern California. *Proceedings of the American Geophysical Union 2007 Joint Assembly* 1–2.

Meave del Castillo MA and Hernández-Becerril DU (1998) "Fitoplancton." In: M. Tapia–García (ed.) *El Golfo de Tehuantepec: El Ecosistema y sus Recursos*. México, D. F.: Universidad Autónoma Metropolitana (Unidad Iztapalapa) 59–74.

Meave del Castillo ME (2002) *Diatomeas planctónicas del Océano Pacífico de México. Informe final SNIB-CONABIO proyecto No. H176*. México, D. F.

Miller GH, Geirsdóttir Á, Zhong Y et al. (2012) Abrupt onset of the Little Ice Age triggered by volcanism and sustained by sea-ice/ocean feedbacks. *Geophysical Research Letters* 39(L02708): 1–5.

Moreno JL, Licea S and Santoyo H (1996) *Diatomeas del Golfo de California. Universidad Autónoma de Baja California Sur*. La Páz, México.

Moreno-Ruiz JL, Tapia-Garcia M, Licea S et al. (2011) Ecological composition and distribution of the diatoms from the Laguna Superior, Oaxaca, Mexico. *Journal of Environmental Biology* 32(4): 425–442.

Naya T (2012) Marine Thalassiosira species from coastal Pleistocene sediments in central Kanto Plain. *Diatom Research* 27(3): 141–163.

Nyberg J, Malmgren BA, Kuijpers A et al. (2002) A centennial-scale variability of tropical North Atlantic surface hydrography during the late Holocene. *Palaeogeography, Palaeoclimatology, Palaeoecology* 183(1–2): 25–41.

Oksanen J, Blanchet FG, Friendly M et al. (2020) Vegan-package Community Ecology Package: Ordination, Diversity and Dissimilarities 298.

Pennington JT, Mahoney KL, Kuwahara VS et al. (2006) Primary production in the eastern tropical Pacific: A review. *Progress in Oceanography* 69(2–4): 285–317.

Pica-Granados, Y, Botello, AV, Villanueva SF (1994) *La contaminación por actividades petroleras en el Puerto de Salina Cruz Oaxaca (1990–199). Serie Grandes Temas de la Hidrobiología: vol. 2. Los sistemas litorales.* Mexico City: UAMI, UNAM.

Pichevin LE, Ganeshram RS, Francavilla S et al. (2010) Interhemispheric leakage of isotopically heavy nitrate in the eastern tropical Pacific during the last glacial period. *Paleoceanography* 25(1).

R Core Team (2021) *R: A language and environment for statistical computing. R Foundation for Statistical Computing, Vienna, Austria.* Available at: https://www.r-project.org/. (accessed 7.1.22).

Reimer RW and Reimer PJ (2016) An Online Application for Δr Calculation. *Radiocarbon* 59(5): 1623–1627.

Ren J, Gersonde R, Esper O et al. (2014) Diatom distributions in northern North Pacific surface sediments and their relationship to modern environmental variables. *Palaeogeography, Palaeoclimatology, Palaeoecology* 402(March): 81–103.

Ricaurte-Villota C, González-Yajimovich O and Sanchez A (2013) Respuesta acoplada de la lluvia y la desnitrificación al forzamiento solar durante el Holoceno en la cuenca Alfonso. *Ciencias Marinas* 39(2): 151–164.

Rines JEB and Hargraves PE (1988) The Chaetoceros Ehrenberg (Bacillariophyceae) flora of Narragansett Bay, Rhode Island, U.S.A. *Bibliotheca Phycologica* 79: 1–196.

Rodríguez-Ramírez A, Caballero M, Roy P et al. (2015) Climatic variability and human impact during the last 2000 years in western Mesoamerica: Evidence of late Classic (AD 600-900) and Little Ice Age drought events. *Climate of the Past* 11(9): 1239–1248.

Romero O, Boeckel B, Donner B et al. (2002) Seasonal productivity dynamics in the pelagic central Benguela system inferred from the flux of carbonate and silicate organisms. *Journal of Marine Systems* 37(4): 259–278.

Romero OE, Hebbeln D and Wefer G (2001) Temporal and spatial variability in export production in the SE Pacific Ocean: Evidence from siliceous plankton fluxes and surface sediment assemblages. *Deep-Sea Research Part I: Oceanographic Research Papers* 48(12): 2673–2697.

Romero OE, Leduc G, Vidal L et al. (2011) Millennial variability and long-term changes of the diatom production in the eastern equatorial Pacific during the last glacial cycle. *Paleoceanography* 26(2): 1–11.

Romero OE, Thunell RC, Astor Y et al. (2009a) Seasonal and interannual dynamics in diatom production in the Cariaco Basin, Venezuela. *Deep-Sea Research Part I: Oceanographic Research Papers* 56(4): 571–581.

Romero OE, Rixen T and Herunadi B (2009b) Effects of hydrographic and climatic forcing on diatom production and export in the tropical southeastern Indian Ocean. *Marine Ecology Progress Series* 384: 69–82.

Romero-Centeno R, Zavala-Hidalgo J and Raga GB (2007) Midsummer gap winds and low-level circulation over the eastern tropical Pacific. *Journal of Climate* 20(15): 3768–3784.

Round FE Crawford RM and Mann DG (1990) *The Diatoms: Biology & Morphology of the genera. The University Cambridge Press*.

Ruiz-Fernández AC, Páez-Osuna F, Machain-Castillo ML et al. (2004). 210Pb geochronology and trace metal fluxes (Cd, Cu and Pb) in the Gulf of Tehuantepec, South Pacific of Mexico. *Journal of Environmental Radioactivity*, *76*(1–2): 161–175.

Ruiz-Fernández AC, Hillaire-Marcel C, de Vernal A et al. (2009) Changes of coastal sedimentation in the Gulf of Tehuantepec, South Pacific Mexico, over the last 100 years from short-lived radionuclide measurements. *Estuarine, Coastal and Shelf Science* 82(3): 525–536.

Ruiz-Fernández AC, Maanan M, Sanchez-Cabeza JA et al. (2014) Cronología de la sedimentación reciente y caracterización geoquímica de los sedimentos de la laguna de Alvarado, Veracruz (suroeste del golfo de México). *Ciencias Marinas* 40(4): 291–303.

Sachs JP, Sachse D, Smittenberg RH et al. (2009) Southward movement of the Pacific intertropical convergence zone AD 1400--1850. *Nature Geoscience* 2: 519–525.

Salvatteci R, Gutiérrez D, Field D et al. (2014) The response of the Peruvian Upwelling Ecosystem to centennial-scale global change during the last two millennia. *Climate of the Past* 10(2): 715–731.

Sancetta C (1992) Comparison of phytoplankton in sediment trap time series and surface sediments along a productivity gradient. *Paleoceanography* 7(2): 183–194.

Sancetta C (1995) Diatoms in the Gulf of California: Seasonal flux patterns and the sediment record for the last 15,000 years. *Paleoceanography* 10(1): 67–84.

Sanchez-Cabeza JA and Ruiz-Fernández AC (2012) 210Pb sediment radiochronology: An integrated formulation and classification of dating models. *Geochimica et Cosmochimica Acta* 82: 183–200.

Sanchez-Cabeza JA, Rico-Esenaro SD, Corcho-Alvarado JA et al. (2021) Plutonium in coral archives: A good primary marker for an Anthropocene type section. *Science of the Total Environment* 771: 145077.

Sanchez-Cabeza JA, Ruiz-Fernández AC, Ontiveros-Cuadras JF et al. (2014) Monte Carlo uncertainty calculation of 210Pb chronologies and accumulation rates of sediments and peat bogs. *Quaternary Geochronology* 23: 80–93.

Sautter LR and Sancetta C (1992) Seasonal associations of phytoplankton and planktic foraminifera in an upwelling region and their contribution to the seafloor. *Marine Micropaleontology* 18(4): 263–278.

Schrader HJ and Gersonde R (1978) Diatoms and silicoflagellates. In: W.J. Zachariasse (ed.) *Microplaeontological counting methods and techniques - an excercise on an eight metres section of the lower Pliocene of Capo Rossello. Sicily*. Odijk: Utrecht Micropaleontology Bulletin 129–176.

Schrader H, Swanberg N, Lycke AK et al. (1993) Diatom-inferred productivity changes in the eastern equatorial Pacific: The quaternary record of ODP leg 111, site 677. *Hydrobiologia* 269–270(1): 137–151.

Sifeddine A, Gutiérrez D, Ortlieb L et al. (2008) Laminated sediments from the central Peruvian continental slope: A 500 year record of upwelling system productivity, terrestrial runoff and redox conditions. *Progress in Oceanography* 79(2–4): 190–197.

Smrzka D, Zwicker J, Bach W et al. (2019) The behavior of trace elements in seawater, sedimentary pore water, and their incorporation into carbonate minerals: a review. *Facies* 65(41): 1-47.

Staines-Urías F, Douglas RG and Gorsline DS (2009) Oceanographic variability in the southern Gulf of California over the past 400 years: Evidence from faunal and isotopic records from planktic foraminifera. *Palaeogeography, Palaeoclimatology, Palaeoecology* 284(3–4): 337–354.

Tapia PM, Velazco F, Sifeddine A et al. (2010) Do dark/light laminae in core sediments from the Peruvian Upwelling Ecosystem represent ENSO events? A look into diatom assemblages. in *XV Congreso Peruano de Geología*. Cusco: Sociedad Geológica del Perú 35–39.

Thunell RC and Kepple AB (2004) Glacial-Holocene δ15N record from the gulf of Tehuantepec, Mexico: Implications for denitrification in the eastern equatorial Pacific and changes in atmospheric N2O. *Global Biogeochemical Cycles* 18(1): 1–12.

Torres-Ariño A, Okolodkov YB and Herrera-herrera NV (2019) Un listado del fitoplancton y microfitobentos del sureste del Pacífico mexicano A checklist of phytoplankton and microphytobenthos of the southeastern Mexican Pacific. *Cymbella* 5(1): 1–97.

Trasviña A, Barton ED, Brown J et al. (1995) Offshore wind forcing in the Gulf of Tehuantepec, Mexico: The asymmetric circulation. *Journal of Geophysical Research* 100(C10): 20649–20663.

Treinen-Crespo C, Barbara L, Villaescusa JA et al. (2021) Revisiting the marine reservoir age in Baja California continental margin sediments using 14C and 210Pb dating. *Quaternary Geochronology* 66(February).

Treppke FU, Lange C and Wefer G (1996) Vertical fluxes of diatoms and silicoflagellates in the eastern equatorial Atlantic, and their contribution to the sedimentary record. *Marine Micropaleontology* 28: 73–96.

Tribovillard N, Algeo TJ, Lyons T et al. (2006) Trace metals as paleoredox and paleoproductivity proxies: An update. *Chemical Geology* 232(1–2): 12–32.

Vázquez-Selem L (2011) Las glaciaciones en las montañas del centro de México. In: Caballero M and Ortega B (ed.) *Escenarios de cambio climático: Registros del Cuaternario en América Latina I*. Universidad Nacional Autónoma de México, México 215–238.

Yamaguchi R and Suga T (2019) Trend and Variability in Global Upper-Ocean Stratification Since the 1960s. *Journal of Geophysical Research: Oceans* 124(12): 8933–8948.

Yan H, Sun L, Wang Y et al. (2011) A record of the Southern Oscillation Index for the past 2,000 years from precipitation proxies. *Nature Geoscience* 4(9): 611–614.

CAPÍTULO 3: Changes on bottom water oxygenation during the last half millennium in the Gulf of Tehuantepec (Eastern Tropical Pacific): a multiproxy approach

Sometido a *Palaeogeography, Palaeoclimatology, Palaeoecology*

Authors:

Laura Almaraz-Ruiz[a], laura.almaraz.ruiz@gmail.com; María Luisa Machain-Castillo[b*], machain@cmarl.unam.mx; Abdelfettah Sifeddine[c-d], abdel.sifeddine@ird.fr; Ana Carolina Ruiz-Fernández[e], caro@ola.icmyl.unam.mx; Joan-Albert Sanchez-Cabeza[e], jasanchez@cmarl.unam.mx; Alejandro Rodríguez-Ramírez[b], alerdz@unam.mx; Mercedes Mendez-Millan[c], mercedes.mendez@ird.fr; Sandrine Caquineau[c], sandrine.caquineau@ird.fr.

[a]Posgrado en Ciencias del Mar y Limnología, Universidad Nacional Autónoma de México; Av. Universidad 3000, Ciudad Universitaria Coyoacán, C.P. 04510, Ciudad de México, México.

[b]Unidad Académica de Procesos Oceánicos y Costeros, Instituto de Ciencias del Mar y Limnología, Universidad Nacional Autónoma de México, Circuito Exterior s/n, Ciudad Universitaria, 04510, México.

[c]IRD, CNRS, SU, MNHN, IPSL, LOCEAN: Laboratoire d'Océanographie et du Climat: Expérimentations et Approches Numériques, 93143 Bondy, France.

[d]ERC2- Université Quisqueya. Port au Prince-Haïti.

[e]Unidad Académica Mazatlán, Instituto de Ciencias del Mar y Limnología, Universidad Nacional Autónoma de México, Calz. Montes Camarena s/n, Col. Playa Sur, 82040 Mazatlán, Sinaloa, México.

*Corresponding author ML Machain-Castillo

Abstract

The Gulf of Tehuantepec (GoT), in the Eastern Tropical North Pacific Ocean, is home to one of the largest and more intense Oxygen Minimum Zones (OMZ). To identify the OMZ variability during the last five hundred years in the GoT, we analyzed the temporal variations of benthic

foraminiferal (BF) assemblages, enrichment of redox-sensitive metals (Mo, V, Cd, U, and Re) and $\delta^{15}N_{sed}$, on a laminated sediment core. During the Little Ice Age (LIA; ~1500 to ~1860 CE), the BF assemblages showed high dominance, and the most abundant BF species in the sediments were *Epistominella sandiegoensis*, *Takayanagia delicata*, and *Buliminella tenuata*. This assemblage can withstand the lowest dissolved oxygen conditions, indicating an intensified OMZ, consistent with the enrichment of Mo, Re, Cd, U, and enhanced denitrification. During the Current Warm Period (CWP; ~1860 CE to present), the BF assemblages were more diverse, and the most abundant species were *Bolivina seminuda, Epistominella* sp.1, *Gyroidina nitidula*, and *Suggrunda eckisi*, an assemblage less tolerant to low dissolved oxygen conditions, together with lower concentrations of redox-sensitive metals and $\delta^{15}N_{sed}$, suggesting a weakening of the OMZ. Bottom-water oxygenation changes appear to respond to increased solar forcing caused by Intertropical Convergence Zone migration and strengthened Pacific Walker Circulation, which in turn modulated productivity, organic matter flux to the seabed, and oxygen consumption in the bottom water. Our findings agree with previous studies further north from the study site, indicating these changes' regional scale.

Keywords: oxygen minimum zone; benthic foraminifera; trace metal; $\delta^{15}N$; Little Ice Age; Current Warm Period.

1. Introduction

An oxygen minimum zone (OMZ) comprises water masses with dissolved oxygen (DO) concentrations permanently below ~0.5 mL/L (Helly and Levin, 2004). They are usually the result of the sluggish circulation of the Intermediate Water Masses (from ~200 to ~700 m depth) (Fiedler and Talley, 2006), high rates of organic matter decomposition (Helly and Levin, 2004; Fiedler and Talley, 2006) and, in tropical regions, a strong thermocline which hinders convection and exchange of oxygen-rich surface water into the deep ocean (local ventilation of subsurface waters) (Stramma et al., 2008; Keeling et al., 2010).

The Eastern Tropical North Pacific (ETNP) hosts the largest and one of the most intense OMZs of the world's modern oceans. Seasonal upwelling generates high fluxes of organic matter that consume DO during its remineralization, thereby enhancing the development of OMZ. Such is the case of the Gulf of Tehuantepec (GoT) in the Mexican Pacific, rich in marine resources and fisheries such as tuna, shrimp, and other pelagic species (Blackburn, 1962; Lluch-Cota et al., 1997). Therefore, OMZ variations may imply severe impacts on the economy and food availability in this region.

The extension and intensity of OMZs vary at diverse time scales (millennial, centennial, decadal, interannual, and seasonal) driven by climatic processes in relation to atmospheric-oceanic changes (Hendy and Kennett, 2003; Thunell and Kepple, 2004; Moffitt et al., 2015; Tems et al., 2016; Choumiline et al., 2019; García-Gallardo et al., 2021, 2022). A cold and dry period called the Little Ice Age (LIA) is recognized in the climate of Europe and North America from ~1400 to ~1850 CE (Crowley, 2000; Mann et al., 2009; Wanner et al., 2011). Several studies have been focused on the OMZ variability during the LIA in the ETNP (e.g., Ricaurte-Villota et al., 2013; Ontiveros-Cuadras et al., 2019; Choumiline et al., 2019; García-Gallardo et al., 2021),

its influence in more tropical latitudes such as the GoT (~15°N), is still poorly known. In the most recent period, a warming trend is observed around the globe (from ~1850s to present, IPCC, 2014), which have implications on the upper water column thermal stratification and, consequently, in the upper OMZ boundary (Deutsch et al., 2014; IPCC, 2014).

With the current warming trend, tropical oceans appear to experience deoxygenation as a consequence of enhanced stratification, leading to lesser oxygen diffusion and decreased oxygen dissolution in the ocean's surface (Stramma et al., 2008; Frölicher et al., 2009; Keeling et al., 2010) resulting in an intensification and expansion of the OMZ. However, other studies have found a weakening of the OMZ (e.g., Deutsch et al., 2014; Tems et al., 2016; Choumiline et al., 2019; Ontiveros-Cuadras et al., 2019) in response to reduced upwelling and productivity, and consequently, less oxygen consumption. This topic has not been resolved yet, nor is the OMZ temporal variability in the GoT during the last ~500 years. The present study aims to reconstruct the changes in the oxygenation in the GoT during the last five centuries and their relationship to ocean-climate variability through micropaleontological and geochemical proxies.

Bottom-water DO conditions can be reconstructed by various proxies, including benthic foraminifera (BF), redox-sensitive metals, and $\delta^{15}N$. Benthic foraminifera are marine protists widely distributed on seafloors, and their populations are affected by diverse factors, primarily DO concentrations and organic matter fluxes. Thus, their populations have been successfully used in sedimentary records as indicators of bottom-water oxygenation and productivity changes in modern oxygen-poor environments (e.g., Sen Gupta and Machain-Castillo, 1993; Bernhard and Sen Gupta, 1999; Murray et al., 2007; Moffitt et al., 2015; Balestra et al., 2018). Sediment redox chemistry is also commonly used to reconstruct past bottom water DO conditions. Redox-sensitive metals such as Mo, V, Cd, U, and Re are more/less soluble under oxidizing/reducing

conditions (Tribovillard et al., 2006). Thus, in the OMZs, these metals' authigenic enrichment is expected (Tribovillard et al., 2006). These metals are useful indicators of oxygen-deficient conditions and allow reconstructing paleoxygenation conditions on different time scales (e.g., Hendy and Pedersen, 2006; Choumiline et al., 2019; Sánchez et al., 2022).

The $\delta^{15}N$ of the bulk sedimentary organic matter ($\delta^{15}N_{sed}$) is a common tracer of changes in water column denitrification. In oxygen-depleted environments, where a high organic matter flux is transported to the seafloor, the extensive isotopic fractionation of nitrate (NO_3^-) results in a residual NO_3^- pool enriched in ^{15}N. Subsequently, these waters are upwelled to the surface, and the ^{15}N-rich NO_3^- is taken by the phytoplankton transferring the isotopic signal to the particulate organic matter, and eventually to sediments (Robinson et al., 2012). Therefore, denitrification within OMZs is coupled to the OMZ variations (Moffitt et al., 2015). However, the $\delta^{15}N$ signal in the sedimentary organic matter can also be affected by other processes such as N_2 fixation by diazotrophic bacteria, nitrification, the extent of surface NO_3^- utilization, and the anammox reaction (Robinson et al., 2012). Additionally, $\delta^{15}N$ can also reflect the organic matter source (e.g., Ruiz-Fernández et al., 2007). In near-shore environments, terrestrial interference could also affect the use of the $\delta^{15}N$ as a denitrification tracer (Altabet et al., 1999; Robinson et al., 2012). Nevertheless, $\delta^{13}C$ and C:N ratio in the GoT suggest that the organic matter has mainly a marine source (Almaraz-Ruiz et al., 2023). Likewise, previous studies in the ETNP (e.g., Altabet et al., 1999; Pichevin et al., 2010; Deutsch et al., 2014; Tems et al., 2016), including the GoT (Thunell and Kepple, 2004), have substantiated the sensitivity of $\delta^{15}N_{sed}$ to fluctuations in the denitrification intensity and its relationship with the OMZ variations.

2. Regional settings

The GoT is located in the southern Mexican Pacific. The convergence of two currents systems influences the region; equatorial waters that reach the GoT as the warm Costa Rica Coastal Current, which later turns offshore to join the North Equatorial Current, and remnants of the cold and subsurface water from the north as the tropical branch of California Current (Kessler 2006). Four water masses are found in the studied site (Machain-Castillo et al., 2008; Fiedler and Talley, 2006): Equatorial Surface Water, Subtropical Subsurface Water, North Pacific Intermediate Water, and Deep Pacific Water.

A well-developed OMZ extends from ~100 to ~800 m water depth in the GoT (Cline and Richards, 1972) (Fig. 1). Its upper boundary varies seasonally. During winter and spring, it moves closer to the surface at ~25 m with concentrations < 0.05 mL/L; during summer, it sinks until ~60 m (García-Gallardo et al., 2021). Sediments are laminated where this OMZ impinges on the seafloor.

From winter to spring, the ITCZ and the high-pressure systems are in their south-eastwardmost position (Lavín et al., 1992; Amador et al., 2006). This setting generates airflows channeled through the low elevation gap of the Isthmus of Tehuantepec, locally known as Tehuano-winds (Trasviña and Barton, 1997). During a Tehuano-wind event, intense winds perpendicular to the coast cause mixing and stress curling of the surface water column on the wind axis, the stratification breaks, and the nutrient-rich and cold sub-superficial waters are brought to the surface (Lavín et al., 1992), fertilizing the euphotic zone resulting in high biological productivity (Meave del Castillo and Hernández-Becerril, 1998). During summer to autumn, the high-pressure systems weaken, and the Tehuano-winds are relatively sporadic and weak (Romero-Centeno et al., 2007). Also, during this time of year, the ITCZ migrates to its northernmost position, resulting in heavy rainfall over the south of Mexico (Amador et al., 2006).

3. Material and methods

3.1. Sampling

A laminated sediment core (Tehua XII E03) was collected using a Reineck box corer in March 2014 aboard RV "El Puma" from the National Autonomous University of Mexico (UNAM). The coring site (15.6442° N and 95.3071° W, 743 m water depth) is within the modern core of the OMZ (Fig. 1A). Two sedimentary sequences were extracted from the Reineck box corer: Subcore Tehua XII E03a (34.5 cm long, 6.5 cm diameter) was sampled at 1 cm resolution and used for ^{210}Pb dating. Subcore Tehua XII E03b (32.5 cm long and 14 x 14 cm wide and high; Fig. 1C) was sampled in 92 laminae (~0.4 cm average thickness; Fig. 1C), which were visually recognized and extracted, using an x-ray digitalized acetate template. Since the Tehua XII E03b was sampled a few months later, it had drained longer and was a bit shorter (~2 cm). The subcores were stratigraphically correlated by visually identifying common light laminae in both subcores and ^{210}Pb-derived dates for subcore Tehua XII E03a were transferred to subcore Tehua XII E03b (Almaraz-Ruiz et al., 2023). Benthic foraminiferal analyses were conducted in each lamina. Redox-sensitive metals (Mo, V, Cd, U, and Re) and δ^{15}N analyses were performed in 24 samples at ~0.5 cm resolution in the Tehua XII E03b, also five radiocarbon (^{14}C) ages were determined at 4.0-4.5, 8.0-8.5, 20.0-20.5, 25.0-25.5 and 29.0-29.5 cm depth. The distinctive laminations observed along the core indicated relatively undisturbed sediments and a lack of bioturbation (Fig. 1C).

3.2. Age model

We used an integrated ^{210}Pb-^{14}C age-depth model produced by a Bayesian approach (Blaauw and Christen, 2011) with the rbacon R package (Blaauw et al., 2022) using the

MARINE20 curve (Heaton et al., 2020) and a local $\Delta R = 247 \pm 30$ years. Detailed information on the estimation of the local ΔR and age model is described in Almaraz-Ruiz et al. (2023).

3.3. Micropaleontological analyses

A portion of wet sediment was taken from each extracted lamina, weighed, and dried at room temperature. Approximately 1.5 g of dried sediment per sample was sieved (63 µm mesh) using tap water. The retained sediment fraction was air-dried in Whatman[TM] filter papers, weighed, and subdivided with an *Otto* microsplitter to obtain aliquots containing 300 to 500 specimens. In four samples (0-0.3, 0.3-0.45, 0.45-0.7, and 1.0-1.5 cm depth), the sediment was insufficient for BF analysis and was discarded in the study. All specimens were counted and identified under a stereoscopic microscope. The taxa were identified using the specialized literature following the Loeblich and Tappan (1988) classification. The total abundance is reported as the BF number per gram of sediment (ind/g), and the species composition as relative abundance (%). The BF counts precision was determined by duplicates in eight samples; the relative standard deviation was 11%.

The diversity was quantified through the species richness (number of species per sample) and dominance ($\lambda = D = \Sigma_i \left(\frac{n_i}{n}\right)^2$, where *ni* is the number of taxon individuals *i*) were computed using *Past 3.0 software* (Hammer and Harper, 2006).

3.4. Trace elements and $\delta^{15}N$ analyses

Dry sediment samples were macerated in an agate mortar, hot-plate acid digested (HNO_3 65%, HF 40%, and $HCLO_4$ 70%) in Polytetrafluoroethylene vessels, and analysed for the major element Al and the trace elements Mo, V, Cd, U, and Re, with a quadrupole-based inductively coupled plasma mass spectrometer (ICP-QMS 7900 Agilent of platform PARI at the Institut de

Physique du Globe de Paris). Element's concentrations accuracy and precision were determined using certified reference materials (MESS-3). Verifications were performed on duplicates in six samples. The duplicates' relative standard deviations were < 2% for Al, < 4% for Mo, V, Cd, and U, and < 9% for Re.

To assess the degree of enrichment or depletion of metals relative to their concentration in the lithogenic background, we calculated the enrichment factor (EF) of redox-sensitive metals using the formula described by Tribovillard et al. (2006): $EF_{element\ X} = (X/Al)_{sample} / (X/Al)_{background}$, where X is the metal analyzed in the sample. If the EFx is > 1, the metal is enriched relative to background values suggesting an authigenic source; conversely, if the EF is < 1, the metal is depleted relative to background values, likely pointing to a lithogenic source (Tribovillard et al., 2006; Valdés et al., 2021). Average upper continental crust or average shale concentrations are commonly used to estimate the lithogenic fraction when reference values local or regional are unavailable (e.g., Nameroff et al., 2002; Ontiveros-Cuadras et al., 2019; Valdés et al., 2021). However, the upper continental crust or average shale values may not necessarily represent the study area (Van der Weijden, 2002; Birch, 2017) and may lead to the wrong estimation of metal enrichments. Therefore, to calculate Efs, we used trace element reference values as the mean concentration of Al and the trace elements from the three bottommost (27.3 to 30.1 cm depth, ~1568 to ~1652 CE) core sections (e.g., Birch, 2017; Ochoa-Contreras et al., 2021; Ruiz-Fernández et al., 2022).

Furthermore, we calculated the Re/Mo ratio, frequently used to distinguish sediment anoxic from suboxic conditions (Crusius et al., 1996; Nameroff et al., 2002; Salvatteci et al., 2014). Under anoxic conditions, the ratio would be close or lesser to the Re/Mo in seawater (0.4

X 10^{-3}, Crusius et al., 1996) because both Re and Mo are being removed from the water column; while under suboxic conditions the ratio increases above the 0.4 X 10^{-3} (Nameroff et al., 2002).

The $\delta^{15}N_{sed}$ analysis was performed on bulk samples with a Flash HT 2000 elemental analyzer, coupled to an isotopic ratio mass spectrometer Delta Vplus via combustion-ConFlow IV interface from Thermo Fisher Scientific at the ALYSES platform (IRD/SU, Bondy France). $\Delta^{15}N$ calibration was performed with a certified material the EMAP2 ($\delta^{15}N=-1.57‰$, Sd=0.18‰, n=8) and an homemade standard, the Tyrosine ($\delta^{15}N= 10.04$ ‰, Sd=0.08‰, n=6). Precision and accuracy were assessed using the certified reference material HOS (high Organic Sediment) ($\delta^{15}N= 4.38‰$, Sd=0.27‰, n=4 – against the certified value $\delta^{15}N= 4.32 \pm 0.29$ ‰), and results are expressed in ‰ against $^{15}N_{air}$.

3.5. Statistical analyses

To identify the significance of the observed variability along the core, non-parametric unequal ANOVA (Analysis of Variance) tests were applied to the benthic foraminiferal assemblages, diversity indices, redox-sensitive metal concentrations, and $\delta^{15}N_{sed}$. In addition, we also applied Pearson's correlation coefficients to our data to determine the positive or negative correspondence between them.

4. Results

4.1. Chronology and sedimentation accumulation rates

According to the integrated age model reported in Almaraz-Ruiz et al. (2023), the samples presented an average temporal resolution of ~6 years (Table S1). In the most recent sediments (from ~1907 to ~2014 CE), the average sedimentation rate was 0.14 ± 0.07 cm/year. For the oldest ones, the average sedimentation rate was 0.08 ± 0.06 cm/year.

4.2. Benthic foraminifera

The total benthic foraminiferal abundance ranged from 32 to 4406 ind/g (average = 1776 ± 1091 ind/g) and showed maxima from ~1726 to ~1747, ~1889 to ~1935 and ~1964 to ~2009 CE. Species richness ranged from 6 to 30 taxa (average = 20 ± 5) and dominance index from 0.08 to 0.42 (average = 0.22 ± 0.08). In general, high benthic foraminiferal abundance periods coincided with high richness (Fig. 2, Table S1).

Forty-eight benthic foraminiferal taxa were determined throughout the core, of which eight species (relative abundances > 3.2 %) accounted for 89.0 % of the total population (Table S1). These species were: *Epistominella sandiegoensis* (38.3%), *Takayanagia delicata* (15.7%), *Buliminella tenuata* (12.9%), *Bolivina seminuda* (7.8%), *Epistominella* sp.1 (4.3%), *Gyroidina nitidula* (3.6%), *Suggrunda eckisi* (3.2%) and *Bolivina subadvena* (3.2%). The highest abundances of the first two taxa occurred mainly from ~1555 to ~1860 CE. The highest abundances of *Buliminella tenuata* were found between ~1660 and ~1880 CE; *B. seminuda*, *Epistominella* sp.1, and *G. nitidula* from ~1872 to ~2009 CE; and *S. eckisi* from ~1906 to ~2009 CE, similar to *B. subadvena*, although this last was more variable (Fig. 3).

4.3. Redox-sensitive metals and $\delta^{15}N_{sed}$

All redox-sensitive metals generally displayed a similar variation downcore (Fig. 4, Table S1). The ranges of the enrichment factors were 0.3 – 1.2 for Mo, 0.6 – 1.1 for V, 0.64 – 1.34 for Cd, 0.53 – 1.41 for U, and 0.38 – 1.82 for Re. Generally, the metals exhibited larger concentrations from ~1500 until ~1840 CE. The Re/Mo ratios ranged from 4.3 to 9.7 X 10^{-3}, whereas $\delta^{15}N_{sed}$ values varied between 6.89 and 9.15‰, with heavier values observed mainly from ~1652 to ~1796 and ~1924 to ~1935 CE.

5. Discussion

5.1. Benthic foraminiferal assemblages

The benthic foraminiferal population was typical of oxygen-deficient environments. Eight taxa accounted for 89.0 % of the total fauna (Fig. 3), which is a common feature of oxygen-poor environments where a few taxa dominate the assemblage (Phleger and Soutar, 1973; Golik and Phleger, 1977; Sen Gupta and Machain-Castillo, 1993; Bernhard et al., 1997; Moffitt et al., 2015).

Epistominella sandiegoensis, T. delicata, and *B. tenuata* showed a similar distribution pattern downcore (Fig. 3). These species have been found in the Eastern North Pacific under low DO concentrations; for instance, for *E. sandiegoensis* and *T. delicata* between < 0.3 to 2.0 mL/L (Bandy, 1961; Blake, 1976; Golik and Phleger, 1977; Douglas and Heitman, 1979; Bernhard et al., 1997; McGann and Conrad, 2018); *B. tenuata* between 0.05 to 0.8 mL/L (Harman, 1964; Blake, 1976; Douglas and Heitman, 1979; Quintero and Gardner, 1987; Bernhard et al., 1997; Páez et al., 2001), and even in complete anoxia (Bernhard et al., 1997; Ohkuchi et al., 2013). In the GoT, the relative abundances of living BF (Rose Bengal stained) indicated that *E. sandiegoensis* was the most abundant species in the samples characterized by the lowest DO concentrations (~0.05 to ~0.06 mL/L) (García-Gallardo et al., 2021), followed by *T. delicata* and *B. tenuata* (García-Gallardo personal communication). Rose Bengal stained *T. delicata,* and *B. tenuata* were not reported in García-Gallardo et al. (2021); however, these taxa were grouped with *E. sandiegoensis*, and therefore, they were used as part of the low oxygen assemblage during the last ~6 ka (García-Gallardo et al., 2021). Since these taxa also showed a similar distribution in the core Tehua XII E03, this assemblage was considered the most tolerant to low DO concentrations in our study (Fig. 4).

The species *B. Seminuda*, *Epistominella* sp.1, *G. nitidula*, and *S. eckisi* exhibited an opposite pattern to the previous species (Fig. 3). *Bolivina seminuda* has been reported in the Eastern Pacific at DO ranging from ~0.03 to ~0.1 mL/L (Bandy, 1961; Harman, 1964; Bernhard et al., 1997; Phleger and Soutar 1973; Perez-Cruz and Machain-Castillo, 1990), while *G. nitidula* was found in El Salvador at ~0.3 mL/L DO (Smith, 1963). *Suggrunda eckisi* has been reported in the Santa Barbara basin and the Gulf of California, ranging from 0.02 to 3.0 mL/L DO (Bandy, 1961; Phleger and Soutar, 1973; Douglas and Heitman, 1979; Bernhard et al., 1997). In the GoT, Rose Bengal stained specimens of *B. seminuda* occurred in samples with DO concentrations between 0.11 to 0.05 mL/L, higher than those where *E. sandiegoensis* was found (García-Gallardo et al., 2021). These authors grouped *Epistominella* sp (*Epistominella* sp 1 in this study), *G. nitidula* and *B. seminuda* in the higher DO assemblage.

5.2 Changes in the OMZ strength during the last ~500 years in the GoT

The benthic foraminiferal assemblages, redox-sensitive metals concentrations, $\delta^{15}N_{sed}$, and the presence of laminations (preserved at < 0.1-0.2 mL/L, Moffitt et al., 2015) along the entire sequence suggest that bottom water DO concentrations have been hypoxic and did not change considerably in the last half-millennium in the GoT. Nonetheless, as revealed by our proxies, it was possible to identify statistically significant variations between them (Anova tests $p < 0.05$) that suggest periods of relatively higher and lower DO levels related to the OMZ variations (Table S2) and that were associated with the LIA and CWP climate conditions. In addition, the Re/Mo values above to seawater ratio indicated that anoxic conditions were not reached during the studied period (Crusius et al., 1996; Nameroff et al., 2002; Salvatteci et al., 2014) (Fig. 4).

5.3. Bottom-water oxygenation during the Little Ice Age (~1500 to ~1860 CE)

The sediments corresponding to LIA were characterized by the predominance of the benthic foraminiferal assemblage most tolerant to low DO (*E. sandiegoensis*, *T. delicata*, and *B. tenuata*), with low abundance and high dominance (Fig. 4). The significant negative correlation ($p < 0.05$) between this assemblage versus richness (r = -0.78,) and faunal abundances (r = -0.71) (Table S3), and the significant positive correlation with dominance (r = 0.77) (Table S3), suggests a strongly stressed environment (such as OMZs) in which few taxa can withstand. Similar findings were previously observed in the benthic foraminiferal population in the last 6 ka in the GoT, in which lower oxygen concentration periods are characterized by the highest dominance (García-Gallardo et al., 2021, 2022).

The highest enrichment of redox-sensitive metals during LIA also suggested a stronger OMZ (Fig. 4). The significant positive correlation ($p < 0.05$) between the lowest DO assemblage *versus* Cd EF (r = 0.50) and Re EF (r = 0.54) (Table S3), showed that when these metals are more enriched, poor oxygen concentrations are found in the bottom water, and reduced redox conditions predominated, which allowed the dominance of the lowest DO benthic foraminiferal assemblage (Fig. 4). The $\delta^{15}N_{sed}$ signal suggested that lower oxygenation conditions in the water column prevailed from ~1650 to ~1750 CE (Fig. 4).

Few studies have focused on the redox and denitrification conditions during the LIA in the Mexican Pacific (Ricaurte-Villota et al., 2013; Tems et al., 2016; Choumiline et al., 2019; Ontiveros-Cuadras et al., 2019). Similar enrichment in redox-sensitive metals and $\delta^{15}N_{sed}$ have been found in Alfonso Basin (Ricaurte-Villota et al., 2013; Choumiline et al., 2019) and the Mazatlan margin (Ontiveros-Cuadras et al., 2019).

The LIA in the ETNP is characterized by high productivity attributed to enhanced upwelling (Goni et al., 2006; Barron and Bukry, 2007; Juárez et al., 2014; Choumiline et al., 2019). Our previous results of C_{org} percentage in core Tehua XII E03 (Almaraz-Ruiz et al., 2023) showed highest C_{org} values and dominance of cold-water and high-productivity diatom taxa in the LIA interval, suggesting an increase in the organic matter flux associated with increased upwelling, which led to an increased oxygen consumption causing the strengthening of the OMZ in the GoT. These conditions are consistent with a southward shift in the average position of the ITCZ (Haug et al., 2001) and the strengthening of Pacific Walker Circulation (PWC) (Griffiths et al., 2016), which are driven mainly by the low solar irradiance that prevailed during the LIA (Bard et al., 2000; Lean, 2018). Under these conditions, the establishment of the benthic foraminiferal assemblage more tolerant to reduced DO levels is promoted, as well as the enrichment of redox-sensitive metals and $\delta^{15}N_{sed}$ (Fig. 4).

5.4. Bottom-water oxygenation during the Current Warm Period (~1860 to ~2009 CE)

The CWP was characterized by the predominance of less tolerant to low DO benthic foraminiferal assemblage (*B. seminuda, Epistominella* sp. 1, *G. nitidula*, and *S. eckisi*), with high abundance, and low diversity (Fig. 4). Significant ($p < 0.05$) positive correlations between the higher DO assemblage *versus* richness (r = 0.78) and faunal abundances (r = 0.47) (Table S3), as well as a significant negative correlation with the dominance (r = -0.77) (Table S3), suggested an improvement of oxygen environmental conditions. Higher DO concentrations in the bottom water led to less environmental stress allowing a more diverse population (low dominance) and higher fossil abundance. These trends coincide with the results observed in periods of greater oxygenation in the last 6 ka in the study site (García-Gallardo et al., 2021, 2022).

The redox-sensitive metals showed lower concentrations during this period, suggesting less hypoxic conditions in the GoT. Significant ($p < 0.05$) negative correlations between the higher DO assemblage *versus* Cd EF (r = -0.55) and Re EF (r = -0.57) (Table S3) corroborated that the higher DO assemblage is dominant when redox conditions are less intense, that is, a weaker OMZ. $\Delta^{15}N_{sed}$ showed low variations from ~1770 CE onwards except from ~1924 to ~1935 CE. In general, the $\delta^{15}N_{sed}$ showed its lower values during the CWP, particularly in the past ~60 years, suggesting lesser denitrification of the water column (Fig. 4). Our redox-sensitive metals and $\delta^{15}N_{sed}$ agree with previous studies in the ETNP, which also reveal lower reducing conditions (Dean et al., 2004; Choumiline et al., 2019; Ontiveros-Cuadras et al., 2019; Sánchez et al., 2022), and a decrease of denitrification during the last ~150 years (Deutsch et al., 2014; Tems et al., 2016).

Climatically, the CWP is characterized by increased solar irradiance (Bard et al., 2000; Lean, 2018). This condition promoted the northward ITCZ migration and a weaker PWC (Haug et al., 2001; Griffiths et al., 2016), weakening the winds that generated upwelling in the ETNP (Goni et al., 2006; Barron and Bukry, 2007; Choumiline et al., 2019). The lowest C_{org} values and the predominance of warm-water and low productivity diatom taxa in the core Tehua XII E03 during the CWP also agree with a lower organic matter flux associated with reduced upwelling (Almaraz-Ruiz et al., 2023), which led to lower oxygen consumption in the bottom water. However, it has been observed that the warming trend has reduced the oxygen supply to the ocean due to a lower dissolution and more stratification in the water column (Stramma et al., 2008; Keeling et al., 2010). Our data indicate that a higher DO concentration could be more influenced by the reduction in upwelling, which can explain the weakening of the OMZ during the CWP in the GoT.

6. Conclusions

The accumulation of Mo, V, Cd, U, and Re, $\delta^{15}N_{sed}$ enrichment, as well as the benthic foraminiferal assemblages in the sedimentary record Tehua XII E03, revealed variations in the bottom water oxygenation during the Little Ice Age and the Current Warm Period.

The Little Ice Age (~1500 to ~1860 CE) was characterized by low abundances, high dominance, and the predominance of a lower dissolved oxygen benthic foraminiferal assemblage (*Epistominella sandiegoensis*, *Takayanagia delicata*, and *Buliminella tenuata*), together with the larger enrichment of redox-sensitives metals and $\delta^{15}N_{sed}$. These conditions indicate the OMZ's strengthening in the GoT, which was primarily associated with increased productivity. In contrast, during the Current Warm Period (~1860 to ~2009 CE), the high abundances, lower dominance, and predominance of a higher dissolved oxygen benthic foraminiferal assemblage (*Bulimina seminuda*, *Epistominella* sp. 1, and *Gyroidina nitidula*), as well as lower enrichment of the redox-sensitive metals and $\delta^{15}N_{sed}$, suggested a weakening of the OMZ in the GoT. This weakening is primarily associated with decreasing upwelling and productivity.

This climate variability in the Eastern Tropical North Pacific is primarily driven by the Intertropical Convergence Zone migration and the strength of the Pacific Walker Circulation, which modulate upwelling, productivity, and the thermocline depth, and consequently the bottom water oxygen. Our findings revealed that the OMZ variability in the GoT during the last five centuries agrees well with other northern records, indicating these changes' regional scale. Likewise, these results highlight the impact of the warming trend of the last ~150 years on the OMZs of tropical regions, which contribute to the study of the impact of recent climate change in these regions.

Acknowledgments

References

Almaraz-Ruiz, L., Machain-Castillo, M.L., Sifeddine, A., Ruiz-Fernandez, A.C., Sanchez-Cabeza, J.A., Rodríguez-Ramírez, A., López-Mendoza, P., Mendez-Millan, M., Caquineau, S., 2023. Diatom-based paleoproductivity and climate change record of the Gulf of Tehuantepec (Eastern Tropical Pacific) during the last ~500 years. The Holocene.

Altabet, M.A., Pilskaln, C., Thunell, R., Pride, C., Sigman, D., Chavez, F., Francois, R., 1999. The nitrogen isotope biogeochemistry of sinking particles from the margin of the eastern North Pacific. Deep. Res. Part I Oceanogr. Res. Pap. 46, 655–679. https://doi.org/10.1016/S0967-0637(98)00084-3

Amador, J.A., Alfaro, E.J., Lizano, O.G., Magaña, V.O., 2006. Atmospheric forcing of the eastern tropical Pacific: A review. Prog. Oceanogr. 69, 101–142. https://doi.org/10.1016/j.pocean.2006.03.007

Balestra, B., Quintana-Krupinski, N.B., Erohina, T., Fessenden-Rahn, J., Rahn, T., Paytan, A., 2018. Bottom-water oxygenation and environmental change in Santa Monica Basin, Southern California during the last 23 kyr. Palaeogeogr. Palaeoclimatol. Palaeoecol. 490, 17–37. https://doi.org/10.1016/j.palaeo.2017.09.002

Bandy, O.L., 1961. Distribution of foraminifera, radiolaria and diatoms in sediments of the Gulf of California. Micropaleontol. 7, 1–26. https://doi.org/10.2307/1484140

Bard, E., Raisbeck, G., 78ou, F., Jouzel, J., 2000. Solar irradiance during the last 1200 years based on cosmogenic nuclides. Tellus, Ser. B Chem. Phys. Meteorol. 52, 985–992.

Barron, J.A., Bukry, D., 2007. Solar forcing of Gulf of California climate during the past 2000 yr suggested by diatoms and silicoflagellates. Mar. Micropaleontol. 62, 115–139. https://doi.org/10.1016/j.marmicro.2006.08.003

Bernhard, J.M., Sen Gupta, B.K., 1999. Foraminifera of oxygen- depleted environments, in: Modern Foraminifera. Pp. 201–216. https://doi.org/10.1007/0-306-48104-9_12

Bernhard, J.M., Sen Gupta, B.K., Borne, P.F., 1997. Benthic foraminifera proxy to estimate dysoxic bottom-water oxygen concentrations: Santa Barbara Basin, U. S. Pacific continental margin. J. Foraminifer. Res. 27, 301–310. https://doi.org//10.2113/gsjfr.27.4.301

Birch, G.F., 2017. Determination of sediment metal background concentrations and enrichment in marine environments – A critical review. Sci. Total Environ. 580, 813–831. https://doi.org/10.1016/j.scitotenv.2016.12.028

Blaauw, M., Christen, J.A., Aquino-Lopez, M.A., Esquivel, V.J., Gonzalez, O.M., Belding, T., Theiler, J., Gough, B., Karney, C., 2022. Package 'rbacon'. Age-Depth Modelling using Bayesian Statistics.

Blaauw, M., Christen, J.A., 2011. Flexible paleoclimate age-depth models using an autoregressive gamma process. Bayesian Anal. 6, 457–474. https://doi.org/10.1214/11-BA618

Blackburn, M., 1962. An oceanographic study of the Gulf of Tehuantepec., Special Scientific Report-Fisheries.

Blake, G.H., 1976. The distribution of benthic foraminifera in the outer borderland and its relationship to Pleistocene facies. M.S. Thesis, University of South Carolina.

Choumiline, K., Pérez-Cruz, L., Gray, A.B., Bates, S.M., Lyons, T.W., 2019. Scenarios of deoxygenation of the Eastern Tropical North Pacific during the past millennium as a window into the future of Oxygen Minimum Zones. Front. Earth Sci. 7. https://doi.org/10.3389/feart.2019.00237

Cline, J.D., Richards, F.A., 1972. Oxygen deficient conditions and nitrate reduction in the Eastern Tropical North Pacific Ocean. Limnol. Oceanogr. 17. https://doi.org/10.4319/lo.1972.17.6.0885

Crowley, T.J., 2000. Causes of climate change over the past 1000 years. Science 289, 270–277. https://doi.org/10.1126/science.289.5477.270

Crusius, J., Calve, S., Pedersen, T., Sage, D., 1996. Rhenium and molybdenum enrichments in sediments as indicators of oxic, suboxic and sulfidic conditions of deposition. Earth Planet. Sci. Lett. 65–78. https://doi.org/10.1016/S0012-821X(96)00204-X

Dean, W., Pride, C., Thunell, R., 2004. Geochemical cycles in sediments deposited on the slopes of the Guaymas and Carmen Basins of the Gulf of California over the last 180 years. Quat. Sci. Rev. 23, 1817–1833. https://doi.org/10.1016/j.quascirev.2004.03.010

Deutsch, C., Berelson, W., Thunell, R., Weber, T., Tems, C., McManus, J., Crusius, J., Ito, T., Baumgartner, T., Ferreira, V., Mey, J., Van Geen, A., 2014. Centennial changes in North Pacific anoxia linked to tropical trade winds. Science 345, 665–668. https://doi.org/10.1126/science.1252332

Douglas, R.G., Heitman, H.L., 1979. Slope and basin benthic foraminifera of the California borderland, in: Larry J. Doyle and Orrin H. Pikey (Ed.), Geology of Continental Slopes. Broken Arrow, OK: SEPM Special Publication, pp. 231–246.

Fiedler, P.C., Talley, L.D., 2006. Hydrography of the eastern tropical Pacific: A review. Prog. Oceanogr. 69, 143–180. https://doi.org/10.1016/j.pocean.2006.03.008

Frölicher, T.L., Joos, F., Plattner, G.K., Steinacher, M., Doney, S.C., 2009. Natural variability and anthropogenic trends in oceanic oxygen in a coupled carbon cycle-climate model ensemble. Global Biogeochem. Cycles 23. https://doi.org/10.1029/2008GB003316

García-Gallardo, Á., Machain-Castillo, M.L., Almaraz-Ruiz, L., 2021. Paleoceanographic evolution of the Gulf of Tehuantepec (Mexican Pacific) during the last ~6 millennia. Holocene 31, 529–544. https://doi.org/10.1177/0959683620981724

García-Gallardo, Á., Almaraz-Ruiz, L., Machain-Castillo, M.L., 2022. Paleoceanography of the Gulf of Tehuantepec during the Medieval Warm Period. Mar. Micropaleontol. 170. https://doi.org/10.1016/j.marmicro.2021.102081

Golik, A., Phleger, F.B., 1977. Benthonic Foraminifera from the Gulf of Panama. J. Foraminifer. Res. 7, 83–99. https://doi.org/10.2113/gsjfr.7.2.83

Goni, M.A., Thunell, R.C., Woodwort, M.P., Müller-Karger, F.E., 2006. Changes in wind-driven upwelling during the last three centuries: Interocean teleconnections. Geophys. Res. Lett. 33, 3–6. https://doi.org/10.1029/2006GL026415

Griffiths, M.L., Kimbrough, A.K., Gagan, M.K., Drysdale, R.N., Cole, J.E., Johnson, K.R., Zhao, J.X., Cook, B.I., Hellstrom, J.C., Hantoro, W.S., 2016. Western Pacific hydroclimate linked to global climate variability over the past two millennia. Nat. Commun. 7, 1–9. https://doi.org/10.1038/ncomms11719

Hammer, O., Harper, D., 2006. Paleontological Data Analysis. Blackwell Publishing, Oxford. https://doi.org/10.1017/S0016756806272480

Harman, R.A., 1964. Distribution of Foraminifera in the Santa Barbara Basin, California. Micropaleontol. 10, 81. https://doi.org/10.2307/1484628

Haug, G.H., Hughen, K.A., Sigman, D.M., Peterson, L.C., Röhl, U., 2001. Southward migration of the intertropical convergence zone through the Holocene. Science 293, 1304–1308. https://doi.org/10.1126/science.1059725

Heaton, T.J., Köhler, P., Butzin, M., Bard, E., Reimer, R.W., Austin, W.E.N., Ramsey, C.B., Grootes, P.M., Hughen, K.A., Kromer, B., Reimer, P.J., Adkins, J., Burke, A., Cook, M.S., Olsen, J., Skinner, L.C., 2020. Marine20 – The Marine Radiocarbon Age Calibration Curve (0-55,000 cal BP). Radiocarbon 62, 779–820. https://doi.org/10.1017/RDC.2020.68

Helly, J.J., Levin, L.A., 2004. Global distribution of naturally occurring marine hypoxia on continental margins. Deep. Res. Part I Oceanogr. Res. Pap. 51, 1159–1168. https://doi.org/10.1016/j.dsr.2004.03.009

Hendy, I.L., Kennett, J.P., 2003. Tropical forcing of North Pacific intermediate water distribution during Late Quaternary rapid climate change? Quat. Sci. Rev. 22, 673–689. https://doi.org/10.1016/S0277-3791(02)00186-5

Hendy, I.L., Pedersen, T.F., 2006. Oxygen minimum zone expansion in the Eastern Tropical North Pacific during deglaciation. Geophys. Res. Lett. 33, 1–5. https://doi.org/10.1029/2006GL025975

IPCC, 2014. Cambio climático 2014: Informe de síntesis., Contribución de los Grupos de trabajo I, II y III al Quinto Informe de Evaluación del Grupo Intergubernamental de Expertos sobre el Cambio Climático. Ginebra, Suiza.

Juárez, M., Sánchez, A., González-Yajimovich, O., 2014. Variabilidad de la productividad biológica marina en el Pacífico nororiental durante el último milenio. Ciencias Mar. 40, 211–220. https://doi.org/10.7773/cm.v40i4.2477

Keeling, R.F., Körtzinger, A., Gruber, N., 2010. Ocean Deoxygenation in a Warming World. Ann. Rev. Mar. Sci. 2, 199–229.

Kessler, W.S., 2006. The circulation of the eastern tropical Pacific: A review. Prog. Oceanogr. 69, 181–217. https://doi.org/10.1016/j.pocean.2006.03.009

Lavín, M.F., Robles, J.M., Argote, M.L., Barton, E.D., Smith, R., Brown, J., Kosro, M., Trasviña, A., Velez, H.S., García, J., 1992. Física del Golfo de Tehuantepec. Cienc. Desarro. XVIII, 97–108.

Lean, J.L., 2018. Estimating Solar Irradiance Since 850 CE. Earth Sp. Sci. 5, 133–149. https://doi.org/10.1002/2017EA000357

Lluch-Cota, S.E., Álvarez-Borrego, S.A., Santamaría del Angel, E.M., Müller-Karger, F.E., Hernández-Vázquez, S., 1997. El Golfo de Tehuantepec y áreas adyacentes: variación espaciotemporal de pigmentos fotosintéticos derivados de satélite. Ciencias Mar. 23, 329–340. https://doi.org/10.7773/cm.v23i3.809

Loeblich A.R. and Tappan H., 1988. Foraminiferal Genera and their Classification. Van Norstrand Reinhold International Company Limited.

Machain-Castillo, M.L., Monreal-Gómez, M.A., Arellano-Torres, E., Merino-Ibarra, M., González-Chávez, G., 2008. Recent planktonic foraminiferal distribution patterns and their relation to hydrographic conditions of the Gulf of Tehuantepec, Mexican Pacific. Mar. Micropaleontol. 66, 103–119. https://doi.org/10.1016/j.marmicro.2007.08.003

Mann, M.E., Zhang, Z., Rutherford, S., Bradley, R.S., Hughes, M.K., Shindell, D., Ammann, C., Faluvegi, G., Ni, F., 2009. Global Signatures and Dynamical Origins of the Little Ice Age and Medieval Climate Anomaly. Science (80). 326, 1256–1260. https://doi.org/10.1126/science.1177303

McGann, M., Conrad, J.E., 2018. Faunal and stable isotopic analyses of benthic foraminifera from the Southeast Seep on Kimki Ridge offshore southern California, USA. Deep. Res. Part II Top. Stud. Oceanogr. 150, 92–117. https://doi.org/10.1016/j.dsr2.2018.01.011

Meave del Castillo, M.A., Hernández-Becerril, D.U., 1998. "Fitoplancton," in: M. Tapia–García. (Ed.), El Golfo de Tehuantepec: El Ecosistema y Sus Recursos. Universidad Autónoma Metropolitana (Unidad Iztapalapa), México, D. F., pp. 59–74.

Moffitt, S.E., Moffitt, R.A., Sauthoff, W., Davis, C. V., Hewett, K., Hill, T.M., 2015. Paleoceanographic insights on recent oxygen minimum zone expansion: Lessons for modern oceanography. PloS One 10, 1–39. https://doi.org/10.1371/journal.pone.0115246

Murray, J.W., Stewart, K., Kassakian, S., Krynytzky, M., DiJulio, D., 2007. Oxic, Suboxic and Anoxic Conditions in the Black Sea, in: Gilbert, A., Yanko-Hombach, V., and Panin, N. (Ed.), The Black Sea Flood Question: Changes in Coastline, Climate and Human Settlement. Kluwer Pub., pp. 1–21. https://doi.org/10.1007/978-1-4020-5302-3

Nameroff, T.J., Balistrieri, L.S., Murray, J.W., 2002. Suboxic trace metal geochemistry in the eastern tropical North Pacific. Geochim. Cosmochim. Acta 66, 1139–1158. https://doi.org/10.1016/S0016-7037(01)00843-2

Ochoa-Contreras, R., Jara-Marini, M.E., Sanchez-Cabeza, J.A., Meza-Figueroa, D.M., Pérez-Bernal, L.H., Ruiz-Fernández, A.C., 2021. Anthropogenic and climate induced trace element contamination in a water reservoir in northwestern Mexico. Environ. Sci. Pollut. Res. 28, 16895–16912. https://doi.org/10.1007/s11356-020-11995-3

Ohkushi, K., Kennett, J.P., Zeleski, C.M., Moffitt, S.E., Hill, T.M., Robert, C., Beaufort, L., Behl, R.J., 2013. Quantified intermediate water oxygenation history of the NE Pacific: A new benthic foraminiferal record from Santa Barbara basin. Paleoceanography 28, 453–467. https://doi.org/10.1002/palo.20043

Ontiveros-Cuadras, J.F., Thunell, R., Ruiz-Fernández, A.C., Benitez-Nelson, C., Machain-Castillo, M.L., Tappa, E., Sanchez-Cabeza, J.A., 2019. Centennial OMZ changes in the NW Mexican Margin from geochemical and foraminiferal sedimentary records. Cont. Shelf Res. 176, 64–75. https://doi.org/10.1016/j.csr.2019.02.009

Páez, M., Zúniga, O., Valdés, J., Ortlieb, L., 2001. Foraminíferos bentónicos recientes en sedimentos micróxicos de la bahía Mejillones del Sur (23° S), Chile. Rev. Biol. Mar. Oceanogr. 36, 129–139. https://doi.org/10.4067/s0718-19572001000200002

Perez-Cruz, L.L., Machain-Castillo, M.L., 1990. Benthic foraminifera of the oxygen minimum zone, continental shelf of the Gulf of Tehuantepec, Mexico. J. Foraminifer. Res. 20, 312–325. https://doi.org/10.2113/gsjfr.20.4.312

Phleger, F.B., Soutar, A., 1973. Production of benthic foraminifera in three east Pacific oxygen minima. Micropaleontology 19, 110–115. https://doi.org/10.2307/1484973

Pichevin, L.E., Ganeshram, R.S., Francavilla, S., Arellano-Torres, E., Pedersen, T.F., Beaufort, L., 2010. Interhemispheric leakage of isotopically heavy nitrate in the eastern tropical Pacific during the last glacial period. Paleoceanography 25. https://doi.org/10.1029/2009PA001754

Quintero, P.J. and Gardner, J.V., 1987. Benthic Foraminifera on the continental shelf and upper slope. Russian River, northern California. J. Foraminifer. Res. 17, 132–152. https://doi.org/10.2113/gsjfr.17.2.132

Ricaurte-Villota, C., González-Yajimovich, O., Sanchez, A., 2013. Respuesta acoplada de la lluvia y la desnitrificación al forzamiento solar durante el Holoceno en la cuenca Alfonso. Ciencias Mar. 39, 151–164. https://doi.org/10.7773/cm.v39i2.2224

Robinson, R.S., Kienast, M., Luiza Albuquerque, A., Altabet, M., Contreras, S., De Pol Holz, R., Dubois, N., Francois, R., Galbraith, E., Hsu, T.C., Ivanochko, T., Jaccard, S., Kao, S.J., Kiefer, T., Kienast, S., Lehmann, M., Martinez, P., McCarthy, M., Möbius, J., Pedersen, T., Quan, T.M., Ryabenko, E., Schmittner, A., Schneider, R., Schneider-Mor, A., Shigemitsu, M., Sinclair, D., Somes, C., Studer, A., Thunell, R., Yang, J.Y., 2012. A review of nitrogen

isotopic   alteration   in   marine   sediments.   Paleoceanography   27.
https://doi.org/10.1029/2012PA002321

Romero-Centeno, R., Zavala-Hidalgo, J., Raga, G.B., 2007. Midsummer gap winds and low-level circulation over the eastern tropical Pacific. J. Clim. 20, 3768–3784. https://doi.org/10.1175/JCLI4220.1

Ruiz-Fernández, A.C., Frignani, M., Tesi, T., Bojórquez-Leyva, H., Bellucci, L.G., Páez-Osuna, F., 2007. Recent sedimentary history of organic matter and nutrient accumulation in the Ohuira Lagoon, northwestern Mexico. Arch. Environ. Contam. Toxicol. 53, 159–167. https://doi.org/10.1007/s00244-006-0122-3

Ruiz-Fernández, A.C., Sanchez-Cabeza, J.A., Pérez-Bernal, L.H., Blaauw, M., Cardoso-Mohedano, J.G., Aquino-López, M.A., Giralt, S., 2022. Recent trace element contamination in a rural crater lake, NW Mexico. J. Paleolimnol. https://doi.org/10.1007/s10933-022-00268-3

Salvatteci, R., Gutiérrez, D., Field, D., Sifeddine, A., Ortlieb, L., Bouloubassi, I., Boussafir, M., Boucher, H., Cetin, F., 2014. The response of the Peruvian Upwelling Ecosystem to centennial-scale global change during the last two millennia. Clim. Past 10, 715–731. https://doi.org/10.5194/cp-10-715-2014

Sánchez, A., Shumilin, E., Rodríguez-Figueroa, G., 2022. Trace elements V, Ni, Mo and U: A geochemical tool to quantify dissolved oxygen concentration in the oxygen minimum zone of the north-eastern Pacific. J. Mar. Syst. 230. https://doi.org/10.1016/j.jmarsys.2022.103732

Sen Gupta, B.K., Machain-Castillo, M.L., 1993. Benthic foraminifera in oxygen-poor habitats. Mar. Micropaleontol. 20, 183–201. https://doi.org/10.1016/0377-8398(93)90032-S

Smith, P.B., 1963. Recent Foraminifera off Central America, Quantitative and qualitative study of the family Bolivinidae. U.S. Geol. Surv. Prof. Pap. 429, 39.

Stramma, L., Johnson, G.C., Sprintall, J., Mohrholz, V., 2008. Expanding Oxygen-Minimum Zones in the Tropical Oceans. Science 320, 655–658. https://doi.org/10.1126/science.1153847

Tems, C.E., Berelson, W.M., Thunell, R., Tappa, E., Xu, X., Khider, D., Lund, S., González-Yajimovich, O., Hamann, Y., 2016. Decadal to centennial fluctuations in the intensity of the eastern tropical North Pacific oxygen minimum zone during the last 1200 years. Paleoceanography 31, 1138–1151. https://doi.org/10.1002/2015PA002904.Received

Thunell, R.C., Kepple, A.B., 2004. Glacial-Holocene $\delta15N$ record from the gulf of Tehuantepec, Mexico: Implications for denitrification in the eastern equatorial Pacific and changes in atmospheric N2O. Global Biogeochem. Cycles 18, 1–12. https://doi.org/10.1029/2002gb002028

Trasviña, A., Barton, E.D., 1997. Los Nortes del Golfo de Tehuantepec: la circulación costera inducida por el viento. Contrib. A la Oceanogr. Física en México. Monogr. No. 3.

Tribovillard, N., Algeo, T.J., Lyons, T., Riboulleau, A., 2006. Trace metals as paleoredox and paleoproductivity proxies: An update. Chem. Geol. 232, 12–32. https://doi.org/10.1016/j.chemgeo.2006.02.012

Valdés, J., Sifeddine, A., Guiñez, M., Castillo, A., 2021. Oxygen minimum zone variability during the last 700 years in a coastal upwelling area of the Humboldt system (Mejillones, 23° S, Chile). A new approach from geochemical signature. Prog. Oceanogr. 193, 102520. https://doi.org/10.1016/j.pocean.2021.102520

Van Der Weijden, C.H., 2002. Pitfalls of normalization of marine geochemical data using a common divisor. Mar. Geol. 184, 167–187. https://doi.org/10.1016/S0025-3227(01)00297-3

Wanner, H., Solomina, O., Grosjean, M., Ritz, S.P., Jetel, M., 2011. Structure and origin of Holocene cold events. Quat. Sci. Rev. 30, 3109–3123. https://doi.org/10.1016/j.quascirev.2011.07.010

Figure captions

Figure 1. A) Sampling site of sediment core Tehua XII E03 (black diamond), B) Dissolved oxygen concentration profile at the collection site. C) Core Tehua XII E03*b* photography.

Figure 2. Benthic foraminiferal abundance (ind/g), species richness, and dominance index in core Tehua XII E03. Dashed lines indicate the average values of each record.

Figure 3. Relative abundances (%) of the most abundant benthic foraminiferal species (> 3.2 %) in core Tehua XII E03. Dashed lines indicate the average value of each record.

Figure 4. Comparison of the proxies analyzed in core Tehua XII E03: benthic foraminiferal abundance (ind/g), dominance index, lower DO benthic foraminiferal assemblage (*E. sandiegoensis*, *T. delicata*, *B. tenuata*), higher DO benthic foraminiferal assemblage (*B. seminuda*, *Epistominella* sp. 1, *G. nitidula*, and *S. eckisi*), enrichment factors of Mo, V, Cd, U, and Re, Re/Mo ratio, and $\delta^{15}N_{sed.}$ C_{org} (%) (Almaraz-Ruiz et al., 2023). Dashed lines indicate average values.
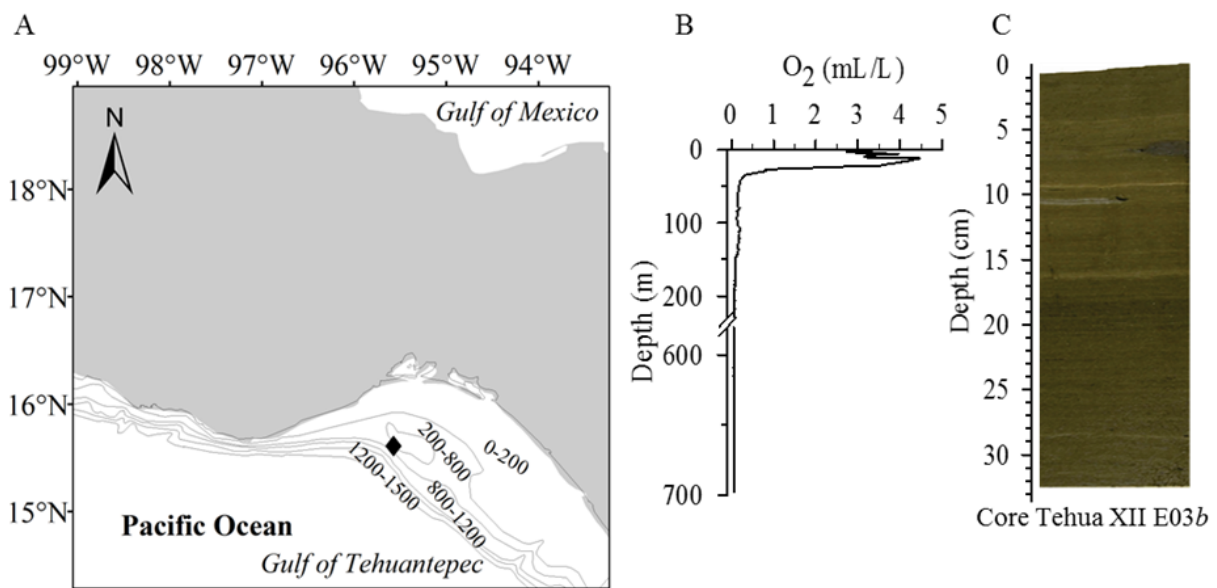
Figure 1.
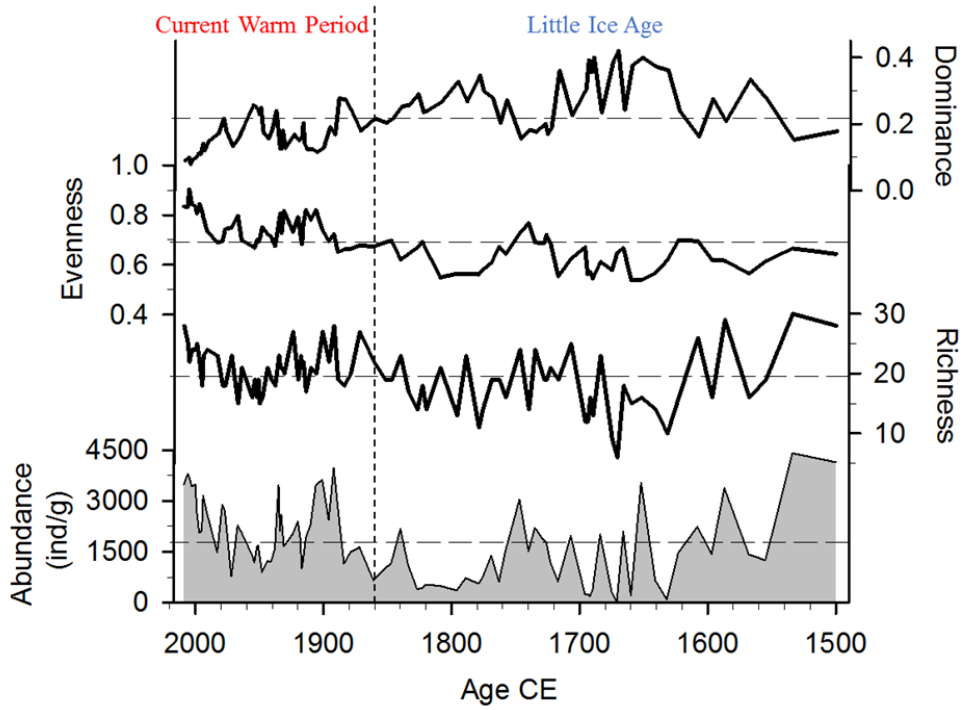
Figure 2.
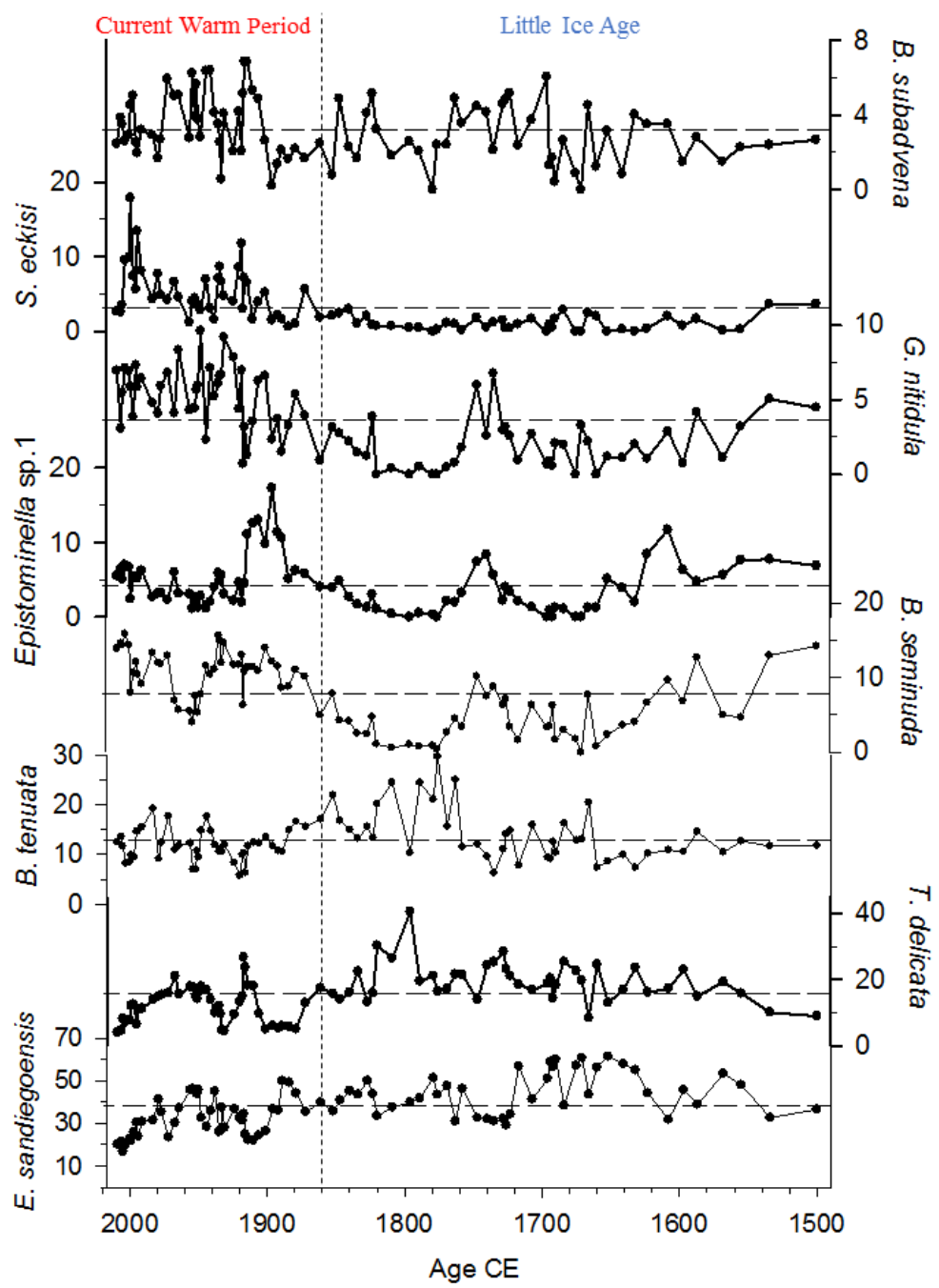
Figure 3.
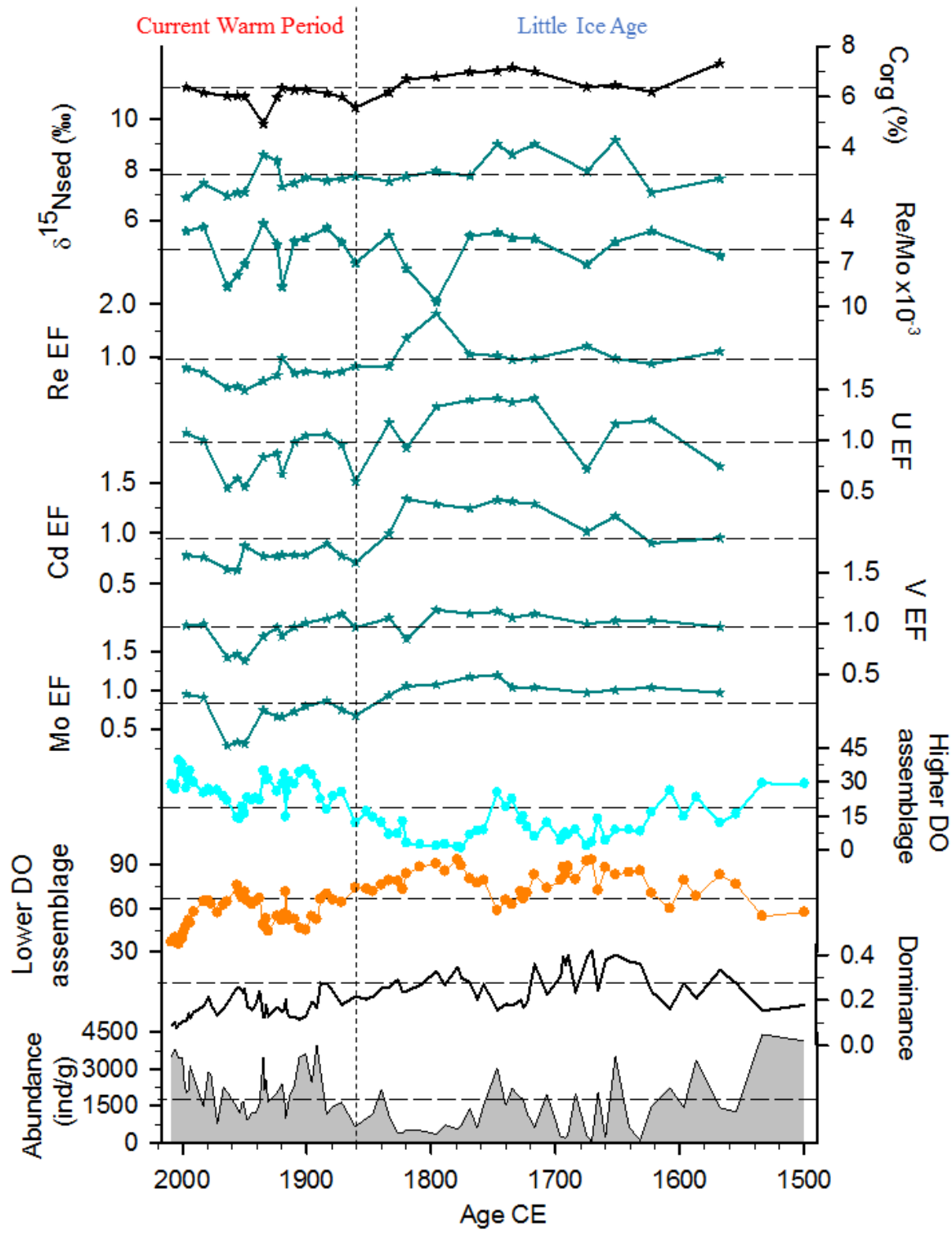
Figure 4.

CAPÍTULO 4: Variabilidad de la paleoproductividad durante el último milenio en el Golfo de Tehuantepec (Pacífico sur mexicano): registro de diatomeas

1. Introducción

El clima del PTNO de los últimos dos milenios (EC) responde con distinta frecuencia e intensidad a las variaciones climático-oceanográficas (ej. Barron y Bukry, 2007; Juárez et al., 2014; Choumiline et al., 2019). Dos periodos climáticos conocidos como el PCM de ~950 a ~1250 EC (Mann et al., 2009) y la PEH de ~1350 a ~1850 EC (Crowley et al., 2008; Mann et al., 2009) destacan dentro de la variabilidad de la EC, excedidos solo por la tendencia de calentamiento de los últimos ~150 años (Man y Jones, 2003).

La variabilidad de la productividad marina en el PTNO durante la EC ha sido asociada principalmente a los cambios en la irradiancia solar, que a su vez tiene influencia en la posición de los sistemas de alta presión del Pacífico Norte y de la migración de la ZCIT (Juárez et al., 2014; Choumiline et al., 2019). Adicionalmente, la actividad volcánica se ha relacionado con el clima de la PEH (Crowley et al., 2008). Más recientemente, la tendencia de calentamiento atribuido principalmente a la influencia antrópica puede explicar gran parte de la tendencia de los últimos ~150 años (IPCC, 2014).

Se han llevado a cabo en la cuenca del Pacífico Nororiental, principalmente en el Golfo de California y en la Península de Baja California, algunos estudios sobre la variabilidad de la productividad en los últimos milenios (ej. Barron et al., 2003; Barron y Bukry, 2007; Ricaurte-Villota et al., 2013; Juárez et al., 2014; Choumiline et al., 2019); sin embargo, en regiones más tropicales como el GT un estudio de este tipo es aún ausente.

El GT es un sitio de interés científico en estudios paleoclimáticos y paleoceanográficos ya que está influenciada por la convergencia del sistema de corrientes frías del Pacífico Nororiental y por el sistema de corrientes cálidas ecuatoriales. Ambos sistemas de corrientes oceánicas responden a la variabilidad climática promedio del Pacífico Oriental; por lo tanto, se espera que las variaciones climáticas de los últimos milenios en el PTNO queden registradas en los sedimentos del GT.

En el presente estudio se propone identificar la variabilidad de la productividad del último milenio, basado en un registro de diatomeas de un núcleo sedimentario colectado en el GT. Dado que la zona de estudio forma parte del PTNO se espera que las señales climáticas más evidentes registradas en latitudes más norteñas, particularmente el PCM (Barron y Bukry, 2007; Ricaute-Villota et al., 2013) y la PEH (Barron y Bukry, 2007; Ricaute-Villota et al., 2013; Juárez et al., 2014; Choumiline et al., 2019), también sean observadas en los sedimentos del GT.

3. Material y métodos

3.1. Núcleo MD02-2521

El núcleo sedimentario MD02-2521 fue colectado a bordo del B/O *Marion Dufresne* en junio de 2002, a una profundidad de 719 m dentro del núcleo de la ZOM del GT (15º 40.25' N; 95º 18.00' W, Fig. 1). La secuencia se colecto con un nucleador de Pistón (Calypso Square Corer) y se recuperaron 571.5 cm de sedimento. Posteriormente, en el Laboratorio de Micropaleontología y Paleoceanografía de la UNAM, el núcleo fue muestreado a 0.5 cm de espesor a 1 cm de resolución. Análisis de diatomeas se realizaron en cada centímetro de los primeros 100 cm de la secuencia sedimentaria (Fig. 1).
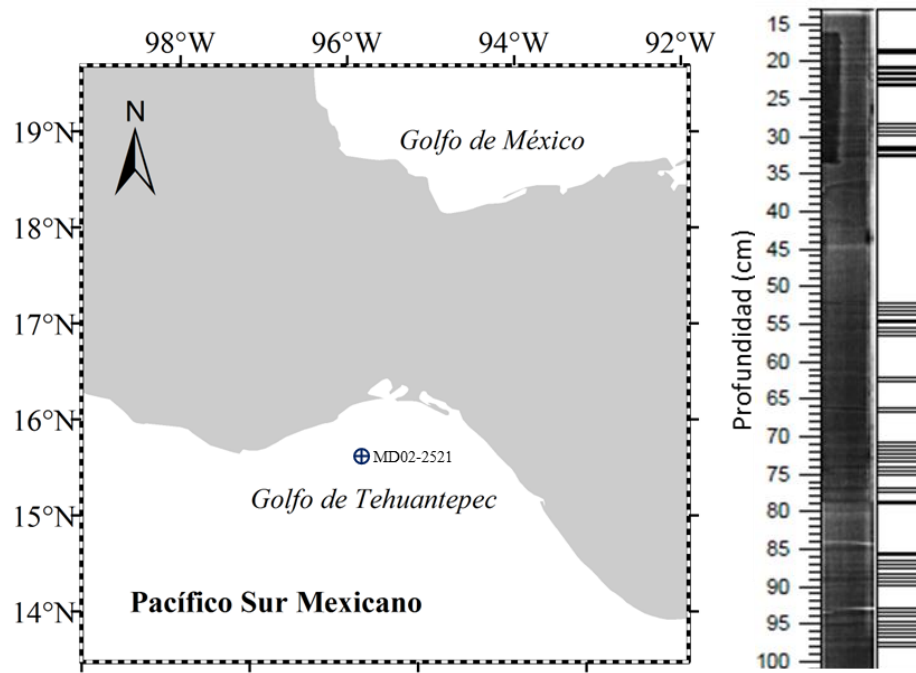
Figura 1. Localización del punto de muestreo de núcleo MD02-2521. Radiografía de los primeros 100 cm de núcleo MD02-2521.

La cronología de los sedimentos se estableció a través del fechado por radiocarbono (^{14}C; AMS, realizados en el laboratorio de Lalonde, Ottawa Canadá) de ocho muestras de sedimento total en las profundidades 0.1-0.6, 9-10, 100-100.5, 192.5-193, 300-300.5, 399.5-400, 500-500.5, 556-556.5 cm (Fig. 2). Las edades de ^{14}C fueron calibrados con la curva Marina 20 (Heaton et al., 2020) y corregidas por el reservorio local de $\Delta R = 247 \pm 30$. (Capítulo 2, Almaraz-Ruiz et al., 2023).

3.2. Obtención de las diatomeas

Se procesaron ~0.5 g de sedimento seco para la obtención de las diatomeas siguiendo la metodología de Schrader y Gersonde (1978). La materia orgánica se eliminó con peróxido de hidrógeno (H_2O_2) al 18% y ácido nítrico al 70% (HNO_3) a una temperatura de ~60°C, y los carbonatos con ácido clorhídrico (HCl) al 10%. Posteriormente, se realizaron enjuagues con agua

destilada hasta neutralizar la acidez de las muestras y eliminar las sales. Una vez limpios los sedimentos se almacenaron en un volumen estándar de 30 mL.

Se realizaron montajes en laminillas permanentes utilizando cubreobjetos de 18 mm de diámetro, en el cual se distribuyeron alícuotas de 200 µl de la muestra. En la mayoría de las muestras fue necesario aplicar diluciones que nos permitieran hacer las identificaciones y conteos, que fueron consideradas en los cálculos de las abundancias. Posteriormente, las muestras fueron fijadas en portaobjetos usando Naphrax como medio de montaje (índice de refracción =1.74).

Las determinaciones taxonómicas y los conteos se realizaron en un microscopio óptico en iluminación de contraste de fases (Nikon eclipse N*i*). Se contaron al menos 500 valvas por muestra siguiendo el criterio de Crosta y Koc (2007). Los organismos fueron identificados usando las claves y descripciones taxonómicas de Cupp (1943), Round et al. (1990), Moreno et al. (1996), Hasle y Syvertsen (1997), Hernández-Becerril et al. (2021), y literatura especializada.

3.3. Procesamiento de los datos

Los conteos fueron estandarizados a número de valvas por gramo de sedimentos seco (valvas/g) para determinar la abundancia absoluta. Se construyó una nueva matriz reducida con las especies más abundantes > 1.0 %, resultando una matriz de 23 taxones y 90 muestras. El corte se realizó al 1% ya que a este nivel se contiene al menos el 85% de la abundancia total de diatomeas y se elimina la influencia de las especies raras. Sobre está matriz reducida, se realizó un análisis de factores modo-Q en el software *Statistica 10*. La selección de las muestras que componen cada factor fue delimitada por cargas factoriales > 0.70. La elección de los taxones que componen cada factor fue delimitada por puntuaciones factoriales > 0.70. Con el conocimiento de la afinidad ecológica de las especies que forman cada asociación se interpretó

la distribución de los factores a lo largo de la secuencia y su relación con las variaciones climáticas del último milenio. Se calculó la riqueza de especies (número de especies por muestra), el índice de equidad de Pielou (J') y la diversidad de Fisher (α) (Fisher et al., 1943) usando el software *Primer* vers. 6.0.

4. Resultados

4.1. Modelo de edad del núcleo MDO02-2521

El modelo de edad de ^{14}C del MD02-2521 actualizado de García-Gallardo et al. (2021) (Fig. 2), revela de acuerdo con la tasa de acumulación sedimentaria promedio del periodo de interés, que es de 1.13 mm/año, que los primeros ~100 cm del núcleo corresponden a los últimos ~1000 años, correspondiente de ~618 ~1610 EC. Se traslapa parcialmente con el núcleo TEHUA XII E 03 en el período de ~1500 a ~1610 EC.
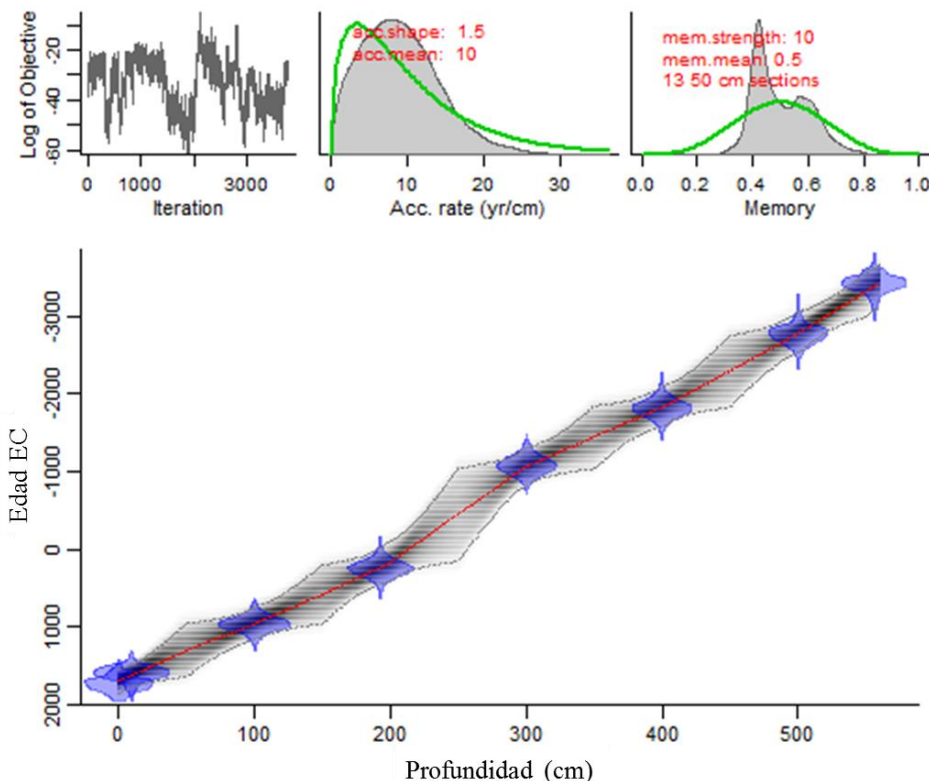

Figura 2. Modelo de edad de ^{14}C del MD02-2521.

4.2. Abundancia e índices de diversidad

La abundancia de diatomeas exhibió valores que oscilan de 7.3 a 22.7 x10^6 valvas/g (promedio de 13.5 ± 3.3 x10^6 valvas/g). Los periodos de mayores abundancias (respecto al promedio) ocurrieron de manera general de ~618 a ~864, ~1025 a ~1074, ~1253 a ~1375, y ~1528 a ~1599 EC (Fig. 3). La riqueza osciló de 36 a 60 taxones (promedio de 49 ± 5), la equidad de 0.64 a 0.79 (promedio de 0.74 ± 0.02) y el índice de Fisher de 20.2 a 63.3 (promedio de 39.0 ± 10.0). En términos generales, los periodos de mayor riqueza y los valores más altos del índice α ocurrieron de ~618 a ~854, ~1135 a ~1375 EC. La equidad fue alta de ~824 a ~1375 EC. De ~1384 EC hacia lo más reciente, todos los índices exhibieron sus valores más bajos (Fig. 3).
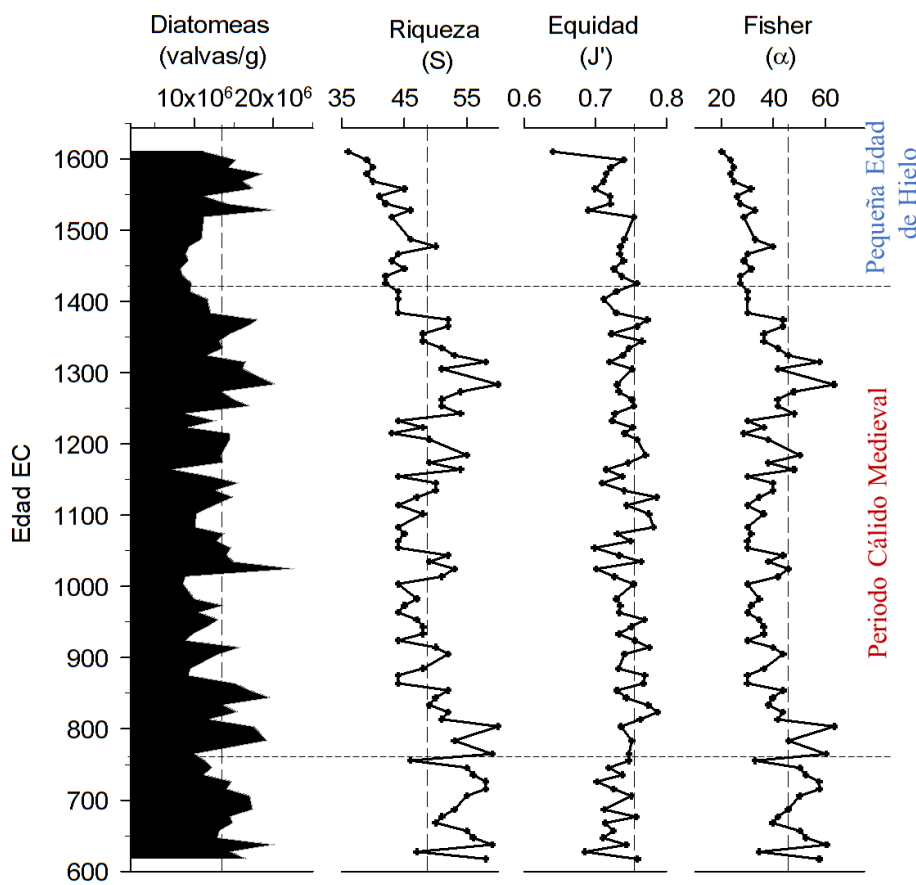

Figura 3. Abundancia de diatomeas (valvas/g), riqueza de especies, índice de Equidad (J') e índice de Fisher (α) de las poblaciones de diatomeas del núcleo MD02-2521. Las líneas punteadas indican el promedio en cada gráfica.

4.3. Composición florística

En el MD02-2521 se reconocieron un total de 110 taxones (se registró la misma flora que en el núcleo Tehua XII E03, Capítulo 2), de los cuales 11 fueron los más abundantes (> 2.5%) (Fig. 4) y en conjunto representaron el 75.8 % de la flora total. Estas especies fueron: *Thalassionema nitzschioides* (21.5%), esporas de *Chaetoceros* spp. (13.6%), *Neodelphineis pelagica* (9.0%), *Lioloma pacificum* (7.3%), *Thalassionema bacillare* (6.5%), *Thalassionema nitzschioides* var. *parvum* (3.9%), *Thalassiosira eccentrica* (3.2%), *Thalassiosira oestrupii* (2.8%), *Cyclotella litoralis* (2.8%), *Fragillariopsis doliolus* (2.7%) y *Thalassiosira lineata* (2.5%).

De manera general, se observa que del inicio del registro ~618 a ~756 EC, *T. nitzschioides*, *T. bacillare* y *L. pacificum* fueron los taxones más abundantes. De ~756 a ~1426 EC los taxones más abundantes fueron *T. nitzschioides*, *N. pelagica*, *T. nitzschioides* var. *parvum* y *T. eccentrica*, y algunos picos de máxima abundancia de *C. litoralis* y *T. lineata*. En el periodo más reciente de ~1426 a ~1610 EC las esporas de *Chaetoceros* spp., *L. pacificum* y *T. bacillare* mostraron sus máximas abundancias, y algunos picos de máxima abundancia de *T. bacillare* y *T. oestrupii* (Fig. 4).

4.4. Análisis de factores

El análisis de factores indica que el 94.9 % de la varianza acumulada es contenida en 2 factores: el Factor 1 contiene el 91.0% y el Factor 2 el 3.9% (Tabla 1). El primer factor se distribuyó principalmente de ~765 a ~1414 EC (84.0-84.5 a 19.0-19.5 cm), mientras que el segundo factor de ~1426 a ~1610 EC (18.0-18.5 a 0.6-1.0 cm). De ~618 a ~756 EC (99.0-99.5 a 85.0-85.5 cm) ambos factores se alternan y no hay una clara dominancia de algunas de los

factores (Fig. 5). El Factor 1 fue caracterizado por la asociación de *T. nitzschioides*, y *N. pelagica*, y el Factor 2 por la asociación de esporas de *Chaetoceros* spp., *T. nitzschioides*, *L. pacificum* y *T. bacillare* (Tabla 2).
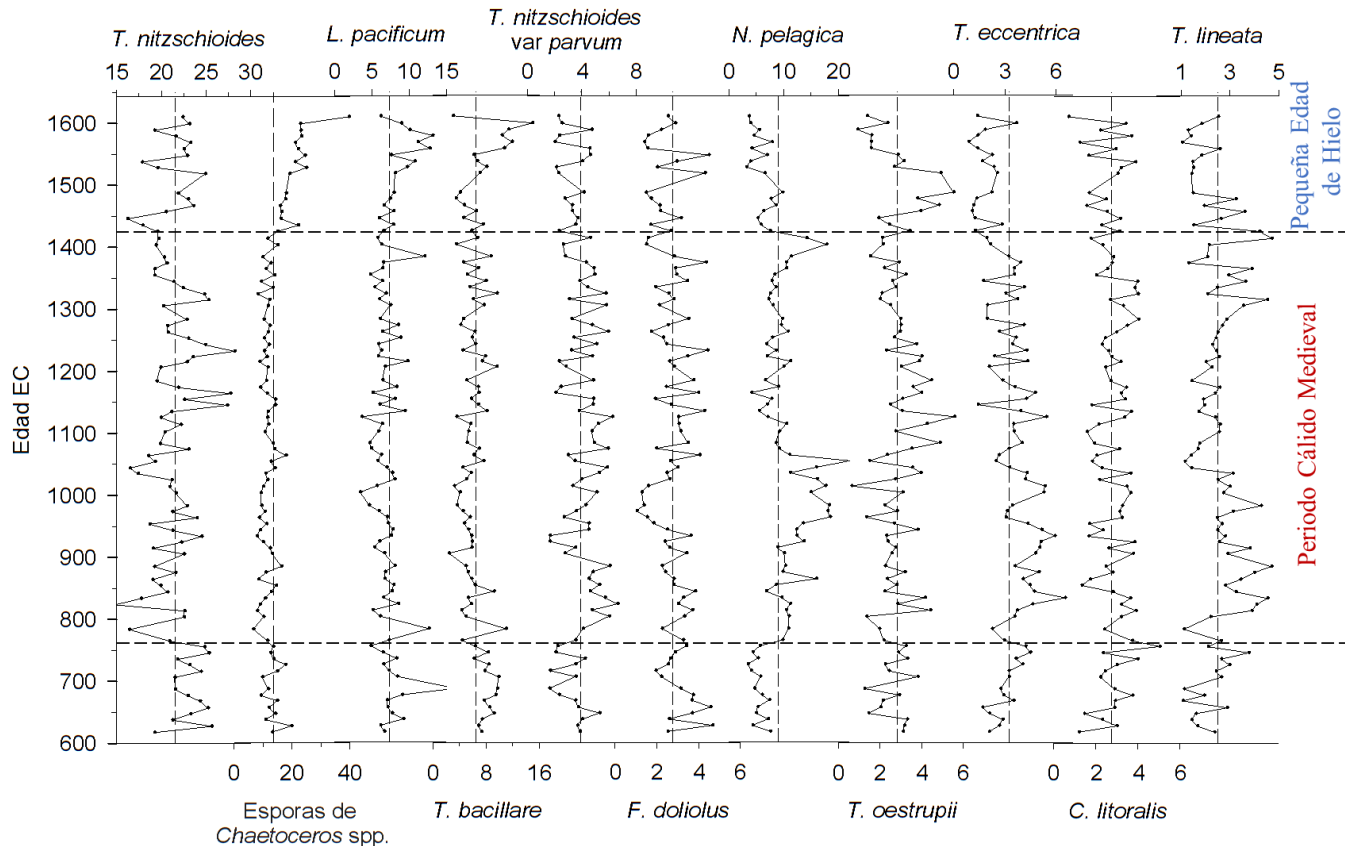
Figura 4. Abundancia relativa (%) de las especies más abundantes del núcleo MD02-2521. Las líneas punteadas indican los valores promedios de cada taxón.

Tabla 1. Eigenvalores del análisis de factores de las diatomeas del núcleo MD02-2521.

|	Eigenvalor	Varianza total %	Eigenvalor acumulado	Varianza acumulada
Factor 1	81.01	91.03	81.01	91.03
Factor 2	3.45	3.88	84.46	94.90
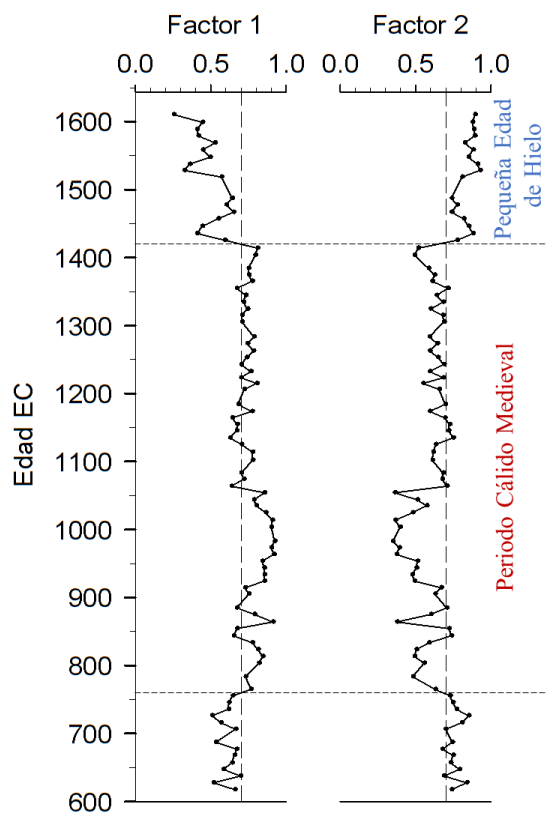
Figura 5. Distribución del Factor 1 y Factor 2 de las diatomeas del núcleo MD02-2521.

Tabla 2. Puntuaciones factoriales del análisis de factores de las diatomeas del núcleo MD02-2521. En rojo valores > 0.80.

Taxón	Factor 1	Factor 2
Azpeitia nodulifera	-0.46	-0.34
Cyclotella litoralis	-0.20	-0.15
Plagiogramma minus	-0.02	-0.72
Esporas de *Chaetoceros* spp.	-0.68	3.41
Fragilariopsis doliolus	-0.32	-0.02
Lioloma pacificum	0.12	0.89
Neodelphineis pelagica	3.08	-1.69
Nitzschia bicapitata	-0.18	-0.38
Nitzschia interruptestriata	-0.38	-0.25
Paralia sulcata	-0.62	-0.34
Rhizossolenia bergonii	-0.60	-0.28
Rhizossolenia setigera	-0.51	-0.36
Roperia tesselata	-0.43	-0.26
Thalassionema bacillare	-0.17	0.84
Thalassionema nitzschioides	3.04	1.99
Thalassionema nitzschioides var. *parva*	0.18	-0.19
Thalassiosira nanolineata	-0.31	-0.27
Thalassiosira oestrupii	-0.22	-0.10

5. Discusión

La flora de diatomeas del núcleo MD02-2521 fue muy similar a la encontrada en el núcleo Tehua XII E03 (Capítulo 2, sección 3.4), al igual que las asociaciones delimitadas con el análisis de factores. Las dos asociaciones encontradas en el MD02-2521 fueron: 1) la asociación caracterizada por *N. pelagica* y *T. nitzschioides* y 2) la asociación caracterizada por esporas de *Chaetoceros* spp., *T. nitzschioides*, *L. pacificum*, y *T. bacillare*. En el PCA, *N. pelagica* fue una de las especies que conformaron la asociación de aguas cálidas y de baja productividad en el núcleo Tehua XII E03 (Capítulo 2). *Thalassionema nitzschioides* es una especie ampliamente distribuida en aguas tropicales y templadas (Hasle y Syvertsen, 1997). En el Golfo de California y en la Cuenca de Cariaco, *T. nitzschioides* se ha encontrado junto con otros taxones de diatomeas cálidas (Sancetta, 1995; Romero et al., 2009). Dado que en este estudio *T. nitzschioides* fue encontrado en conjunto con *N. pelagica* consideramos que la asociación en conjunto refleja las condiciones cálidas y de baja productividad en el núcleo MD02-2521.

Las esporas de *Chaetoceros* spp., *T. nitzschioides* y *L. pacificum* conformaron la asociación de condiciones frías y de alta productividad, y fue la asociación que caracterizó las condiciones de la PEH en el núcleo Tehua XII E03 (Capítulo 2). Las esporas de *Chaetoceros* spp. del MD02-2521 fueron las mismas formas identificadas en el núcleo Tehua XII E03, pertenecientes a *Chaetoceros affinis*, *Chaetoceros costatus*, *Chaetoceros curvisetus*, y *Chaetoceros radicans*. *Thalassionema bacillare* fue agrupada en la asociación de condiciones templadas en el núcleo Tehua XII E03. Sin embargo, dado que en este núcleo se agrupó a las especies antes mencionadas, se consideró que esta asociación sugiere la predominancia de condiciones frías a templadas y de alta a moderada productividad en el núcleo MD02-2521.

La distribución de estas asociaciones a lo largo del núcleo coincidió con los periodos climáticos del PCM y la PEH. Al inicio del registro de ~618 a ~756 EC (Fig. 5), la riqueza de especies y la equidad estuvieron generalmente arriba del promedio. En este periodo ambas asociaciones presentaron cargas factoriales muy semejantes, y no hay una clara dominancia de algunas de las asociaciones, probablemente debido a que es la transición entre el final de las condiciones frías de la Edad Oscura (la cual abarca de ~400 a ~800 EC, Neukom et al., 2019) y el inicio de las condiciones cálidas del PCM. Del ~765 a ~ 1414 EC se estableció la asociación de condiciones cálidas y baja productividad con índices de diversidad variables; este periodo coincide con la temporalidad del PCM (~950 a ~1250 EC; Mann et al., 2009). En la parte superior del registro de ~1426 a ~1610 EC fue predominante la asociación de diatomeas de condiciones frías a templadas y de alta a moderada productividad (similar a lo que se encontró en la parte correspondiente a la PEH en el núcleo Tehua XII E03, Fig. 6). Asimismo, fue evidente una disminución de los índices de diversidad en este periodo, el cual coincide con el inicio de la PEH (~1350 a ~1850 EC; Crowley et al., 2008; Mann et al., 2009).
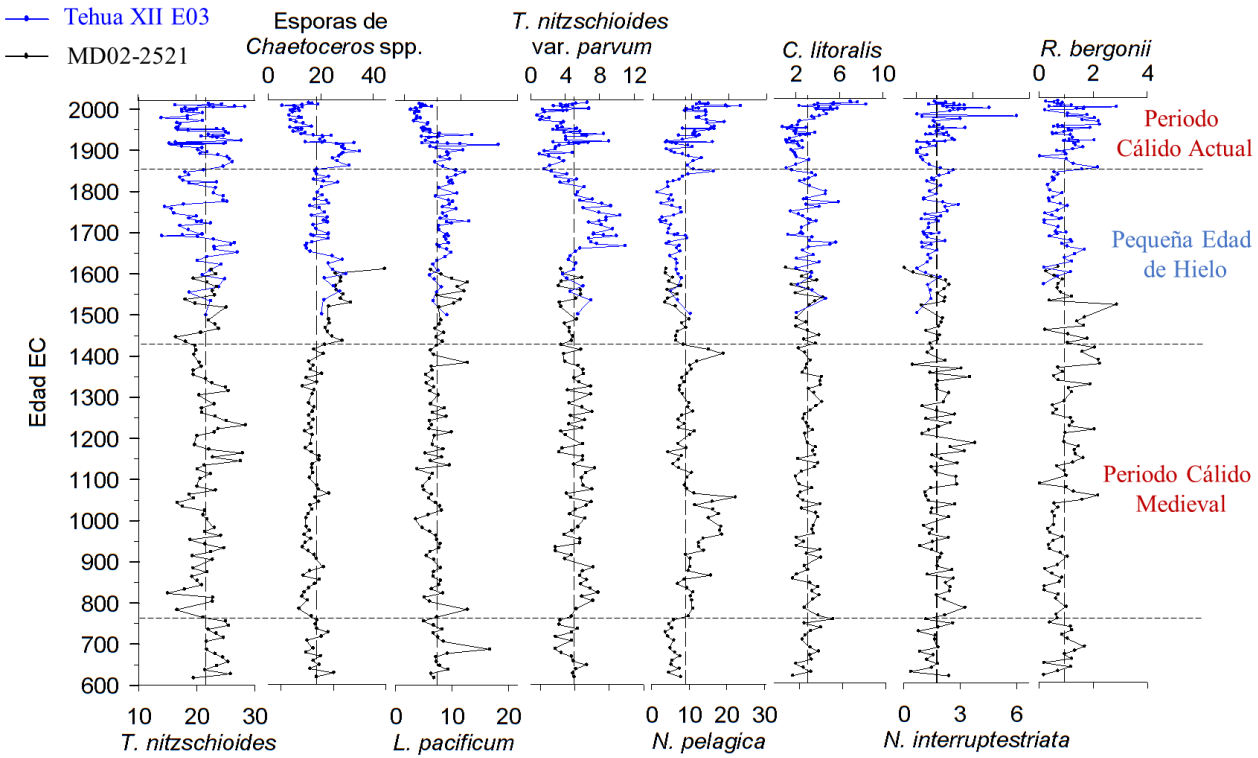
Figura 6. Distribución de las principales diatomeas durante el periodo de estudio en una secuencia combinada de los núcleos MD02-2521 y Tehua XII E03.

El PCM en el PTNO ha sido identificado como un periodo cálido y poco productivo. En el Golfo de California, Barron y Bukry (2007) señalan que el PCM (~900 a ~1250 EC), fue caracterizado por una distintiva asociación de diatomeas y silicoflagelados de condiciones cálidas (*Azpeitia nodulifera* y *Dictyocha stapedia*). En la cuenca Alfonso Ricaurte-Villota et al. (2013) encuentran condiciones de baja productividad durante el PCM (~700 a 1150 EC) de acuerdo con sus registros de COT (% Carbono Orgánico Total) y sílice biogénico. Resultados similares se reportaron en el margen de Magdalena (BCS) por Juárez et al. (2014) quienes encontraron que durante el PCM el contenido de C_{org} (%) y el ópalo biogénico fue mucho menor que durante la PEH (Fig. 7).

Por el contrario, la PEH en el PTNO es reconocido como un periodo frío de alta productividad. En el Golfo de California, Barron y Bukry (2007) señalaron que durante la PEH

(~1300 a ~1850 EC) predominaron asociaciones silíceas de condiciones frías (*Roperia tesselata* y *Octatis pulchra*), y su registro de sílice biogénico sugirió condiciones más productivas que las del PCM. Resultados similares fueron encontrados en la cuenca Alfonso y en el margen de Magdalena (BCS), donde los registros de COT y C_{org}, respectivamente, también sugiere condiciones más productivas durante la PEH (Ricaurte-Villota et al., 2013; Juárez et al., 2014) (Fig. 7). El registro de diatomeas, C_{org}, Ni/Al y Cu/Al del núcleo Tehua XII E03, el cual abarca gran parte de la PEH (~1500 a ~1860 EC), también sugiere que este periodo fue caracterizado por condiciones frías y de alta productividad (Capítulo 2).
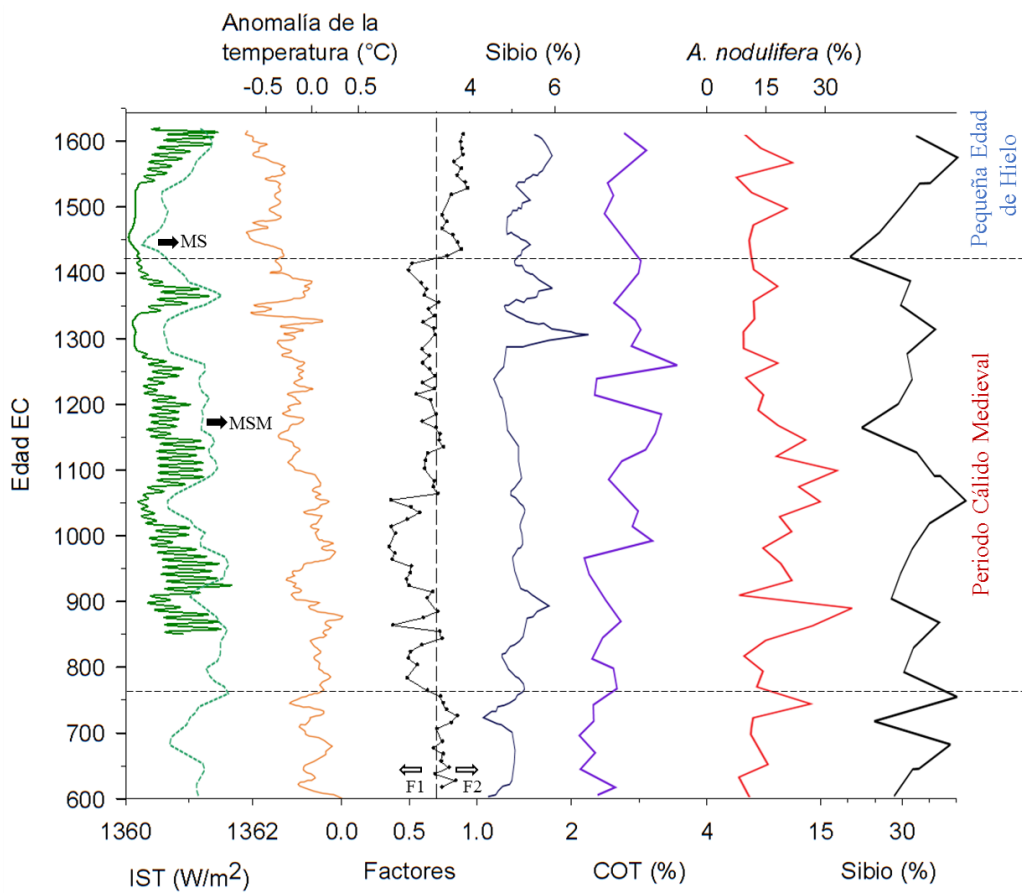

Figura 7. Registros paleoclimáticos y el registro del MD02-2521 durante el periodo estudiado: a) Irradiancia solar total (IST), MSM (máximo solar medieval, MS (mínimo de Spörer) (Lean, 2018 en línea continua; Wu et al., 2018 en línea punteada); b) Anomalía de la temperatura (°C) (Mann et al., 2009); c) distribución de los factores del MD02-2521, factor (F1), factor (F2); d)

sílice biogénico (sibio) y e) Carbono orgánico total (COT) de Baja California (Ricaurte-Villota et al., 2013); f) *Azpeitia nodulifera,* y g) sibio del Golfo de California (Barron y Bukry, 2007).

Climatológicamente, estos cambios en la productividad del PTNO durante el Holoceno tardío han sido relacionados con los cambios en la irradiancia solar (Barron y Bukry, 2007; Juárez et al., 2014; Choumiline et al., 2019). Las condiciones cálidas del PCM se han relacionado con el aumento en la irradiancia solar y con el máximo solar medieval de ~1100 a 1250 EC (Damon y Jirikowic, 1994) (Fig. 7) y temperaturas más intensas en el hemisferio norte (Mann et al., 2009). Bajo estas condiciones se infiere que el sistema de alta presión del Pacífico Norte se debilitó (Barron y Bukry, 2007; Barron et al., 2010; Juárez et al., 2014; Choumiline et al., 2019) y la ZCIT migró hacia su posición más norteña (Haug et al., 2001; Griffiths et al., 2016), lo cual a su vez conlleva a que los vientos que generan las surgencias en el Golfo de California y en el margen de Magdalena se debilitaron y, consecuentemente, disminuyó la productividad (Barron y Bukry, 2007; Juárez et al., 2014). Dado que el GT también es influenciado por esta dinámica atmosférica, en este escenario cálido del PCM se infiere que menos frentes polares alcanzaron el Golfo de México (Nyberg et al., 2002) y el GT, por lo que los vientos Tehuanos fueron menos frecuentes e intensos sobre el área de estudio. Con la disminución de los vientos Tehuanos, las surgencias y los procesos de mezcla disminuyeron lo que permitió la predominancia de la asociación de diatomeas de condiciones cálidas y de baja productividad en el GT.

Las condiciones climáticas de la PEH en el PTNO son más conocidas que el PCM (ej. Glynn et al., 1993; Goni et al., 2006; Staines-Urías et al., 2009; Barron y Bukry, 2007; Juárez et al., 2014; Choumiline et al., 2019). La PEH es caracterizada por una baja actividad solar, la predominancia de los mínimos solares (Wolf, Spörer, Maunder, y Dalton) (Bard et al., 2000; Lean, 2018), y temperaturas más frías en el hemisferio norte (Mann et al., 2009) (Fig. 7). En estas condiciones de baja irradiancia solar, el sistema de alta presión del Pacífico Norte se intensificó

y la ZCIT migró hacia el sur, promoviendo que los vientos que propician las surgencias en el Golfo de California y el margen de Magdalena fueran más intensos, y por lo tanto la productividad se viera favorecida (Barron y Bukry, 2007; Staines-Urías et al., 2009; Juárez et al., 2014; Choumiline et al., 2019). Bajo este escenario frío de la PEH, los vientos Tehuanos fueron más intensos y frecuentes debido a la mayor incidencia de frentes fríos sobre el Golfo de México (Lozano et al, 2007; Nyberg et al., 2002) y el GT. En el Golfo de Papagayo, el cual también está influenciado por los frentes fríos (Amador et al., 2006), Glynn et al. (1983) reportaron la muerte de arrecifes de coral causada por las bajas temperaturas del agua que asociaron a un incremento en intensidad y duración de las surgencias, debido a una mayor frecuencia de frentes fríos durante la PEH.

6. Conclusiones

Los hallazgos sobre la variabilidad de la productividad durante el PCM y el inicio de la PEH en el presente estudio están en concordancia con la variabilidad climática del PTNO. Asimismo, indican que las variaciones de la productividad superficial, derivada de las diatomeas en el periodo estudiado, fueron impulsadas principalmente por la dinámica atmosférica, específicamente en los movimientos latitudinales de la ZCIT y de los sistemas de alta presión, los cuales a su vez responde a los cambios en la irradiancia solar.

Este estudio provee el primer registro de la influencia del Periodo Cálido Medieval (~765 a ~1414 EC) sobre los cambios en la productividad de diatomeas en el GT. La asociación que caracterizó el PCM fue *N. pelagica-T. nitzschioides*, la cual indica que durante este periodo predominaron condiciones cálidas y de baja productividad comparadas con el inicio de la PEH (~1426 a ~1610 EC). La baja productividad del PCM fue la respuesta a una mayor irradiancia (ej. máximo solar medieval) que ocasionó un desplazamiento hacia el norte de la ZCIT y el

debilitamiento de los sistemas de alta presión en el hemisferio norte, lo que a su vez ocasionó la menor incidencia de frentes fríos en el sur del Golfo de México y eventualmente la disminución en la intensidad y frecuencia de los vientos Tehuanos sobre el GT, lo que a su vez resultó en surgencias menos intensas y por tanto menor productividad superficial, como así lo revelan las diatomeas.

Por el contrario, el inicio de la PEH (~1426 a ~1610 EC), se caracterizó por la asociación de esporas de *Chaetoceros* spp, *T. nitzschioides*, *L. pacificum* y *T. bacillare,* la cual sugiere que condiciones frías a templadas y una mayor productividad predominaron durante este periodo en el GT. Además, las asociaciones de diatomeas (*T. nitzschioides*, esporas de *Chaetoceros* spp, *L. pacificum* y *R. setigera*) y los valores altos de C_{org}, NT, Ni/Al y Cu/Al del núcleo Tehua XII E03 (Capítulo 2), sugieren que estas condiciones frías y de alta productividad prevalecieron en el resto del periodo frío de la PEH (~1500 a ~1860 EC). La PEH se caracterizó por una menor actividad solar, como fue la presencia del mínimo solar de Spörer a inicios de la PEH. Bajo estas condiciones, la ZCIT se desplazó hacia el sur y los sistemas de alta presión del hemisferio norte se intensificaron, lo cual promovió la influencia de más frentes polares en el sur del Golfo de México, y por tanto mayor frecuencia e intensidad de vientos Tehuanos en el GT, que ocasionaron surgencias más intensas y consecuentemente mayor productividad superficial.

7. Referencias

Almaraz-Ruiz, L., Machain-Castillo, M.L., Sifeddine, A., Ruiz-Fernandez, A.C., Sanchez-Cabeza, J.A., Rodríguez-Ramírez, A., López-Mendoza, P., Mendez-Millan, M., Caquineau, S., 2023. Diatom-based paleoproductivity and climate change record of the Gulf of Tehuantepec (Eastern Tropical Pacific) during the last ~500 years. The Holocene.

Amador, J.A., Alfaro, E.J., Lizano, O.G., Magaña, V.O. 2006. Atmospheric forcing of the eastern tropical Pacific: A review. Prog. Oceanogr. 69, 101–142. https://doi.org/https://doi.org/10.1016/j.poc ean.2006.03.007

Bard, E., Raisbeck, G., Yiou, F., Jouzel, J. 2000. Solar irradiance during the last 1200 years based on cosmogenic nuclides. Tellus, Ser. B Chem. Phys. Meteorol. 52, 985–992. https://doi.org/10.1034/j.1600-0889.2000.d01-7.x

Barron, J.A. y Bukry, D. 2007. Solar forcing of Gulf of California climate during the past 2000 yr suggested by diatoms and silicoflagellates. Mar. Micropaleontol. 62, 115–139. https://doi.org/10.1016/j.marmicro.2006.08.003

Barron, J.A., Bukry, D., Bischoff, J.L. 2003. A 2000-yr-long record of climate from the Gulf of California, in: West, G.J. and Blomquist, N.L. (Ed.), Proceedings of t h e Nineteenth Pacific Climate Workshop. Asilomar, Pacific Grove, CA, pp. 1–15.

Barron, J.A., Bukry, D., Field, D. 2010. Santa Barbara Basin diatom and silicoflagellate response to global climate anomalies during the past 2200 years. Quat. Int. 215, 34–44. https://doi.org/10.1016/j.quaint.2008.08.007

Choumiline, K., Pérez-Cruz, L., Gray, A.B., Bates, S.M., Lyons, T.W. 2019. Scenarios of Deoxygenation of the Eastern Tropical North Pacific During the Past Millennium as a Window Into the Future of Oxygen Minimum Zones. Front. Earth Sci. 7. https://doi.org/10.3389/feart.2019.00237

Crosta, X., Koc, N. 2007. Diatoms: From Micropaleontology to Isotope Geochemistry. Dev. Mar. Geol. 1, 327–369. https://doi.org/10.1016/S1572-5480(07)01013-5

Crowley, T.J., Zielinski, G., Vinther, B., et al. 2008. Volcanism and the little ice age. *PAGES News* 16(2): 22–23.

Cupp, E. 1943. Marine Plankton Diatoms of the West Coast of North America. Bull. Scripps Inst. Oceanogr. 5, 1–238.

Damon, P.E., Jirikowic, J.L. 1994. Solar Forcing of Global Climate Change. *Environmental Science*. Universidad de Arizona, Tucson, USA. 301-314.

Fiedler, P.C., Talley, L.D. 2006. Hydrography of the eastern tropical Pacific: A review. Prog. Oceanogr. 69, 143–180. https://doi.org/10.1016/j.pocean.2006.03.008

Fisher, R.A., Corbet, A.S., Williams, C.B. 1943. The Relation Between the Number of Species and the Number of Individuals in a Random Sample of an Animal Population. J. Anim. Ecol. 12, 42–58.

García-Gallardo, Á., Almaraz-Ruiz, L., Machain-Castillo, M.L. 2022. Paleoceanography of the Gulf of Tehuantepec during the Medieval Warm Period. Mar. Micropaleontol. 170. https://doi.org/10.1016/j.marmicro.2021.102081

García-Gallardo, Á., Machain-Castillo, M.L., Almaraz-Ruiz, L. 2021. Paleoceanographic evolution of the Gulf of Tehuantepec (Mexican Pacific) during the last ~6 millennia. Holocene 31, 529–544. https://doi.org/10.1177/0959683620981724

Glynn, P.W., Druffel, E.M., Dunbar, R.B. 1983. A dead Central American coral reef tract: possible link with the Little Ice Age (Costa Rica, Gulf of Papagayo, Gulf of Panama)., Journal of Marine Research. https://doi.org/10.1357/002224083788519740

Goni, M. A., Thunell, R. C., Woodwort, M.P., et al. (2006) Changes in wind-driven upwelling during the last three centuries: Interocean teleconnections. *Geophysical Research Letters* 33(15): 3–6.

Griffiths, M.L., Kimbrough, A.K., Gagan, M.K., Drysdale, R.N., Cole, J.E., Johnson, K.R., Zhao, J.X., Cook, B.I., Hellstrom, J.C., Hantoro, W.S. 2016. Western Pacific hydroclimate linked to global climate variability over the past two millennia. Nat. Commun. 7, 1–9. https://doi.org/10.1038/ncomms11719

Hasle, G.R. y Syvertsen, E.E. 1997. Marine Diatoms, in: Tomas, C.R. (Ed.), Identifying Marine Diatoms. Academic Press, San Diego, California, pp. 5–386.

Haug, G.H., Hughen, K.A., Sigman, D.M., Peterson, L.C., Röhl, U. 2001. Southward migration of the intertropical convergence zone through the Holocene. Science 293, 1304–1308. https://doi.org/10.1126/science.1059725

Heaton, T.J., Köhler, P., Butzin, M., Bard, E., Reimer, R.W., Austin, W.E.N., Ramsey, C.B., Grootes, P.M., Hughen, K.A., Kromer, B., Reimer, P.J., Adkins, J., Burke, A., Cook, M.S., Olsen, J., Skinner, L.C., 2020. Marine20 - The Marine Radiocarbon Age Calibration Curve (0-55,000 cal BP). Radiocarbon 62, 779–820. https://doi.org/10.1017/RDC.2020.68

Hernández-Becerril, D. U., Barón-Campis, S. A., Ceballos-Corona, J. G. A., et al. 2021. *Catálogo de fitoplancton del Pacífico central mexicano, Cruceros "MareaR" (2009-2019). B/O "El Puma." Universidad Nacional Autónoma de México*. México: Universidad Nacional Autónoma de México.

IPCC, 2014. Climate Change 2014: Synthesis Report. Contribution of Working groups I, II and III to the Fifth Assessment Report of the Intergovernmental Panel on Climate Change. Geneva, Switzerland.

Juárez, M., Sánchez, A., González-Yajimovich, O. 2014. Variabilidad de la productividad biológica marina en el Pacífico nororiental durante el último milenio. Ciencias Mar. 40, 211–220.

Lean, J. L. 2018. Estimating Solar Irradiance Since 850 CE. *Earth and Space Science* 5(4): 133–149.

Lozano-García, M.D.S., Caballero, M., Ortega, B., Rodríguez, A., Sosa, S. 2007. Tracing the effects of the Little Ice Age in the tropical lowlands of eastern Mesoamerica. Proc. Natl. Acad. Sci. U. S. A. 104, 16200–16203. https://doi.org/10.1073/pnas.0707896104

Mann, M.E., Zhang, Z., Rutherford, S., Bradley, R.S., Hughes, M.K., Shindell, D., Ammann, C., Faluvegi, G., Ni, F. 2009. Global Signatures and Dynamical Origins of the Little Ice Age and Medieval Climate Anomaly. Science 326, 1256–1260.

Moreno, J. L., Licea, S. Santoyo, H. 1996. *Diatomeas del Golfo de California. Universidad Autónoma de Baja California Sur*. La Páz, México.

Neukom, R., Steiger, N., Gómez-Navarro, J.J. et al. 2019. No evidence for globally coherent warm and cold periods over the preindustrial Common Era. *Nature* 571, 550–554. https://doi.org/10.1038/s41586-019-1401-2

Nyberg, J., Malmgren, B.A., Kuijpers, A., Winter, A., 2002. A centennial-scale variability of tropical North Atlantic surface hydrography during the late Holocene. Palaeogeogr. Palaeoclimatol. Palaeoecol. 183, 25–41. https://doi.org/10.1016/S0031-0182(01)00446-1

Pennington, J.T., Mahoney, K.L., Kuwahara, V.S., Kolber, D.D., Calienes, R., Chavez, F.P., 2006. Primary production in the eastern tropical Pacific: A review. Prog. Oceanogr. 69, 285–317. https://doi.org/10.1016/j.pocean.2006.03.012

Pielou, E.C., 1966. The measurement of diversity in different types of biological collections. J. Theor. Biol. 15, 177. https://doi.org/10.1016/0022-5193(67)90048-3

Ricaurte-Villota, C., Gonz´alez-Yajimovich, O., S´anchez, A., 2013. Coupled response of rainfall and denitrification to solar forcing during the Holocene in Alfonso Basin. Ciencias Marinas 39 (2), 151–164. https://doi.org/10.7773/cm.v39i2.2224.

Romero, O.E., Thunell, R.C., Astor, Y., Varela, R., 2009. Seasonal and interannual dynamics in diatom production in the Cariaco Basin, Venezuela. Deep. Res. Part I Oceanogr. Res. Pap. 56, 571–581. https://doi.org/10.1016/j.dsr.2008.12.005

Round, F. E., Crawford, R. M. Mann, D. G. 1990 *The Diatoms: Biology & Morphology of the genera. The University Cambridge Press*.

Salvatteci, R., Gutiérrez, D., Field, D., Sifeddine, A., Ortlieb, L., Bouloubassi, I., Boussafir, M., Boucher, H., Cetin, F., 2014. The response of the Peruvian Upwelling Ecosystem to centennial-scale global change during the last two millennia. Clim. Past 10, 715–731. https://doi.org/10.5194/cp-10-715-2014

Sancetta, C. 1995. Diatoms in the Gulf of California: Seasonal flux patterns and the sediment record for the last 15,000 years. Paleoceanography 10, 67–84. https://doi.org/10.1029/94PA02796

Schrader, H. J. y Gersonde, R., 1978. Diatoms and silicoflagellates in Micropaleontological counting methods and techniques-An exercise on an eight meters section of the Lower Pliocene of Capo Rossello, Sicily. Micropaleotol. Bull. 17, pp 129–176.

Staines-Urías, F., Douglas, R.G., Gorsline, D.S., 2009. Oceanographic variability in the southern Gulf of California over the past 400 years: Evidence from faunal and isotopic records from planktic foraminifera. Palaeogeogr. Palaeoclimatol. Palaeoecol. 284, 337–354. https://doi.org/10.1016/j.palaeo.2009.10.016

Thunell, R.C., 1998. Particle fluxes in a coastal upwelling zone: Sediment trap results from Santa Barbara Basin, California. Deep. Res. Part II Top. Stud. Oceanogr. 45, 1863–1884. https://doi.org/10.1016/S0967-0645(98)80020-9

Trasviña, A., Barton, E.D., Brown, J., Velez, H.S., Kosro, P.M., Smith, R.L., 1995. Offshore wind forcing in the Gulf of Tehuantepec, Mexico: The asymmetric circulation. J. Geophys. Res. 100, 20649–20663.

Treppke, F.U., Lange, C. y Wefer, G., 1996. Vertical fluxes of diatoms and silicoflagellates in the eastern equatorial Atlantic, and their contribution to the sedimentary record. Mar. Micropaleontol. 28, 73–96.

Wu, C.J., Krivova, N.A., Solanki, S.K., Usoskin, I.G., 2018. Solar total and spectral irradiance reconstruction over the last 9000 years. Astron. Astrophys. 620, 1–12.

CAPÍTULO 5: Conclusiones generales

A través de un modelo de edad-profundidad en el que se integraron fechados con ^{210}Pb y ^{14}C a través de un modelo bayesiano, se determinó un reservorio local $\Delta R = 247 \pm 30$, 1 sigma, para los sedimentos de los últimos ~500 años en el GT. La tasa de sedimentación fue muy similar a lo largo del periodo estudiado, de 0.11 cm/año de ~618 ~1610 EC, de 0.08 ± 0.05 cm/año de ~1500 ~1907 EC y de 0.14 ± 0.07 de ~1907 a 2014 EC.

De acuerdo con los resultados obtenidos, la variabilidad más importante de la ZOM y de la productividad durante el último milenio estuvo relacionada con los eventos climáticos del PCM, la PEH y el PCA. Los cambios en la ZOM y en la productividad fueron determinados a través de las asociaciones de FB y de diatomeas, respectivamente, y para los últimos ~500 años, se incluyeron proxies geoquímicos de oxigenación (Mo, V, Cd, U y Re, y $\delta^{15}N_{sed}$) y de productividad (C_{org}, NT, Ni/Al y Cu/Al). Las poblaciones de FB encontrada en los sedimentos de los núcleos MD0225-21 y Tehua XII E03 fueron características de ambientes pobres en oxígeno, lo que sugiere que las condiciones de fondo no han cambiado drásticamente en el periodo estudiado. Además, la razón Re/Mo durante los últimos ~500 años sugiere que no se alcanzaron condiciones de anoxia, ya que está fue mayor a la razón del agua de mar (0.4×10^{-3}).

Estudios previos sobre el PCM (~800 a ~1375 EC) en el núcleo MD02-2521 (García-Gallardo et al., 2022) a través de FB, revelaron que la concentración de OD del agua de fondo de la ZOM del GT presentó ciclicidades casi seculares (~90 años), cercanas a los ciclos de Gleissberg, sugiriendo que la ZOM durante el PCM no fue un periodo homogéneo, sino variable. Esta ciclicidad ocurrió en tres fases: periodos de mayor oxigenación, caracterizados por la asociación más tolerante a la disminución de OD (*Bolivina seminuda, Epistominella* sp.1, *Epistominella obesa*, *Gyroidina nitidula* y *Pseudoparella bradyana*), seguidos de periodos de

menor oxigenación caracterizados por la asociación más tolerante a la disminución de OD (*Epistominella sandiegoensis, Bolivina seminuda* y *Buliminella tenuata*) y periodos de anoxia donde no se preservaron los FB. Esta variabilidad de la ZOM fue atribuida a la actividad solar ya que está determina la posición promedio de la ZCIT y la fortaleza de los sistemas de alta presión en el hemisferio norte. Ambos procesos determinan el patrón e intensidad de vientos predominante en el PTNO, y consecuentemente las variaciones en la productividad, la cual tiene influencia sobre la oxigenación del agua de fondo. Durante este periodo, las asociaciones de diatomeas revelaron que el PCM (~765 a ~1414 EC) fue caracterizado por una asociación indicadora de condiciones cálidas y de baja productividad (*Neodelphineis pelagica* y *Thalassionema nitzschioides*). Es probable que las periodicidades casi seculares encontradas en la ZOM también estén presentes en los registros de productividad, por lo que sería un tema de estudio que queda por hacer a futuro.

La PEH (~1500 a ~1860 EC) analizada en el núcleo Tehua XII E03 fue caracterizada por bajas abundancias de FB, alta dominancia y la predominancia de la asociación más tolerante a la disminución de la concentración de OD (*E. sandiegoensis, B. seminuda* y *B. tenuata*) y los metales-redox (Mo, V, Cd, U, y Re) y el $\delta^{15}N$ exhibieron sus mayores enriquecimientos. Estas condiciones sugieren la intensificación de la ZOM en el GT durante este periodo. La productividad de diatomeas reveló que el inicio de la PEH (~1426 a ~1610 EC), registrada en el núcleo MD02-2521, se caracterizó por la asociación de diatomeas de condiciones frías a templadas y de alta a moderada productividad (esporas de *Chaetoceros* spp, *T. nitzschioides*, *Lioloma pacificum* y *Thalassionema bacillare*). La parte de la PEH (~1500 a ~1860 EC) registrada en el núcleo Tehua XII E03, fue evidenciada por la asociación indicadora de condiciones frías y alta productividad (esporas de *Chaetoceros* spp, *T. nitzschioides, L. pacificum Thalassiosira nanolineata* y *Rhizossolenia setigera*) y por altos valores de C_{org}, NT, Ni/Al y

Cu/Al. La alta productividad de la PEH fue atribuida a la baja actividad solar que promovió la migración más al sur de la ZCIT, la cual fortaleció el sistema de alta presión del Pacífico Norte y la Circulación de Walker del Pacífico. Bajo estas condiciones, se infiere que más frentes fríos llegaron al GT y los vientos Tehuanos fueron probablemente más intensos y/o frecuentes promoviendo surgencias más intensas y mayor productividad. El aumento de la productividad conllevó a un mayor trasporte de la materia orgánica al fondo oceánico y mayor consumo de OD debido a la degradación de esta materia orgánica, acentuando las bajas concentraciones de OD del agua de fondo de la ZOM durante este periodo (Fig. 1).

El PCA (~1860 a ~2009 EC) analizado en el núcleo Tehua XII E03 se caracterizó por altas abundancias y baja dominancia de las poblaciones de FB y la predominancia de la asociación de FB indicadora de mayor oxigenación (*B. seminuda*, *Epistominella* sp. 1, *G. nitidula*, y *Suggrunda eckisi*), así como un menor enriquecimiento de los metales redox-sensitivos y $\delta^{15}N_{sed}$. En conjunto estas condiciones sugieren un debilitamiento de la ZOM en el GT durante este periodo. La productividad de diatomeas reveló un periodo de transición entre la PEH y el PCA (~1860 a ~1919 EC) caracterizado por la abundancia de la asociación de condiciones frías y baja productividad (*T. nitzschioides*, *Chaetoceros* spores y *L. pacificum*) así como la abundancia de algunos taxones de condiciones cálidas y baja productividad (*N. pelagica*, *Thalassiosira tenera* y *Rhizossolenia bergonii*), además de la disminución del C_{org}, NT, Ni/Al y Cu/Al. El PCA (~1920 a ~2014 EC) se caracterizó por la predominancia de la asociación cálida y de baja productividad (*N. pelagica, Fragillariopsis doliolus*, *Cyclotella litoralis*, *Thalassiosira oestrupii*, *Cymatodiscus. planetophorus*, *Nitzschia interruptestriata*, y *R. bergonii*), y valores bajos de C_{org}, NT, Ni/Al y Cu/Al. En conjunto los proxies sugirieron condiciones de menor productividad desde ~1860 EC que fueron atribuidas al aumento en la irradiancia solar y al aumento de la temperatura global debido a la influencia antrópica. La mayor irradiación

promovió la migración hacia el norte de la ZCIT, el debilitamiento del sistema de alta presión del Pacífico Norte y de la Circulación de Walker del Pacífico. Bajo este escenario se infiere que menos frentes fríos llegaron al GT y, por lo tanto, los vientos Tehuanos fueron menos intensos y/o frecuentes, disminuyendo los procesos de surgencia en el GT, lo cual se reflejó en la disminución de la productividad. Además, el aumento de la temperatura global también propició el aumento de la temperatura superficial del mar y consecuentemente una mayor estratificación que afectó de manera negativa a los procesos de surgencia y a la productividad. Por lo tanto, la disminución de la productividad en el GT puede explicar el debilitamiento de la ZOM ya que a menor productividad se produce menos materia orgánica que alcance a llegar al fondo marino, y menos OD es consumido, permitiendo que la ZOM esté menos intensificada (Fig. 1).
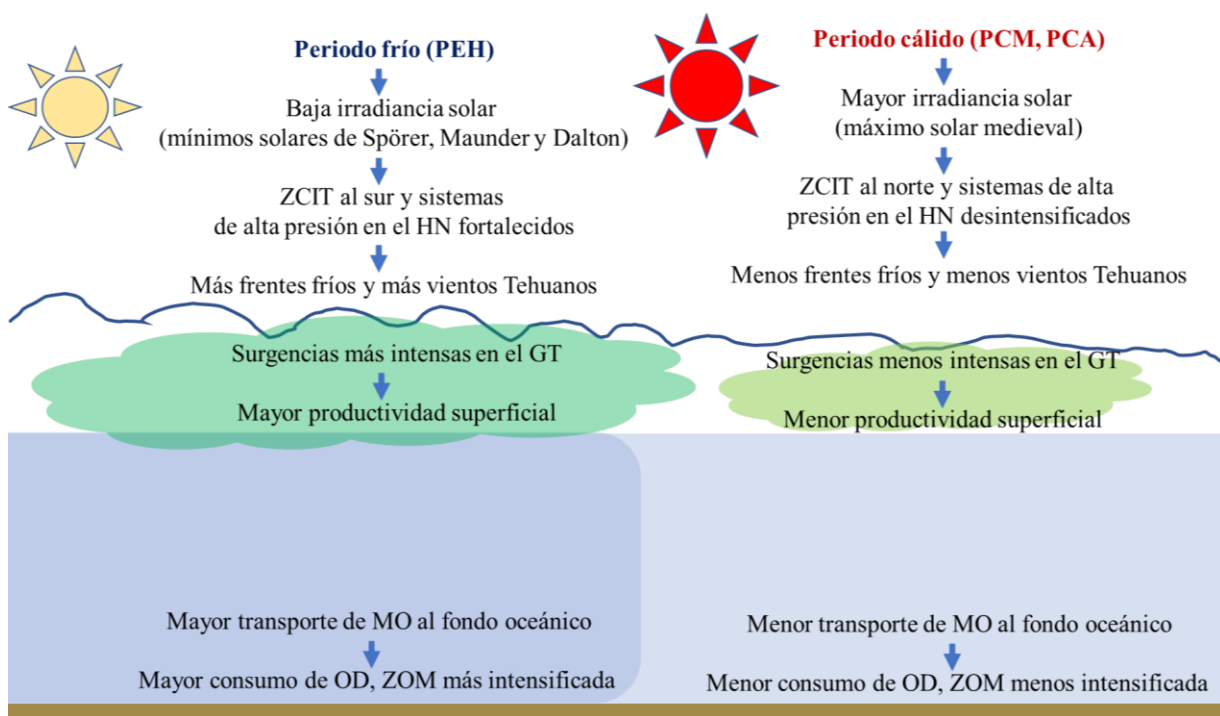

Figura 1. Influencia de la irradiancia solar en la variabilidad de la productividad superficial y la zona de oxígeno mínimo en el PTNO durante el último milenio.

Estas observaciones de la variabilidad de la ZOM del GT durante el periodo estudiado coinciden con lo reportado previamente en latitudes más norteñas, lo que confirma la escala regional de estos cambios y que estos responden a los mismos forzamientos. No obstante, es probable que otros forzamientos estén actuando en conjunto con la productividad, como pueden ser los cambios en la circulación del agua de fondo, así como la señal de ENOS. Este último, tiene un efecto importante en la variabilidad del límite superior de la ZOM y de la productividad, sin embargo, dado que la resolución temporal de las muestras analizadas (~6 años) fue mayor a la resolución de ENOS, no fue posible hacer una comparación directa, por lo que este es un tópico que también debería ser abordado en estudios posteriores.